KINETICS OF REDOX POLYMER MEDIATED BIOANODES

Ву

Harshal M Bambhania

A THESIS

Submitted to
Michigan State University
in partial fulfillment of the requirements
for the degree of

MASTER OF SCIENCE

Chemical Engineering

2011

ABSTRACT

KINETICS OF REDOX POLYMER MEDIATED BIOANODES

By

Harshal M Bambhania

Osmium-based redox polymer mediated glucose oxidase electrodes were characterized in the absence and presence of O_2 for use as anodes in glucose/ O_2 based biofuel cells. In N_2 saturated conditions, glucose oxidation current density of up to 2 mA/cm² was observed whereas significant loss in current was noticed in the presence of O_2 saturated conditions. Mediating performance of the synthesized redox polymers with respect to GOx and effect of oxygen in the system was quantitatively studied in terms of mediator redox potential, osmium loading and diffusivities.

A one-dimensional model of a redox polymer-mediated, enzyme electrode was developed in order to account for the presence of oxygen. Kinetic parameters were determined by fitting to the experimental current density measurements for varying potential, glucose and O₂ concentrations. Kinetic parameters specific to the mediator reaction were an order of magnitude higher than other homogeneous mediated systems ascribed to better mediation efficiency of the synthesized redox polymers. Bimolecular rate constants for GOx-oxygen reaction were found to be an order of magnitude lower than that of the free solution, which can be attributed to the reduced activity of immobilized GOx. Performance of the system was analyzed via simulation under various conditions.

Copyright by

HARSHAL M BAMBHANIA

2011

DEDICATION

This work is dedicated to my parents.

ACKNOWLEDGEMENTS

First of all, I would like to thank my parents for their love, support and encouragement.

Then I would like to thank my Advisor Dr. Scott Calabrese Barton for his help and contributions.

It was an interesting and constructive journey under his guidance and I have learned a lot from that. It has not only helped me to evolve as a better researcher but it has also honed my professional skills.

I would like to give special thanks to a special person Deboleena Chakraborty, who was sort of my co-advisor without whom synthesis of redox polymers would have been an arduous task and cannot thank her enough for all the technical and non-technical teachings.

I also like to thank my colleagues/friends Hao, Durga, Hanzi, Nate, Yira, Piyush, Katie for being there for me whenever I needed any help.

My stint here at MSU has helped me to become a better person and my best wishes will be always there with you all.

TABLE OF CONTENTS

| LIST OF TABLE | S | VII |
|---------------|--|------|
| LIST OF FIGUR | ES | VIII |
| CHAPTER 1: IN | TRODUCTION | 1 |
| Re | ferences | 26 |
| CHAPTER 2: SY | NTHESIS AND CHARACTERIZATION OF OSMIUM REDOX POLY | MER |
| | EDIATED GLUCOSE OXIDASE ELECTRODES | |
| | ostract | |
| | roduction | |
| | perimental | |
| | sults | |
| | scussion | |
| | nclusions | |
| | knowledgements | |
| | ferences | |
| CHAPTER 3. KI | NETICS OF OSMIUM REDOX POLYMER MEDIATED GLUCOSE | |
| | KIDASE ELECTRODES | 62 |
| | ostract | |
| | roduction | |
| | e Model | |
| | sults and discussion. | |
| | onclusions | |
| | ferences | |
| CHAPTER 4: SU | MMARY AND FUTURE OUTLOOK | 92 |
| APPENDIX A· N | MATLAB CODE FOR ONE DIMENSIONAL FILM-MODEL IN N ₂ | |
| | TURATED CONDITIONS | 96 |
| APPENDIX B. W | MATLAB CODE FOR ONE-DIMENSIONAL FILM MODEL IN THE | |
| | ESENCE OF AIR AND O ₂ | 99 |
| ADDENING C. D | NPUT FILE FOR THE BP PROJECT N2(IN) FUNCTION (FOR RP A | |
| | EDIATED SYSTEM) | 104 |

LIST OF TABLES

| Table 2.1: | Redox polymer properties | 47 |
|------------|---|----|
| Table 3.1: | (a) Redox polymer properties. (b) Extracted kinetic parameters of the polymer-GOx films | |
| Table 3.2: | Parameters and nominal values used in the model | 81 |

LIST OF FIGURES

| Figure 1.1: | Schematic representation of a fuel cell. (For interpretation of references to color in this and all other images, the reader is referred to the electronic version of this thesis) |
|-------------|---|
| Figure 1.2: | Illustration of mechanisms for electron transfer from an electrode surface to an enzyme. (a) Direct electron transfer (DET). (b) Mediated electron transfer (MET) where the electron is carried by a redox-active mediator capable of communication with both the enzyme active site and the electrodes |
| Figure 1.3: | Potential schematic of a glucose-oxygen biofuel cell. The potentials are specified versus standard hydrogen electrode (SHE) |
| Figure 1.4: | (a) Graph of second order rate constant between reduced GOx and diffusive osmium complexes of varying potentials. (b) Graph of bimolecular rate constant for laccase-mediator (k_{cat}/K_m) and laccase-oxygen (k_{cat}/K_s) reaction for different redox polymers with varying potentials |
| Figure 1.5: | General structure of the osmium based redox polymers elucidating the role of the chelated ligands in governing redox potential of the mediator |
| Figure 1.6: | Ligand electrochemical parameter series for Os(III)/Os(II) couple in water. Square and circle markers represent the literature and predicted redox potential values of the osmium based redox polymers |
| Figure 1.7: | Structure of the GOx dimer <i>from Aspergillus</i> niger. Two FAD active sites are shown as red spheres. Figure generated from its crystal structure using PyMol24 |
| Figure 2.1: | Structure of synthesized redox mediators. A - poly(N -vinylimidazole[Os(2,2'-bipyridine) $_2$ Cl] $^{+/2+}$) , B - poly(N -vinylimidazole[Os(4,4'-dimethyl-2,2'-bipyridine) $_2$ Cl] $^{+/2+}$) |
| | Cyclic voltammograms (CVs) of GOx enzyme electrodes mediated by (a) RP A and (b) RP B in the presence of N ₂ , Air and O ₂ saturated conditions. Experiments were conducted in the 245 mM phosphate buffer (No NaCl), pH 7, 38 °C, 50 mV/s scan rate. Redox hydrogel composition was 59.5 % redox polymer, 39.5 % GOx and 1 % cross linker by mass with a total material loading of 0.726 mg/cm ² 50 |
| Figure 2.3: | Anode performance of the GOx electrodes in the presence of N ₂ , Air and O ₂ . Polarization curves of (a) RP A and (b) RP B mediated GOx electrodes. Experiments conducted in the 38 °C, 245 mM phosphate buffer (No NaCl), pH 7 containing 50 mM glucose substrate at 1000 rpm rotation. Scan rate 1 mV/s. Total |

| | material loading of 0.726 mg/cm ² with same composition as mentioned in Figure 2.2 |
|-------------|--|
| Figure 2.4: | Substrate dependence curves of (a) RP A and (b) RP B mediated GOx electrodes. Electrodes were poised at 0.6 V re:SHE and rotated at 1000 rpm. Other experimental conditions are same as mentioned in Figure 2.2 |
| Figure 2.5: | (a) Scan rate dependence of redox polymer A and B as a Randles-Sevcik plot. Fitted line vanishes to the origin, indicating semi-infinite diffusion. (b) Apparent e diffusivity (D_m) of mediators as a function of oxygen fraction. Experimental conditions are same as mentioned in Figure 2.2 |
| Figure 2.6: | AFM image showing the cross section of RP A-GOx film. Material loading was 0.726 mg/cm ² with 59.5 % redox polymer, 39.5 % GOx and 1 % cross linker by weight |
| Figure 2.7: | Glucose oxidation stability of the GOx electrodes in the chronoamperometry test mediated by (a) RP A and (b) RP B poised at 0.6 V SHE. Experiments were conducted under N ₂ , Air and O ₂ in 245 mM, pH 7 phosphate buffer (No NaCl) with 50 mM glucose at 38 $^{\circ}$ C, 1000 rpm. |
| Figure 3.1: | (a) Schematic representation of the immobilized redox polymer mediated enzymer electrode showing the processes considered in the model. (b) Sample concentration profiles for the one-dimensional film model. Diffuse layer thickness for glucose substrate is shown as $\delta_{I}.[S]_{\infty}$ and $[O_2]_{\infty}$ are the bulk concentration of glucose substrate and oxygen in the electrolyte. [S] and $[O_2]$ are the glucose and oxygen concentration in the film respectively. M_{ox} and M_{red} represents the oxidized and reduced form of the mediators respectively. D_S , D_m and D_o represents the diffusivities of substrate, mediator and oxygen respectively. |
| Figure 3.2: | Comparison of experimental data to the numerical prediction. Kinetic parameters used in the fitted curve accounts for the mass transfer correction of glucose and oxygen at the film-solution interface. (a) and (c) are the plateau current density for polymer A and B mediated GOx electrodes for varying glucose concentration under N ₂ , Air and O ₂ . (c) and (d) are the ohmic resistance corrected polarization curves or polymer A and B in 50 mM glucose solution, 250 mM PBS buffer (pH 7, 38 °C). Dashed lines in all graphs indicate numerical model results simultaneously fitted to the glucose variation and polarization curves. |
| Figure 3.3: | Simulated concentration and reaction rate profiles within the electrode film for A mediated GOx electrode in the presence of (a) N_2 (b) Air and (c) O_2 . Simulation parameters are taken from the Table 3.1 and 3.2. R/R_{max} represents the ratio of mediator reaction rate to its maximum value |

Chapter 1: Introduction

Fuel cell background

The increasing difficulty of contemporary energy supplies and associated problems of pollution and global warming are a major impetus for research into alternative renewable energy technologies. Fuel cells, as an efficient chemical energy conversion technology and clean energy carrier have a great potential to quench the insatiable global energy demand. William R. Grove and C.F. Schoenbein identified fuel cell technology in 1839 and it has transformed into a huge area of research in the modern era.

As shown in Figure 1.1, fuel cells are the electrochemical devices that convert chemical energy into electrical energy. They can be related to batteries in having anodes and cathodes, but unlike batteries, a constant supply of fuel (glucose, methanol, H_2 etc.) at the anode and oxidant (O_2 or air) at the cathode is required for a continuous operation. Ions generated during oxidation and reduction are transported from one electrode to the other through ionically conductive but electronically insulating electrolyte.³

Conventional fuel cells are based on polymeric electrolyte, alkaline, molten carbonate or phosphoric acid and ion-conductive oxide that are used mainly for stationary (on-site power generation) and portable applications (motor vehicle).⁴ Each type of fuel cell has its own advantages and disadvantages. Alkaline fuel cells allow the use of non-precious metal catalysts but suffer from electrolyte degradation due to CO₂ contamination from air. Molten carbonate

fuel cells can tolerate high concentration of carbon monoxide in fuel streams but suffers from slow start-up due to high temperature (~650 °C) and sealing problems. Solid oxide fuel cells offer high performance but high operating temperature (~600-1000 °C), precluding rapid startup and demanding compatibility between materials in terms of thermal expansion. ⁴ The wellresearched polymer electrolyte membrane fuel cell (PEMFC)^{5,6} gains advantage over other fuel cell systems due to its low-temperature operation (~ 60-140 °C), high power density, fast startup and system robustness. Numerous efforts have been made to reduce the use of platinum and to develop non-precious metal catalysts. ⁷⁻⁹ However, activity and stability issues present significant challenges for state-of-the-art non-precious metal catalysts in practical PEMFC applications. This has motivated research into other categories of power generating devices, which could answer the challenges associated with the contemporary fuel cell technologies. Bio fuel cells are be a promising candidate due to their ability to oxidize high molecular weight fuels, leading to high theoretical energy density, and can operate at room temperature and neutral pH. 10

Biofuel cells

The notion of a biofuel cell was recognized in the early 19th century when M.C. Potter observed the liberation of electrical energy due to disintegration of organic compounds by microorganisms.¹¹ The first working biofuel cell, based on the glucose-glucose oxidase system using microbes, was reported by Davis and Yarborough in 1962.¹² Biofuel cell research

escalated in the 1990s due to emergence of advanced electrode designs and increasing demand from applications requiring small energy generating sources. 10,13-16

Compared to conventional fuel cell technology, commercial development of bio fuel cells are still in the fundamental research stage because of their low stability and power output, but they have successfully spread their wings in the area of bioelectronics like biosensors, ^{10,17,18} portable electronic and implantable devices, ^{10,19,20} music players, ²¹ by taking an advantage of inherent biocatalytic properties of enzymes like low temperature, mild pH operation, specificity towards its substrates and low cost. They also possesses huge potential to make their way into medium-scale electronic devices like cell phones and laptops because of the high theoretical energy density of biofuel such as methanol (1000-3200 W h kg⁻¹).²³ as compared to conventional Li⁺ storage material in Li-ion batteries (100-250 W h kg⁻¹).²³

From the several classes of biofuel cells, three main categories can be distinguished depending upon their working mechanism and type of biochemical species used to produce the electric power. Firstly, the enzymatic fuel cells ¹⁰ (EFCs) which utilizes enzymes as renewable biocatalysts that convert alternative fuels like sugars, methanol and higher alcohols to electric power. In contrast, microbial fuel cells ²⁴ (MFCs), utilize microorganisms rather than enzymes for energy conversion. Finally, hybrid biofuel cells, ¹³ which can utilize photochemical and biological systems for the generation of an electric power.

MFCs use entire microorganisms as small reactors that eliminate the need for isolation of a particular enzyme. Though MFCs offer longer lifetimes²⁵ as compared to EFCs, electron transfer to an electrode can be significantly hindered,¹⁹ leading to small power densities²⁶ and lower volumetric efficiency¹⁶ resulting from the usage of entire microbe as opposed to an isolated enzyme in the case of an EFCs system.

Enzymatic fuel cells (EFCs)

Composed of high molecular weight protein structure assembled around the catalytically reactive atoms, enzymes accelerate the rate of specific chemical reactions at mild temperature and physiological conditions to yield variety of species. Enzymes may be purified from animal tissues, plants and microbes by taking advantage of specific enzyme properties. Enzymes gain advantage over precious metal catalysts like platinum and palladium in terms of the selectivity towards its substrate, cost and catalyzing restricted number of reactions per type. Out of six major classes of enzymes, oxidoreductase enzymes (redox enzymes) catalyze electron-transfer reactions, making them viable for use as electrocatalysts, provided that efficient electrical connection is made between an enzyme and the electronically conductive electrode.

As opposed to metallic catalysts, enzyme active centers are often buried deep in the polypeptide structure, which necessitates efficient electrical contact. This can be achieved via two ways depending upon the location of an enzyme active site. Firstly, enzymes such as laccase and peroxidases, in which the redox active centers are located on the surface of a protein shell, can undergo direct electron transfer (DET) with the adjacent electrode. ^{10,29,30} Secondly,

enzymes like glucose oxidase (GOx), with active centers deeply buried in their polypeptide shell shows poor DET with the current collector and require the use of small redox molecules called mediators to shuttle electrons from the electrode, known as a mediated electron transfer (MET). ^{10,30} Enzymes like glucose dehydrogenase (GDH) and alcohol dehydrogenase can also be categorized under MET mechanism due to diffusive action of nicotinamide adenine dinucleotide (NADH/NAD⁺) redox center, which is often loosely bound to the protein structure. ³⁰ Figure 1.2 illustrates these two approaches for the electrical communication of laccase enzyme to the electrode. ³¹

Mediated electron transfer

The main purpose of mediators is to increase the rate of electron transfer between enzyme active site by eliminating orientation dependence and by facilitating electron transfer over 10-100 nm length scales, enabling immobilization of enzymes far from the electrode surface.

Mediators and enzymes may coexist in solution, only the mediator may be present in a solution with the enzyme immobilized on the electrode surface, 32 or both mediators and the enzymes may be entrapped on the electrode surface using materials such as Nafion $^{\circledR}$, chitosan or silica gel matrix. $^{33-35}$ Mediators or enzymes can be immobilized using crosslinkers, 36,37 electrodeposition 38,39 or via layer-by layer mechanisms 40 . Freely diffusing mediators achieve electron transport by translation back and forth from the electrode whereas immobilized mediators undergo electron self-exchange with neighboring mediator moieties. Both of these operations can be characterized via apparent electron diffusion coefficient (D_{app}). 10,41,42 For the

diffusional mediators such Ferrocenes and Ferri/ferrocynaide ($K_3[Fe(CN)_6]$) D_{app} values are in the order of 10^{-5} cm² s⁻¹ as compared to 10^{-9} cm² s⁻¹ for the immobilized mediators attributed to restricted motion of the confined species.

Quantitative performance of biofuel cells

As an energy-producing device, a biofuel cell must generate high current density (i) and high cell potential (E_{cell}) to yield the maximum power density (P) per geometric electrode area.

$$P = iE_{cell}$$
 [1.1]

Where, $E_{cell} = E_{cathode} - E_{anode}$. Figure 1.3 shows the schematic of mediated enzyme design found in a glucose/O₂ biofuel cell operating at pH $7.^{10,43}$ Enzyme catalyzed anodic and cathodic reactions are shown below (Equation 1.2 and 1.3).

Anodic reaction:
$$C_6H_{12}O_6 \xrightarrow{\text{glucose oxidase}} C_6H_{10}O_6 + 2H^+ + 2e^-$$
 (gluconolactone) [1.2]

Cathodic reaction:
$$\frac{1}{2}O_2 + 2H^+ + 2e^- \xrightarrow{\text{laccase}} H_2O$$
 [1.3]

Overall reaction:
$$C_6H_{12}O_6 + \frac{1}{2}O_2 \longrightarrow C_6H_{10}O_6 + H_2O$$
 [1.4] (glucose) (gluconolactone)

Generally, the power output of EFCs depends on the difference in redox potential of the two mediators employed on each biocatalytic electrode (Equation 1.5). ¹⁰

$$E_{fuel}^{0} < E_{a-enzyme}^{0} < E_{a-mediator}^{0} \parallel \text{Power} \parallel E_{c-mediator}^{0} < E_{c-enzyme}^{0} < E_{O_{2}}^{0} \qquad [1.5]$$

where E_{fuel}^0 represents the redox potential of the fuel such as glucose. $E_{a-enzyme}^0$ and $E^0_{c-enzyme}$ denotes the redox potentials of the employed enzymes on anode and cathode respectively. $E^0_{a-mediator}$ and $E^0_{c-mediator}$ represents the redox potential of the chosen mediators for anode and cathode side respectively. Therefore, in order to extract the maximum power from the mediated EFCs, selection of the appropriate mediators are limited to those with redox potentials close to that of the chosen enzyme. For example, the selection of an anodic mediator having redox potential very close to that of an anode enzyme will increase the cell potential. However, this approach leads to reduction in the catalytic rates governed by the enzyme-mediator overpotential or the electron transfer driving force, $(\Delta E_T = E_{mediator}^0 - E_{enzyme}^0)$, which influences the electron transfer efficiency.³⁶ The ramifications of ΔE_T on electron transfer kinetics have been evaluated for various freely diffusive mediated systems. 44-46 One of such system, in which Zakeeruddin and co-workers synthesized a series of iron, osmium and ruthenium based diffusive complexes in the context of biosensor applications and from the bimolecular rate constant of GOx-mediator reaction (Figure 1.4a), it was found that the efficient mediation window (ΔE_T) for GOx is between 0.14 to 0.54 V relative to standard hydrogen electrode (SHE) for tris-(4,4'-substituted-2,2'-bipyridine) complexes of osmium.⁴⁷ Recently, Gallaway et al.,³⁶ extended this inquiry for the oxygen cathodes catalyzed by laccase, in which both the biocatalyst and mediator were immobilized where the optimum mediator potential based on the bimolecular rate constant between laccase

and mediator reaction (Figure 1.4b) was found to be 0.17 V/SHE below the laccase enzyme potential with an anode poised at 0 V/SHE. In an MET system, electrode potential controls the relative concentrations of the mediator redox states at the electrode surface, as governed by the Nernst equation (Equation 1.6), which correlates the chemical activity and electric potential of an electrochemical cell.

$$E = E^{0} + \frac{RT}{nF} \ln \frac{C_{O}^{*}}{C_{R}^{*}}$$
 [1.6]

where, E is the electrode potential, E^0 is the redox potential of the mediator which is defined as the oxidation/reduction potential measured under standard conditions, C_O^* and C_R^* are the respective bulk concentrations of the oxidized and reduced mediator species at a given electrode potential. In any electrochemical cell, three types of overpotential exists: 10,19,48 1) Activation overpotential which stem from the finite rate of reaction at the electrode surfaces. 2) Ohmic overpotential, which arises due to resistances associated with the electrolyte, ion-conducting membrane and electrical connections. 3) Concentration overpotential attributed to the mass transport limitations at high current regime in the electrode polarization curves. Though incorporation of the mediator introduces an additional overpotential-that between enzyme active center and the mediator, appropriate mediator selection increases the reaction rate by interacting with the electrode at a rate faster than the DET system, which requires specific orientation of enzyme towards the electrode.

Even though the first enzyme-based biofuel cell was reported in 1964 which used GOx as an anodic catalyst and glucose as the fuel, ⁴⁹ use of mediator to facilitate the electron transfer in

EFCs was recognized in 1981. Phenazine methosulphate and phenazine ethosulphate were used as a mediators but instability of these salts at high pH made them unsuitable for further use in the biofuel cell. This encouraged the use of N.N.N'.N'-tetramethyl-4-phenylenediamine (TMPD) as a mediator in quinoprotein methanol dehydrogenase based biofuel cell with platinum electrodes that produced 2 µW cm⁻² power.⁵¹ In the same period, Kulys et al., studied tetracyanoquinodimethane mediator based glucose oxidizing GOx electrode for various enzyme concentrations and electrode potentials. ⁵² In 1984, Cass et al., ⁵³ used various ferrocene derivatives with range of redox potentials (0.35 V to 0.65 V/SHE), as oxidants for GOx in the context of biosensors for amperometric determination of glucose. Since then, electrocatalytic enzyme mediation has been demonstrated using quinones. 54,55 conducting salts such as Tetrathiafulvalene (TTF) and Tetrathiafulvalene-tetracynoquinodimethane (TTF-TCNQ),⁵⁶ K₃[Fe(CN)₆], Methylene blue, ⁵⁷ ABTS, ⁵⁸ Methyl viologen, ⁵⁹ Methylene green, ⁶⁰ complexes of iron, ruthenium, cobalt, osmium and many other compounds. 45,47

Osmium redox polymer mediation

Albeit vast literature on various formats of MET based biofuel cells, the most successful designs are based on the osmium based redox polymer mediators due to their stability, fast redox kinetics, rich organometallic chemistry and broad range of oxidation-reduction potentials. ^{21,36,61} Redox polymers are electrochemically active macromolecules, in which the redox active moieties are incorporated into the polymer backbones like polyvinylimidazole (PVI), polyvinylpyridine (PVP), poly(allylamine), polypyrrole, poly(ethylenimine) (PEI), either by

electropolymerization or at the complexation stage of the redox polymer synthesis. $^{38,62-67}$ "Redox hydrogel", is a term often used for such water-soluble polymers, which swell upon cross-linking to form a substrate-permeable, electron-conductive redox-active network. 36,41 Heller et at. 68 employed such osmium-based redox polymer mediators for immobilization and mediation of GOx for amperometric detection of glucose. Since then variety of osmium based mediated systems have been developed and characterized depending on the desired applications. 36,69,70 However, the mobility of the redox pendants becomes limited when such polymers are immobilized on the electrode surface, such that electron transport take place by hopping between neighboring active centers as described through an expression developed by Blauch and Savént which relates the mediator diffusivity, D_{app} to the redox site concentration, c_m in bounded-diffusion systems:

$$D_{app} = \frac{1}{6} k_{ex} (\delta^2 + 3\lambda^2) c_m$$
 [1.7]

where k_{ex} is the electron self-exchange rate constant, δ is the electron tunneling distance, λ is the range of bounded motion for the redox centers.

The redox potential is a key parameter that controls the overall performance of mediated enzymatic fuel cells. Redox potential of the osmium-based complexes can be tailored by altering the ligands attached to the Os active site. 63,72 Utilizing electron-withdrawing (terpyridine, dipyridyl, PVP) or electron-donor (chloride ion) characteristics of the attached ligand, redox potential of the Os center can be effectively tuned to the chosen enzyme. As shown in Figure 1.5,

co-ordination number of six and attachment of two similar bidentate ligands (2,2'-Bipyridine, 4,4'-Dimethyl-2,2'-Bipyridine or 4,4'-Dimethoxy-2,2'-Bipyridine) and chloride to the Os center gives low potential mono-valent redox sites, whereas mixed ligands (2,2':6',6"-terpyridine and 2,2'-Bipyridyl or 4,4'-Dimethyl-2,2'-dipyridyl and 2,2':6'2"-Terpyridine) with no chloride ligand generates high potential bi-valent redox active moieties. 31,36,63,73,74 As shown in Figure 1.6, hypothetical redox potential of such organometallic complexes can be predicted using "Lever analysis", 36,74 based on the following expression, which was obtained by fitting a straight line through literature redox potential value data:

$$E_{pred}^{0} / V = 0.711 \sum a_i E_L(L_i) - 0.236$$
 [1.8]

where, E_{pred}^0 is the theoretical redox potential of the mediator, E_L is the ligand parameter for a particular ligand L_i , a_i is the degree of chelation of the ligand. For example, the redox potential of PVI- $[Os(2,2'-bipyridine)_2Cl]^{+/2+}$ redox polymer mediator can be speculated as follows: E_L of PVI, 2,2'-bipyridine and Cl^- are 0.181, 0.26 and -0.24 respectively. A a_i for PVI, 2,2'-bipyridine and cl^- are 1, 2 and 1 respectively. Substituting these values in equation 1.8 yields the hypothetical redox potential of 0.45 V/SHE. Similarly, the redox potential of the PVI- $[Os(4,4'-dimethyl-2,2'-bipyridine)_2Cl]^{+/2+}$ can be predicted as 0.33 V/SHE. General structures of the osmium-based mediators are shown in Figure 1.5.

Glucose oxidase enzyme for enzymatic fuel cell anodes

Enzymes used in the enzymatic biofuel cells or biosensors must have high activity toward a cheap and easily available fuel or commercially important analyte, high turnover number and high stability. Glucose oxidase (GOx) is one of the most widely used oxidoreductase enzymes for this purpose, catalyzing the oxidation of β -D-glucose to glucono- δ -lactone and hydrogen peroxide.⁷⁵ In 1928, Muller et al.⁷⁶ reported the activity of GOx in the extracts of Aspergillus *niger* and subsequently this enzyme has been isolated from this fungal mold and other sources like bacteria, algae, insects and citrus fruits. ⁷⁸⁻⁸¹ As shown in Figure 1.7, GOx is a dimeric flavoprotein, made up of two identical subunits of molecular weight of ~80000 Daltons each, and containing one molecule of noncovalently bound coenzyme flavin adenine dinucleotide (FAD/FADH₂), that undergoes two-electron, two-proton redox reaction. FAD is typically bound within the enzyme but it can be removed from the enzyme shell (apoenzyme) and covalently attached to a mediator species previously immobilized on the electrode surface. 82 The reversible potential of FAD/FADH₂ is -0.23 V/SHE at pH 7 and when immobilized in a GOx enzyme, it is -0.12 V/SHE. ^{30,83} In a GOx-catalyzed redox reaction, the substrate of GOx can be separated into two groups:⁸⁴ 1) Where FAD works as an initial electron acceptor and is reduced to $FADH_2$ in the reductive half reaction by oxidation of substrate like β -D-glucose which has the highest specificity towards GOx. 2) In the oxidative half reaction where, FADH2 is being oxidized by one (Ferri/ferrocyanide, ⁸⁵ Ferrocene salts ⁸⁶, Osmium redox polymers ⁶⁸) or two

electron acceptors (O_2 , ⁸⁷ Quinones ⁸⁵) out of which O_2 is the natural electron acceptor of GOx enzyme. Apart from its role in the biofuel cells and biosensors, GOx finds uses in food and beverage additives, wine production, gluconic acid production, oral hygiene and many more. ⁸¹

The minimum distance between the FAD site and the electrode-contacting periphery of GOx is more than 13 Å which is a major reason for poor DET of GOx due to increased electron tunneling distance with respect to the adjacent current collector. However, several cases of DET have been reported for the GOx enzyme, where it was immobilized either on a thiol-modified gold surface or on a nanotubes assembly 90,91 to increase the electron transfer rate from the FAD. Also, the catalytic current of 450 μ A cm⁻² have been observed via oxidation of glucose when GOx was immobilized with PEI on nanotubes-coated carbon paper. Recently, Mano *et al.*, 93 deglycosylated (removal of sugar residues) the GOx that produced highly DET active deglycosylated GOx enzyme (dGOx) capable of oxidizing the glucose on a glassy carbon electrode at an unusual potential of -0.29 V/SHE (redox potential of the GOx enzyme) with the production of 240 μ A cm⁻² of current density.

Heller and co-workers were the first to incorporate the GOx into cross-linked redox polymer film, using polyethylene glycol diglycidyl ether (PEGDGE) as a cross-linker and PVP-Os(bpy)₂Cl redox polymer for the context of amperometric biosensors producing ~0.5 mA cm⁻² of glucose oxidation current density.⁶⁸ Since then various osmium polymer derivative based enzymatic biofuel cells have been reported. EFCs with two 7 µm diameters 2 cm long carbon

fiber based micro enzyme electrode producing 137 μW cm⁻² have been demonstrated.⁹⁴ These electrodes were also implanted in a grape and the resulting cell exhibited power density of 240 μW cm⁻² at a cell potential of 0.52 V.⁹⁵ Another example in which the introduction of 13-atom long flexible spacer arm between polymer backbone and osmium pendent in the anodic polymer produced the power of 268 μW cm⁻² at 0.78 V in 15 mM glucose solution in combination with a laccase-based cathode. ⁹⁶ Willner and Katz ⁸² presented a different class of biofuel cell by noncompartmentalizing the glucose/ O_2 biofuel cell where active site of the anodic enzyme GOx was removed from the enzyme shell and covalently attached to pyrroloquinoline quinone (PQQ) species previously immobilized on a gold electrode, whereas on the cathode side immobilized cytochrome c was complexed with cytochrome oxidase and was subsequently cross-linked with glutaric dialdehyde. A cell comprising of these two electrodes generated maximum power density of 5 μ W cm⁻² at pH 7 in 1 mM glucose and air-saturated buffer at 0.04 V of cell potential.

Recently, a similar class of biofuel cell based on GOx and laccase was constructed with monoolein cubic phase as an immobilization matrix producing 7 µW cm⁻² of power density at 0.125 V potential output. Other examples of EFCs based on common enzymes for glucose oxidation like GDH and cellobiose dehydrogenase (CDH) can also be found in the literature. One noteworthy achievement was the biofuel cell developed by Kano and coworkers that produced maximum power density of 1.5 mW cm⁻² at 0.3 V. This was accomplished by using carbon fiber (CF) based bioanode made up of GDH, NADH and vitamin

K3 (as a mediator) combined with Bilirubin oxidase (BOD) and $K_3[Fe(CN)_6]$) mediated CF-biocathode separated by cellophane, which enabled the fabrication of passive-type biofuel cell with high output.²¹

In glucose/ O_2 based EFC, presence of O_2 affects the mediation efficiency by scavenging electrons from the reduced active site of GOx (Equation 1.9) and hence current at the electrode surface due to competing reaction of O_2 with mediator at the GOx-based anode, which lowers the overall performance of such biofuel cell. ^{99,100}

$$O_2 + E_{red} \rightarrow H_2 O_2 + E_{ox}$$
 [1.9]

Loss in performance can also be ascribed to the formation of hydrogen peroxide (H_2O_2) due to reaction between GOx enzyme and O_2 , which adversely affects the reduced active site (E_{red}) of GOx. This necessitates the extraction and comprehension of kinetic information of such immobilized redox polymer mediated electrodes for its use in GOx based EFC.

Overview of this work

The overall objective of this work is to quantify and elucidate the effect of oxygen on the catalytic performance of the osmium redox polymer mediated GOx electrodes from the experimental outcomes and extraction of the kinetic parameters via simulation using one-dimensional mathematical model, which incorporates the effect of oxygen.

Chapter 2 describes the synthesis of such redox polymer mediated GOx electrodes and their characterization in the presence of N_2 , air and O_2 saturated conditions.

Chapter 3 demonstrates the modeling of such enzymatic fuel cell electrode to obtain the kinetic parameters pertinent to the system in the absence and in the presence of oxygen. It is demonstrated that in the presence of oxygen, redox polymer competes for the electrons of the glucose at the active site of GOx, which is responsible for the reduction in performance of such GOx based redox polymer mediated electrodes in the presence of O_2 .

Chapter 4 summarizes this work and discusses about the future outlook.

FIGURES

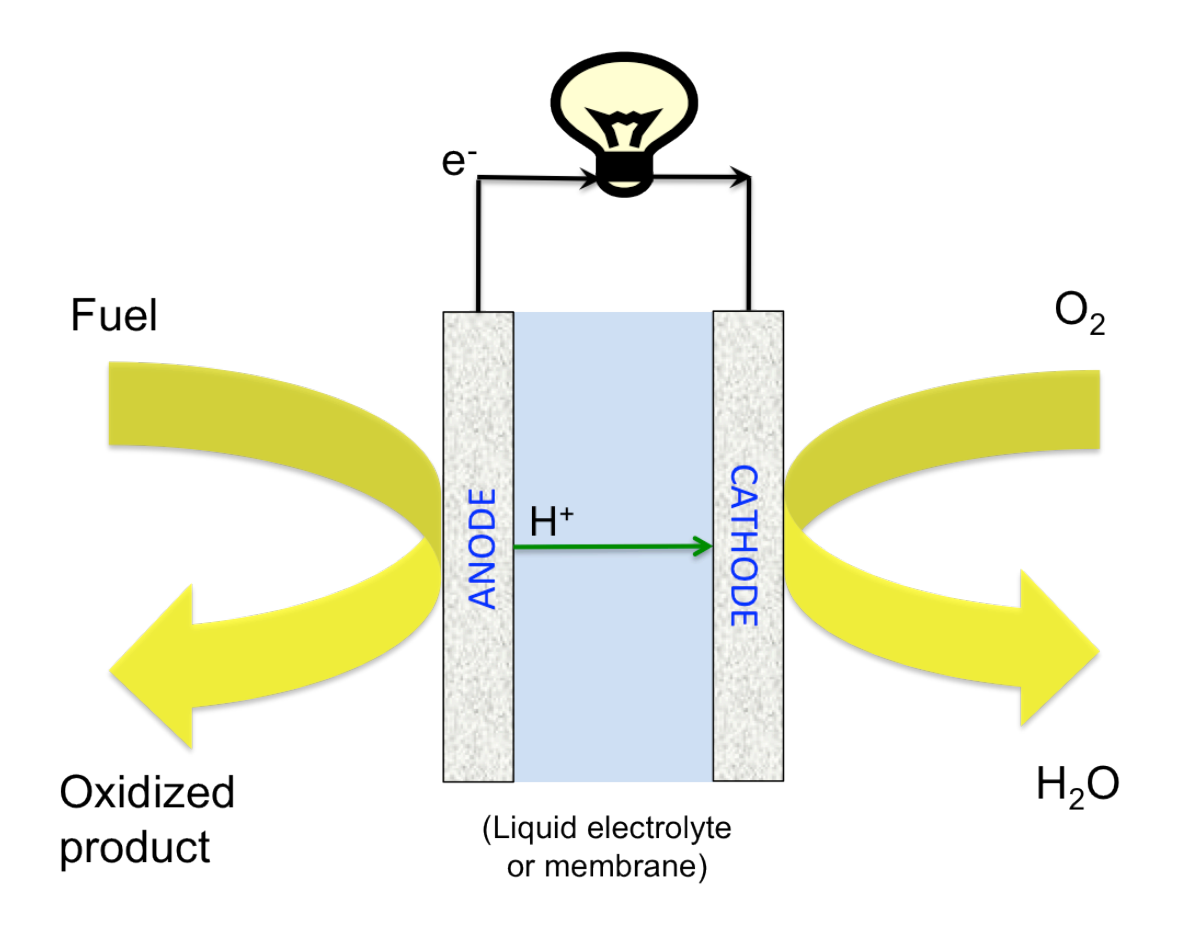


Figure 1.1: Schematic representation of a fuel cell. (For interpretation of references to color in this and all other images, the reader is referred to the electronic version of this thesis)

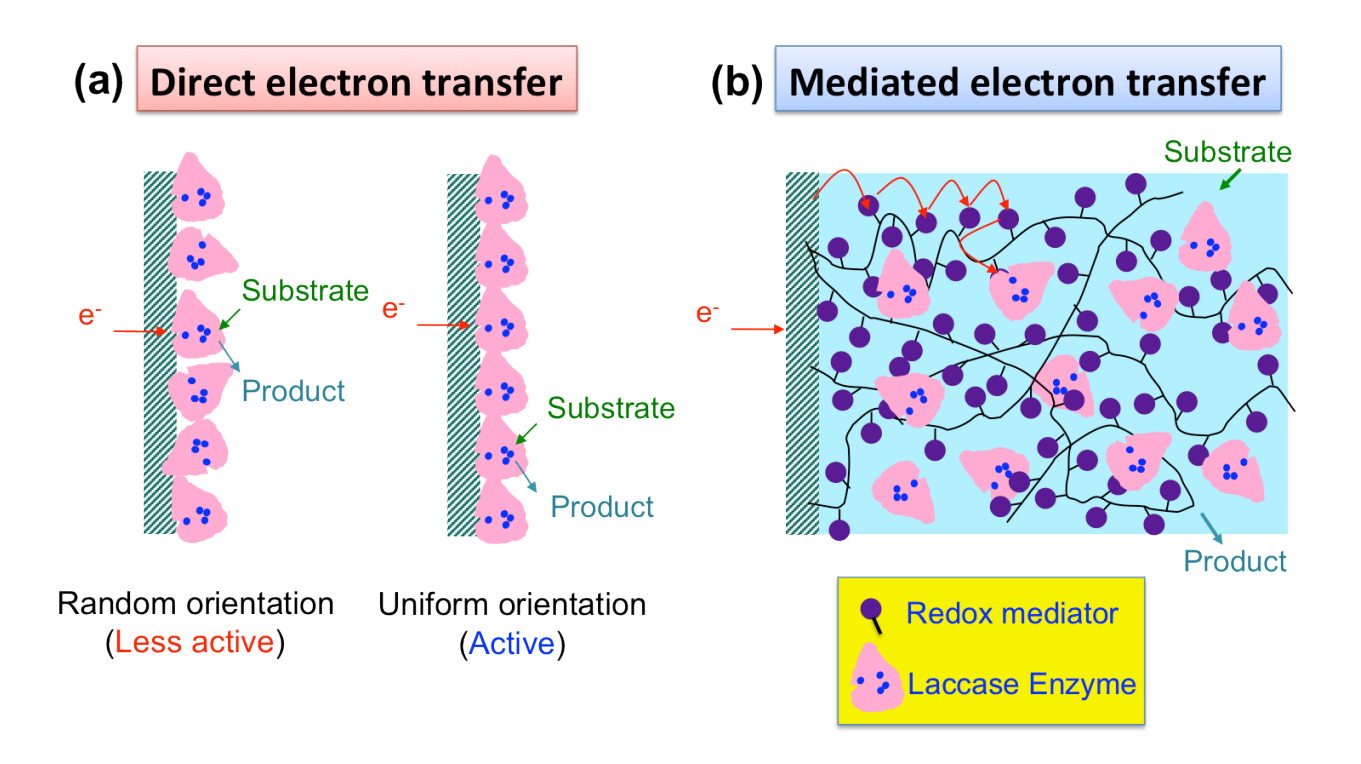


Figure 1.2: Illustration of mechanisms for electron transfer from an electrode surface to an enzyme. (a) Direct electron transfer (DET). (b) Mediated electron transfer (MET) where the electron is carried by a redox-active mediator capable of communication with both the enzyme active site and the electrodes.

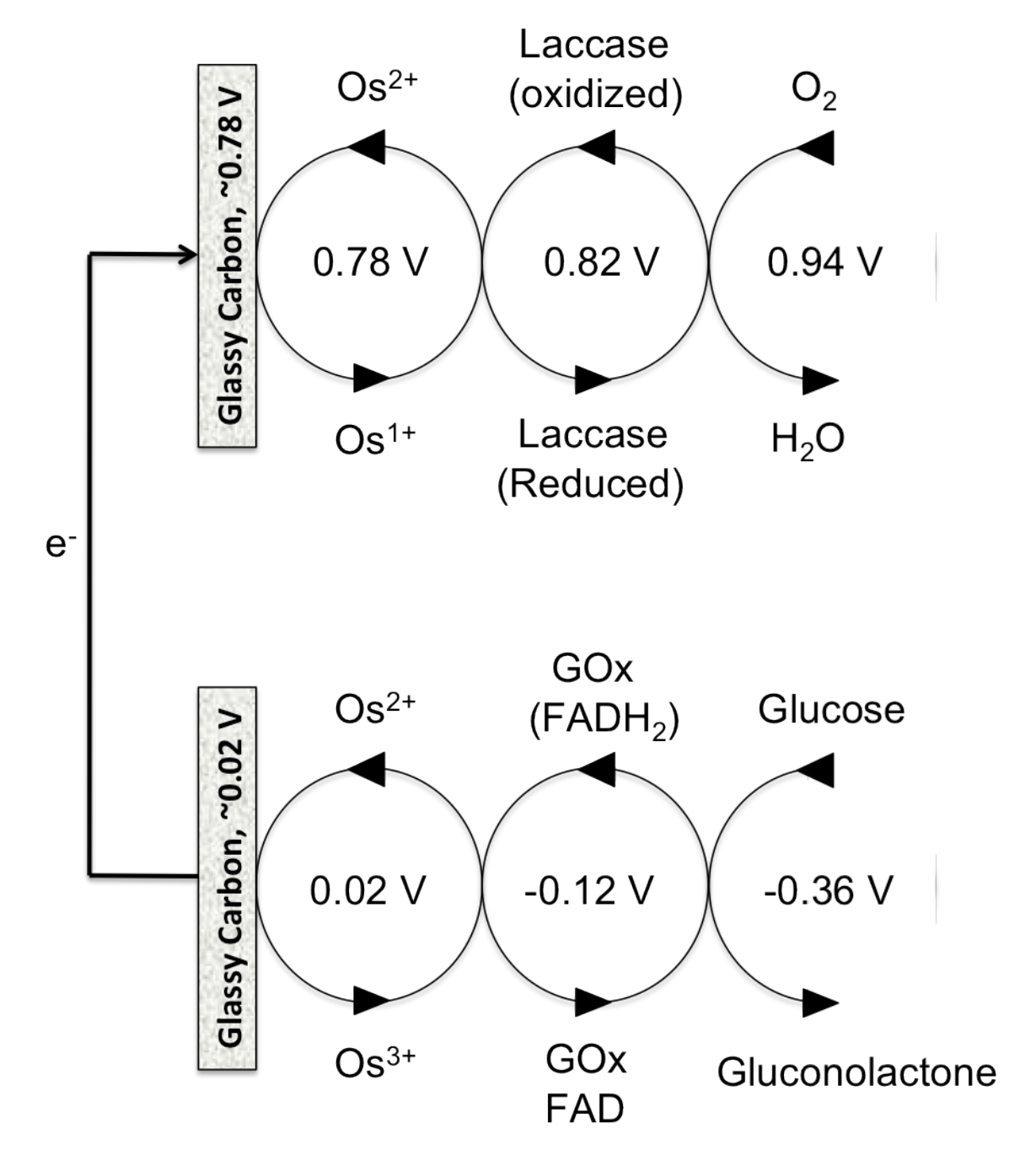


Figure 1.3: Potential schematic of a glucose-oxygen biofuel cell. The potentials are specified versus standard hydrogen electrode (SHE). ¹⁰

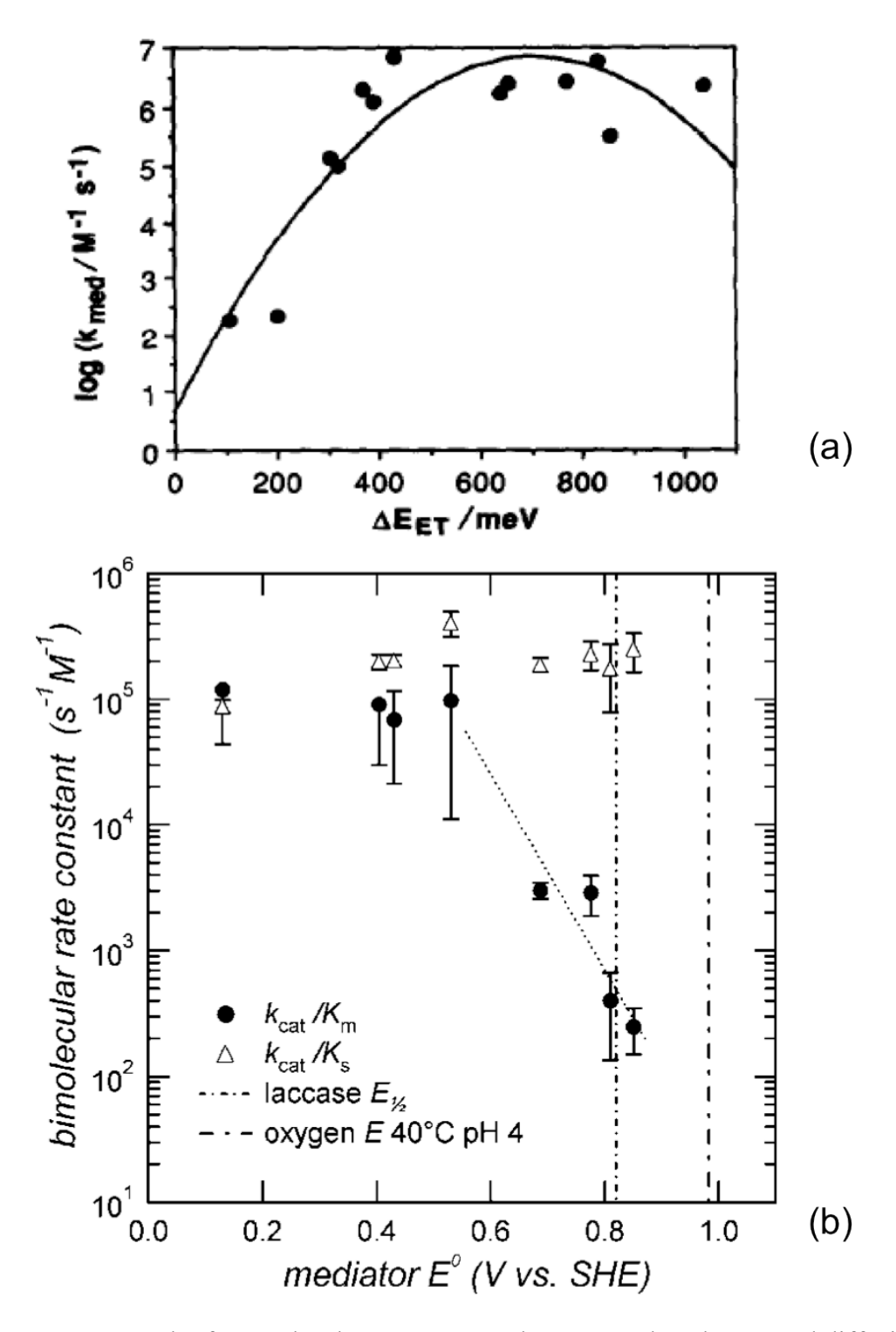


Figure 1.4: (a) Graph of second order rate constant between reduced GOx and diffusive osmium complexes of varying potentials. ⁴⁷ (b) Graph of bimolecular rate constant for laccase-mediator (k_{cat}/K_m) and laccase-oxygen (k_{cat}/K_s) reaction for different redox polymers with varying potentials. ³⁶

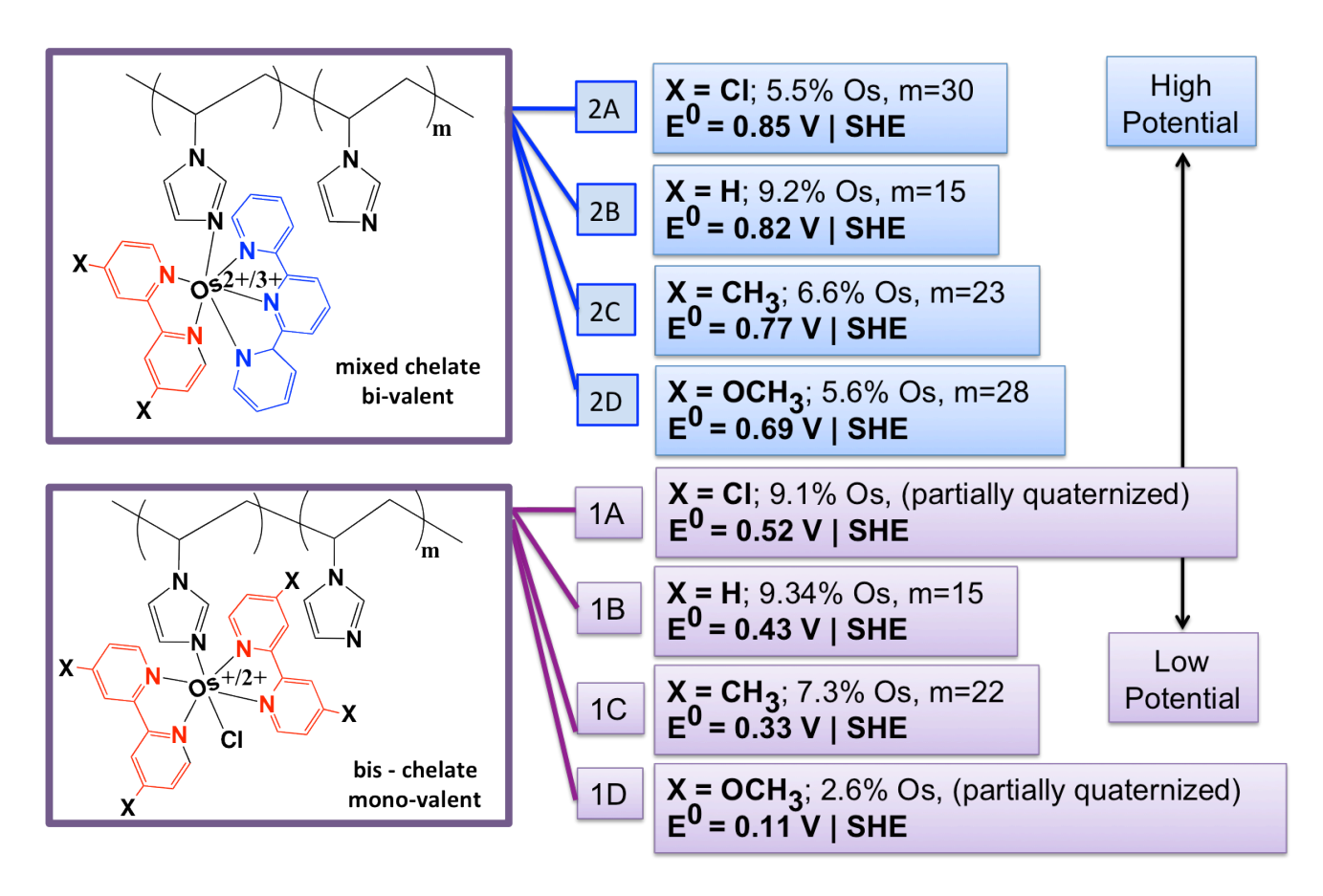


Figure 1.5: General structure of the osmium based redox polymers elucidating the role of the chelated ligands in governing redox potential of the mediator. ³⁴

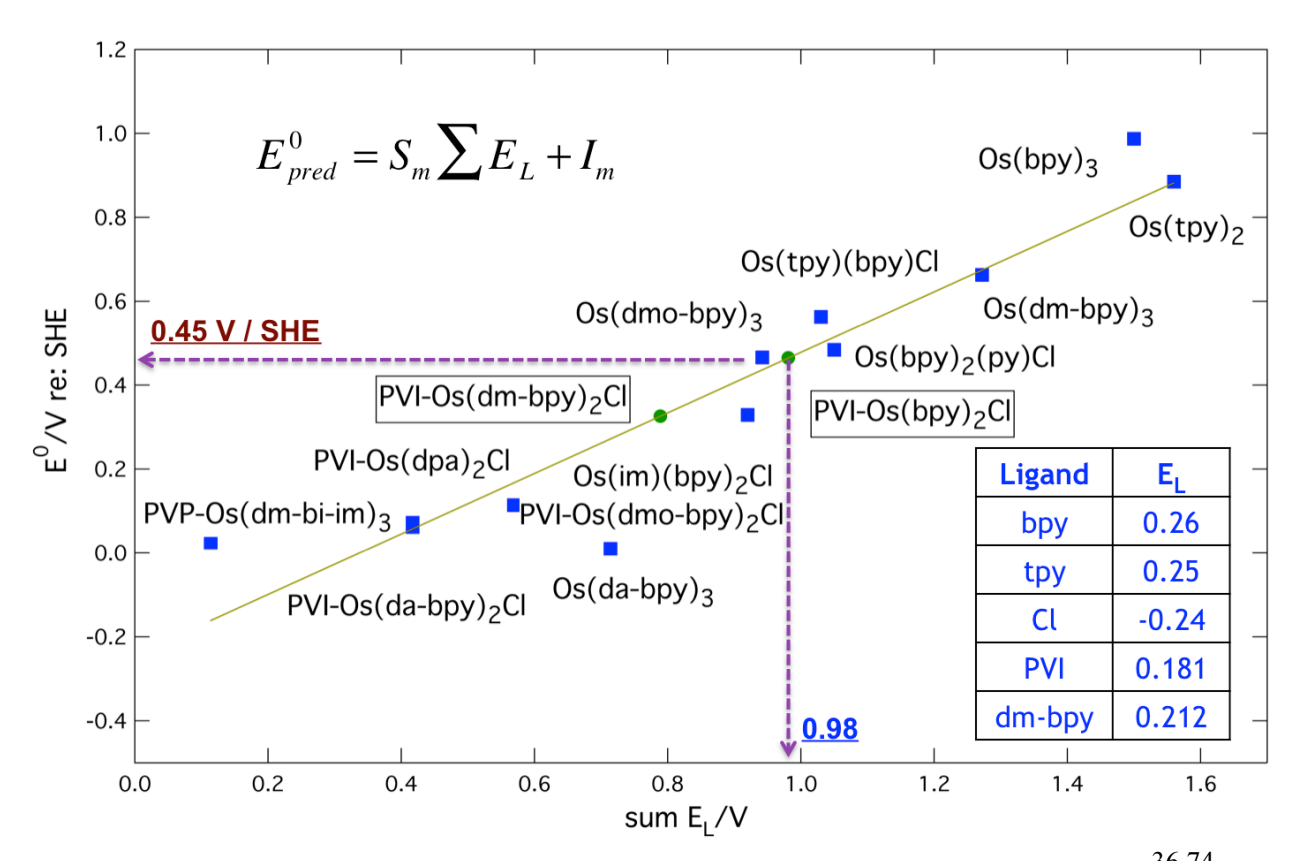


Figure 1.6: Ligand electrochemical parameter series for Os(III)/Os(II) couple in water. ^{36,74} Square and circle markers represent the literature and predicted redox potential values of the osmium based redox polymers.

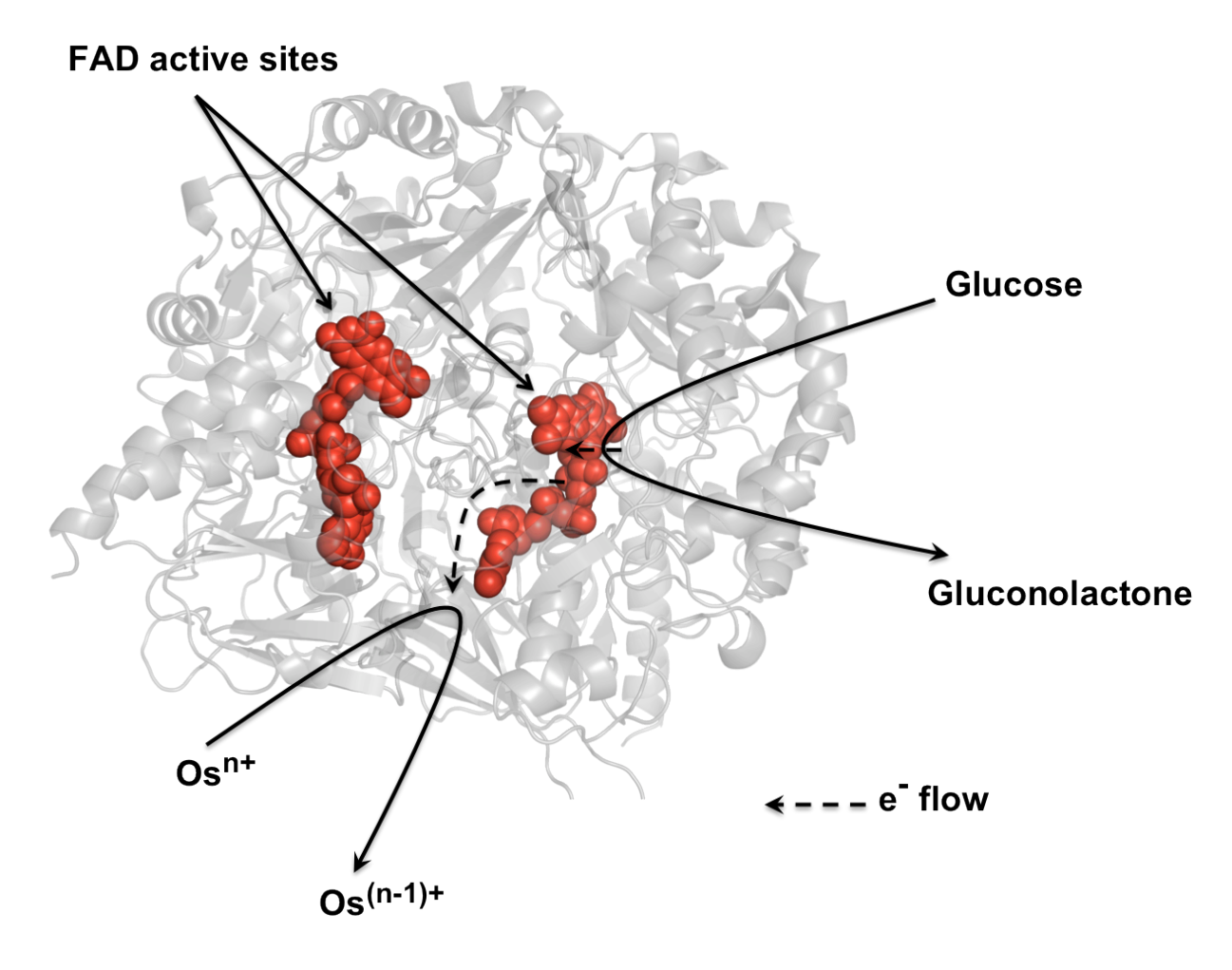


Figure 1.7: Structure of the GOx dimer *from Aspergillus* niger. Two FAD active sites are shown as red spheres. Figure generated from its crystal structure using PyMol.

REFERENCES

References

- 1. W. R. Grove, "On Voltaic Series and the Combination of Gases by Platinum," *Philosophical Magazine and Journal of Science*, **14**(127) (1839).
- 2. C. F. Schoenbein, *Philosophical Magazine Series*, 43-45 (1839).
- 3. K. A. F. a. U. S. L. Carrette, "Fuel Cells Fundamentals and Applications," *Fuel Cells*, **1**(1), 5-39 (2001).
- 4. L. Carrette, K. A. Friedrich and U. Stimming, "Fuel cells: Principles, types, fuels, and applications," *Chemphyschem,* **1**(4), 162-193 (2000).
- 5. P. Costamagna and S. Srinivasan, "Quantum jumps in the PEMFC science and technology from the 1960s to the year 2000 Part I. Fundamental scientific aspects," *Journal of Power Sources*, **102**(1-2), 242-252 (2001).
- 6. V. Mehta and J. S. Cooper, "Review and analysis of PEM fuel cell design and manufacturing," *Journal of Power Sources*, **114**(1), 32-53 (2003).
- 7. R. Bashyam and P. Zelenay, "A class of non-precious metal composite catalysts for fuel cells," *Nature*, **443**(7107), 63-66 (2006).
- 8. R. Kothandaraman, V. Nallathambi, K. Artyushkova and S. C. Barton, "Non-precious oxygen reduction catalysts prepared by high-pressure pyrolysis for low-temperature fuel cells," *Applied Catalysis B-Environmental*, **92**(1-2), 209-216 (2009).
- 9. F. Charreteur, F. Jaouen, S. Ruggeri and J. P. Dodelet, "Fe/N/C non-precious catalysts for PEM fuel cells: Influence of the structural parameters of pristine commercial carbon blacks on their activity for oxygen reduction," *Electrochimica Acta*, **53**(6), 2925-2938 (2008).
- 10. S. C. Barton, J. Gallaway and P. Atanassov, "Enzymatic biofuel cells for Implantable and microscale devices," *Chemical Reviews*, **104**(10), 4867-4886 (2004).
- 11. M. C. Potter, "Electrical effects accompanying the decomposition of organic compounds," *Proceedings of the Royal Society of London Series B-Containing Papers of a Biological Character*, **84**(571), 260-276 (1911).
- 12. J. B. Davis and H. F. Yarbrough, "Preliminary Experiments on a Microbial Fuel Cell," *Science*, **137**(3530), 615-& (1962).
- 13. F. Davis and S. P. J. Higson, "Biofuel cells Recent advances and applications," *Biosensors & Bioelectronics*, **22**(7), 1224-1235 (2007).

- 14. A. K. Sarma, P. Vatsyayan, P. Goswami and S. D. Minteer, "Recent advances in material science for developing enzyme electrodes," *Biosensors & Bioelectronics*, **24**(8), 2313-2322 (2009).
- 15. A. Heller, "Miniature biofuel cells," *Physical Chemistry Chemical Physics*, **6**(2), 209-216 (2004).
- 16. G. T. R. Palmore and G. M. Whitesides, "Microbial and Enzymatic Biofuel Cells," *Enzymatic Conversion of Biomass for Fuels Production*, **566**, 271-290 (1994).
- 17. A. Heller and B. Feldman, "Electrochemical glucose sensors and their applications in diabetes management," *Chemical Reviews*, **108**(7), 2482-2505 (2008).
- 18. R. L. Arechederra and S. D. Minteer, "Self-powered sensors," *Analytical and Bioanalytical Chemistry*, **400**(6), 1605-1611 (2011).
- 19. R. P. G. Tayhas, *Bioelectrochemistry: Fundamentals, Experimental Techniques and Applications* (ed. Bartlett, P. N.) (2008).
- 20. J. A. Cracknell, K. A. Vincent and F. A. Armstrong, "Enzymes as working or inspirational electrocatalysts for fuel cells and electrolysis," *Chemical Reviews*, **108**(7), 2439-2461 (2008).
- 21. H. Sakai, T. Nakagawa, Y. Tokita, T. Hatazawa, T. Ikeda, S. Tsujimura and K. Kano, "A high-power glucose/oxygen biofuel cell operating under quiescent conditions," *Energy & Environmental Science*, **2**(1), 133-138 (2009).
- 22. K. M. McGrath, G. K. S. Prakash and G. A. Olah, "Direct methanol fuel cells," *Journal of Industrial and Engineering Chemistry*, **10**(7), 1063-1080 (2004).
- J. M. Tarascon and M. Armand, "Issues and challenges facing rechargeable lithium batteries," *Nature*, **414**(6861), 359-367 (2001).
- 24. B. E. Logan, B. Hamelers, R. A. Rozendal, U. Schrorder, J. Keller, S. Freguia, P. Aelterman, W. Verstraete and K. Rabaey, "Microbial fuel cells: Methodology and technology," *Environmental Science & Technology*, **40**(17), 5181-5192 (2006).
- 25. G. C. Gil, I. S. Chang, B. H. Kim, M. Kim, J. K. Jang, H. S. Park and H. J. Kim, "Operational parameters affecting the performance of a mediator-less microbial fuel cell," *Biosensors & Bioelectronics*, **18**(4), 327-334 (2003).
- 26. H. Liu, S. A. Cheng and B. E. Logan, "Power generation in fed-batch microbial fuel cells as a function of ionic strength, temperature, and reactor configuration," *Environmental Science & Technology*, **39**(14), 5488-5493 (2005).

- 27. D. L. N. Albert L. Lehninger, Michael M. Cox, *Principles of biochemistry* (ed. Lehninger, A. L.) (2004).
- 28. A. Fersht, *Enzyme Structure and Mechanism* (San Francisco: W.H. Freeman, 1985).
- 29. A. L. Ghindilis, P. Atanasov and E. Wilkins, "Enzyme-catalyzed direct electron transfer: Fundamentals and analytical applications," *Electroanalysis*, **9**(9), 661-674 (1997).
- 30. S. C. Barton, "Enzyme catalysis in biological fuel cells" in Handbook of Fuel Cells Fundamentals, Technology and Applications (ed. Wolf Vielstich, H. Y., Hubert Andreas Gasteiger) (2009).
- 31. D. Chakraborty, *PhD Thesis, Enzyme Electrocatalysis in Mediated Bioelectrodes*, Michigan State University (2010).
- 32. G. T. R. Palmore and H. H. Kim, "Electro-enzymatic reduction of dioxygen to water in the cathode compartment of a biofuel cell," *Journal of Electroanalytical Chemistry*, **464**(1), 110-117 (1999).
- 33. S. Topcagic and S. D. Minteer, "Development of a membraneless ethanol/oxygen biofuel cell," *Electrochimica Acta*, **51**(11), 2168-2172 (2006).
- 34. M. J. Moehlenbrock and S. D. Minteer, "Extended lifetime biofuel cells," *Chemical Society Reviews*, **37**(6), 1188-1196 (2008).
- W. E. Farneth and M. B. D'Amore, "Encapsulated laccase electrodes for fuel cell cathodes," *Journal of Electroanalytical Chemistry*, **581**(2), 197-205 (2005).
- 36. J. W. Gallaway and S. A. C. Barton, "Kinetics of redox polymer-mediated enzyme electrodes," *Journal of the American Chemical Society*, **130**(26), 8527-8536 (2008).
- 37. T. Delumleywoodyear, P. Rocca, J. Lindsay, Y. Dror, A. Freeman and A. A. Heller, "Polyacrylamide-Based Redox Polymer for Connecting Redox Centers of Enzymes to Electrodes," *Analytical Chemistry*, **67**(8), 1332-1338 (1995).
- 38. Z. Q. Gao, G. Binyamin, H. H. Kim, S. C. Barton, Y. C. Zhang and A. Heller, "Electrodeposition of redox polymers and co-electrodeposition of enzymes by coordinative crosslinking," *Angewandte Chemie-International Edition*, **41**(5), 810-+ (2002).
- 39. N. S. Hudak, J. W. Gallaway and S. C. Barton, "Formation of mediated biocatalytic cathodes by electrodeposition of a redox polymer and laccase," *Journal of Electroanalytical Chemistry*, **629**(1-2), 57-62 (2009).
- 40. E. S. Forzani, M. Otero, M. A. Perez, M. L. Teijelo and E. J. Calvo, "The structure of layer-by-layer self-assembled glucose oxidase and Os(Bpy)(2)CIPyCH2NH-

- Poly(allylamine) multilayers: Ellipsometric and quartz crystal microbalance studies," *Langmuir*, **18**(10), 4020-4029 (2002).
- 41. A. Heller, "Electron-conducting redox hydrogels: design, characteristics and synthesis," *Current opinion in Chemical Biology,* **10**(6), 664-672 (2006).
- 42. D. N. Blauch and J. M. Saveant, "Dynamics of Electron Hopping in Assemblies of Redox Centers Percolation and Diffusion," *Abstracts of Papers of the American Chemical Society*, **203**, 343-PHYS (1992).
- 43. H. H. Kim, N. Mano, X. C. Zhang and A. Heller, "A miniature membrane-less biofuel cell operating under physiological conditions at 0.5 V," *Journal of the Electrochemical Society*, **150**(2), A209-A213 (2003).
- 44. L. A. Coury, R. W. Murray, J. L. Johnson and K. V. Rajagopalan, "Electrochemical Study of Kinetics of Electron-Transfer between Synthetic Electron-Acceptors and Reduced Molybdoheme Protein Sulfite Oxidase," *Journal of Physical Chemistry*, **95**(15), 6034-6040 (1991).
- 45. K. Takagi, K. Kano and T. Ikeda, "Mediated bioelectrocatalysis based on NAD-related enzymes with reversible characteristics," *Journal of Electroanalytical Chemistry*, **445**(1-2), 211-219 (1998).
- 46. Y. Nakabayashi, A. Omayu, S. Yagi and K. Nakamura, "Evaluation of osmium(II) complexes as electron transfer mediators accessible for amperometric glucose sensors," *Analytical Sciences*, **17**(8), 945-950 (2001).
- 47. S. M. Zakeeruddin, D. M. Fraser, M. K. Nazeeruddin and M. Gratzel, "Towards Mediator Design Characterization of Tris-(4,4'-Substituted-2,2'-Bipyridine) Complexes of Iron(Ii), Ruthenium(Ii) and Osmium(Ii) as Mediators for Glucose-Oxidase of Aspergillus-Niger and Other Redox Proteins," *Journal of Electroanalytical Chemistry*, 337(1-2), 253-283 (1992).
- 48. A. J. Bard, and Faulkner, *Electrochemical methods: fundamentals and applications* (2001).
- 49. L. S. Yahiro AT, Kimble DO., "Bioelectrochemistry I Enzyme utilizing biofuel cell studies," *Biochim Biophys Acta*, **88**, 375 383 (1964).
- 50. E. V. Plotkin, I. J. Higgins and H. A. O. Hill, "Methanol Dehydrogenase Bioelectrochemical Cell and Alcohol Detector," *Biotechnology Letters*, **3**(4), 187-192 (1981).
- 51. G. Davis, H. A. O. Hill, W. J. Aston, I. J. Higgins and A. P. F. Turner, "Bioelectrochemical Fuel-Cell and Sensor Based on a Quinoprotein, Alcohol-Dehydrogenase," *Enzyme and Microbial Technology*, **5**(5), 383-388 (1983).

- 52. N. K. Cenas and J. J. Kulys, "Biocatalytic Oxidation of Glucose on the Conductive Charge-Transfer Complexes," *Bioelectrochemistry and Bioenergetics*, **8**(1), 103-113 (1981).
- 53. A. E. G. Cass, G. Davis, G. D. Francis, H. A. O. Hill, W. J. Aston, I. J. Higgins, E. V. Plotkin, L. D. L. Scott and A. P. F. Turner, "Ferrocene-Mediated Enzyme Electrode for Amperometric Determination of Glucose," *Analytical Chemistry*, **56**(4), 667-671 (1984).
- 54. T. Ikeda, T. Shibata and M. Senda, "Amperometric Enzyme Electrode for Maltose Based on an Oligosaccharide Dehydrogenase-Modified Carbon Paste Electrode Containing Para-Benzoquinone," *Journal of Electroanalytical Chemistry*, **261**(2B), 351-362 (1989).
- 55. S. Zhao and R. B. Lennox, "Pyrroloquinolinequinone Enzyme Electrode Based on the Coupling of Methanol Dehydrogenase to a Tetrathiafulvalene Tetracyanoquinodimethane Electrode," *Analytical Chemistry*, **63**(11), 1174-1178 (1991).
- 56. J. J. Kulys, "Enzyme Electrodes Based on Organic Metals," *Biosensors*, **2**(1), 3-13 (1986).
- 57. B. Q. Wang, B. Li, Z. X. Wang, G. B. Xu, Q. Wang and S. J. Dong, "Sol-gel thin-film immobilized soybean peroxidase biosensor for the amperometric determination of hydrogen peroxide in acid medium," *Analytical Chemistry*, **71**(10), 1935-1939 (1999).
- 58. S. Tsujimura, B. Tatsumi, J. Ogawa, S. Shimizu, K. Kano and T. Ikeda, "Bioelectrocatalytic reduction of dioxygen to water at neutral pH using bilirubin oxidase as an enzyme and 2,2 '-azinobis (3-ethylbenzothiazolin-6-sulfonate) as an electron transfer mediator," *Journal of Electroanalytical Chemistry*, **496**(1-2), 69-75 (2001).
- 59. J. M. Zen and C. W. Lo, "A glucose sensor made of an enzymatic clay-modified electrode and methyl viologen mediator," *Analytical Chemistry*, **68**(15), 2635-2640 (1996).
- 60. C. M. Moore, N. L. Akers, A. D. Hill, Z. C. Johnson and S. D. Minteer, "Improving the environment for immobilized dehydrogenase enzymes by modifying Nafion with tetraalkylammonium bromides," *Biomacromolecules*, **5**(4), 1241-1247 (2004).
- 61. F. Gao, O. Courjean and N. Mano, "An improved glucose/O-2 membrane-less biofuel cell through glucose oxidase purification," *Biosensors & Bioelectronics*, **25**(2), 356-361 (2009).
- 62. J. S. Facci, R. H. Schmehl and R. W. Murray, "Effect of Redox Site Concentration on the Rate of Electron-Transport in a Redox Co-Polymer Film," *Journal of the American Chemical Society*, **104**(18), 4959-4960 (1982).

- 63. R. J. Forster and J. G. Vos, "Synthesis, Characterization, and Properties of a Series of Osmium-Containing and Ruthenium-Containing Metallopolymers," *Macromolecules*, **23**(20), 4372-4377 (1990).
- 64. J. Hodak, R. Etchenique, E. J. Calvo, K. Singhal and P. N. Bartlett, "Layer-by-layer self-assembly of glucose oxidase with a poly(allylamine)ferrocene redox mediator," *Langmuir*, **13**(10), 2708-2716 (1997).
- 65. K. Habermuller, A. Ramanavicius, V. Laurinavicius and W. Schuhmann, "An oxygeninsensitive reagentless glucose biosensor based on osmium-complex modified polypyrrole," *Electroanalysis*, **12**(17), 1383-1389 (2000).
- 66. M. T. Meredith, D. Y. Kao, D. Hickey, D. W. Schmidtke and D. T. Glatzhofer, "High Current Density Ferrocene-Modified Linear Poly(ethylenimine) Bioanodes and Their Use in Biofuel Cells," *Journal of the Electrochemical Society*, **158**(2), B166-B174 (2011).
- 67. D. A. Guschin, H. Shkil and W. Schuhmann, "Electrodeposition polymers as immobilization matrices in amperometric biosensors: improved polymer synthesis and biosensor fabrication," *Analytical and Bioanalytical Chemistry*, **395**(6), 1693-1706 (2009).
- 68. A. Heller, "Electrical Wiring of Redox Enzymes," *Accounts of Chemical Research*, **23**(5), 128-134 (1990).
- 69. F. Mao, N. Mano and A. Heller, "Long tethers binding redox centers to polymer backbones enhance electron transport in enzyme "wiring" hydrogels," *Journal of the American Chemical Society*, **125**(16), 4951-4957 (2003).
- 70. D. A. Guschin, J. Castillo, N. Dimcheva and W. Schuhmann, "Redox electrodeposition polymers: adaptation of the redox potential of polymer-bound Os complexes for bioanalytical applications," *Analytical and Bioanalytical Chemistry*, **398**(4), 1661-1673 (2010).
- 71. D. N. Blauch and J. M. Saveant, "Dynamics of Electron Hopping in Assemblies of Redox Centers Percolation and Diffusion," *Journal of the American Chemical Society*, **114**(9), 3323-3332 (1992).
- 72. D. A. Buckingham, F. P. Dwyer, H. A. Goodwin and A. M. Sargeson, "Mono- + Bis-(2,2]-Bipyridine) +)1,10-Phenanthroline) Chelates of Ruthenium + Osmi17 .4. Bis Chelates of Bivalent + Tervalent Osmium," *Australian Journal of Chemistry*, **17**(3), 325-& (1964).
- 73. J. W. Gallaway and S. A. C. Barton, "Effect of redox polymer synthesis on the performance of a mediated laccase oxygen cathode," *Journal of Electroanalytical Chemistry*, **626**(1-2), 149-155 (2009).

- 74. A. B. P. Lever, "Electrochemical Parametrization of Metal-Complex Redox Potentials, Using the Ruthenium(Iii) Ruthenium(Ii) Couple to Generate a Ligand Electrochemical Series," *Inorganic Chemistry*, **29**(6), 1271-1285 (1990).
- 75. R. Wilson and A. P. F. Turner, "Glucose-Oxidase an Ideal Enzyme," *Biosensors & Bioelectronics*, **7**(3), 165-185 (1992).
- 76. D. Muller, "Oxidation von Glukose mit Extrakten aus Aspegillus niger.," *Biochemische Zeitschrift,* **199** (1928).
- 77. B. E. P. Swoboda and V. Massey, "Purification and Properties of Glucose Oxidase from Aspergillus Niger," *Journal of Biological Chemistry*, **240**(5), 2209-& (1965).
- 78. J. H. Dowling and H. B. Levine, "Hexose Oxidation by an Enzyme System of Malleomyces-Pseudomallei," *Journal of Bacteriology*, **72**(4), 555-560 (1956).
- 79. R. C. Bean and W. Z. Hassid, "Carbohydrate Oxidase from a Red Alga,Iridophycus-Flaccidum," *Journal of Biological Chemistry*, **218**(1), 425-436 (1956).
- 80. R. C. Bean, G. G. Porter and Steinber.Bm, "Carbohydrate Metabolism of Citrus Fruits .2. Oxidation of Sugars by an Aerodehydrogenase from Young Orange Fruits," *Journal of Biological Chemistry*, **236**(5), 1235-& (1961).
- 81. C. M. Wong, K. H. Wong and X. D. Chen, "Glucose oxidase: natural occurrence, function, properties and industrial applications," *Applied Microbiology and Biotechnology*, **78**(6), 927-938 (2008).
- 82. E. Katz, I. Willner and A. B. Kotlyar, "A non-compartmentalized glucose vertical bar O-2 biofuel cell by bioengineered electrode surfaces," *Journal of Electroanalytical Chemistry*, **479**(1), 64-68 (1999).
- 83. M. T. Stankovich, L. M. Schopfer and V. Massey, "Determination of Glucose Oxidase Oxidation-Reduction Potentials and Oxygen Reactivity of Fully Reduced and Semi-Quinoid Forms," *Journal of Biological Chemistry*, **253**(14), 4971-4979 (1978).
- 84. V. Leskovac, S. Trivic, G. Wohlfahrt, J. Kandrac and D. Pericin, "Glucose oxidase from Aspergillus niger: the mechanism of action with molecular oxygen, quinones, and one-electron acceptors," *International Journal of Biochemistry & Cell Biology*, **37**(4), 731-750 (2005).
- 85. G. Wohlfahrt, S. Trivic, J. Zeremski, D. Pericin and V. Leskovac, "The chemical mechanism of action of glucose oxidase from Aspergillus niger," *Molecular and Cellular Biochemistry*, **260**(1), 69-83 (2004).
- 86. C. Bourdillon, C. Demaille, J. Moiroux and J. M. Saveant, "New Insights into the Enzymatic Catalysis of the Oxidation of Glucose by Native and Recombinant Glucose-

- Oxidase Mediated by Electrochemically Generated One-Electron Redox Cosubstrates," *Journal of the American Chemical Society*, **115**(1), 2-10 (1993).
- 87. Q. H. Gibson, V. Massey and B. E. P. Swoboda, "Kinetics + Mechanism of Action of Glucose Oxidase," *Journal of Biological Chemistry*, **239**(11), 3927-& (1964).
- 88. H. J. Hecht, D. Schomburg, H. Kalisz and R. D. Schmid, "The 3d Structure of Glucose-Oxidase from Aspergillus-Niger Implications for the Use of God as a Biosensor Enzyme," *Biosensors & Bioelectronics*, **8**(3-4), 197-203 (1993).
- 89. L. Jiang, C. J. Mcneil and J. M. Cooper, "Direct Electron-Transfer Reactions of Glucose-Oxidase Immobilized at a Self-Assembled Monolayer," *Journal of the Chemical Society-Chemical Communications*(12), 1293-1295 (1995).
- 90. J. Q. Liu, A. Chou, W. Rahmat, M. N. Paddon-Row and J. J. Gooding, "Achieving direct electrical connection to glucose oxidase using aligned single walled carbon nanotube arrays," *Electroanalysis*, **17**(1), 38-46 (2005).
- 91. Y. D. Zhao, W. D. Zhang, H. Chen and Q. M. Luo, "Direct electron transfer of glucose oxidase molecules adsorbed onto carbon nanotube powder microelectrode," *Analytical Sciences*, **18**(8), 939-941 (2002).
- 92. D. Ivnitski, B. Branch, P. Atanassov and C. Apblett, "Glucose oxidase anode for biofuel cell based on direct electron transfer," *Electrochemistry Communications*, **8**(8), 1204-1210 (2006).
- 93. O. Courjean, F. Gao and N. Mano, "Deglycosylation of Glucose Oxidase for Direct and Efficient Glucose Electrooxidation on a Glassy Carbon Electrode," *Angewandte Chemie-International Edition*, **48**(32), 5897-5899 (2009).
- 94. T. Chen, S. C. Barton, G. Binyamin, Z. Q. Gao, Y. C. Zhang, H. H. Kim and A. Heller, "A miniature biofuel cell," *Journal of the American Chemical Society*, **123**(35), 8630-8631 (2001).
- 95. N. Mano, F. Mao and A. Heller, "Characteristics of a miniature compartment-less glucose-O-2 biofuel cell and its operation in a living plant," *Journal of the American Chemical Society*, **125**(21), 6588-6594 (2003).
- 96. N. Mano, F. Mao, W. Shin, T. Chen and A. Heller, "A miniature biofuel cell operating at 0.78 V," *Chemical Communications*(4), 518-519 (2003).
- 97. X. Li, L. Zhang, L. Su, T. Ohsaka and L. Mao, "A Miniature Glucose/O-2 Biofuel Cell With a High Tolerance Against Ascorbic Acid," *Fuel Cells*, **9**(1), 85-91 (2009).
- 98. F. Tasca, L. Gorton, W. Harreither, D. Haltrich, R. Ludwig and G. Noll, "Highly efficient and versatile anodes for biofuel cells based on cellobiose dehydrogenase from

- Myriococcum thermophilum," *Journal of Physical Chemistry C*, **112**(35), 13668-13673 (2008).
- 99. T. J. Ohara, R. Rajagopalan and A. Heller, "Glucose Electrodes Based on Cross-Linked [Os(Bpy)(2)](+/2+) Complexed Poly(L-Vinylimidazole) Films," *Analytical Chemistry*, **65**(23), 3512-3517 (1993).
- 100. N. Mano, F. Mao and A. Heller, "On the parameters affecting the characteristics of the "wired" glucose oxidase anode," *Journal of Electroanalytical Chemistry*, **574**(2), 347-357 (2005).

Chapter 2: Synthesis and Characterization of Osmium Redox Polymer Mediated Glucose Oxidase Electrodes

Abstract

Two osmium based redox polymer mediated glucose oxidase (GOx) electrodes were synthesized and characterized in the presence of N_2 , air and O_2 . We report glucose oxidation current density up to 2 mA/cm² for poly(n-VI₁₂[Os(bpy)₂Cl]^{+/2+} redox polymer mediated GOx electrode which is approximately 1.5 times higher than previously reported values for similar electrodes. Mediating performance of the synthesized redox polymers with respect to GOx and effect of oxygen in the system was quantitatively elucidated in terms of mediator redox potential, osmium loading and diffusivities.

Introduction

Biofuel cell technology is gradually finding its space in the area of bioelectronics by taking an advantage of unrivaled biocatalytic attributes of the enzymes to convert chemical energy directly to electrical energy. ¹⁻⁴ Biofuel cells gains advantage over other contemporary fuel cell technologies due to biocatalysis aspects of the enzyme that are unmatched by other catalysts like Pt due to selectivity towards its substrate, near room temperature and neutral pH operation. ⁵ Enzymatic electrodes suffer in terms of low activity when compared with noble metal catalysts. However, as in the case of micro-scale size power producing devices requiring low power output, enzymatic biofuel cell gains upper hand over other energy producing devices. ¹

In the present work, we synthesize and characterize two osmium redox polymer mediated GOx electrodes, and examine the effect of O_2 on the performance of such enzyme-catalyzed electrodes. We have used two different redox polymers for this purpose: (**A**)- poly(*N*-vinylimidazole[Os(2,2'-bipyridine)₂Cl]^{+/2+}) and (**B**)- poly(*N*-vinylimidazole[Os(4,4'-dimethyl-2,2'-bipyridine)₂Cl]^{+/2+}).²¹ The structure of these two polymers is shown in Figure 2.1. As shown in Table 1, the physical properties of these polymers mainly differ in three important aspects: First, the redox potential of the central osmium atom, which is modulated by the type of ligands attached to it ³⁷ and hence affecting the thermodynamic driving force of mediation or the electron transfer driving force (ΔE_T).²¹ Second and third being the osmium loading and apparent electron diffusivity or mediator diffusivity (D_m) respectively, which greatly influence the catalytic performance of such redox polymer mediated enzyme electrodes.²¹

Experimental

Reagents and Chemicals

Ultrapure N₂, air and O₂ were purchased from the Airgas (Great Lakes, MI). Potassium hexachloroosmiate (K₂OsCl₆) was purchased from the Alfa Aesar (Ward hill, MA). 4,4'-dimethyl-2,2'-bipyridine (dm-bpy), 2,2'-bipyridine (bpy), Sodium hydrosulphite,

Dimethylformamide (DMF), ethylene glycol, ethanol, acetone, diethyl ether, 1-vinylimidazole (VI), Azobisisobutylonitrile (AIBN), and Glucose oxidase (GOx) from *Aspergillus niger* were purchased from the Sigma-Aldrich (St. Louis, MO). Sodium phosphate monobasic and dibasic,

Sodium bicarbonate and Dextrose were purchased from the J.T. Baker (Phillipsburg, NJ). Sodium periodate was purchased from the Acros organics (NJ). Polyethylene glycol diglycidyl ether (PEGDGE) was obtained from the Polysciences Inc., (Warrington, PA). All the chemicals were used as received. Ultrapure deionized (DI) water was used to make all the solutions.

Redox Polymer Synthesis

Redox polymers **A** and **B** were synthesized in-house following the literature procedures²¹ but it is briefly explained in this section. Overall synthesis method can be divided into three parts. The first step is preparation of polymer backbone like polyvinylimidazole (PVI) or polyvinylpyridine (PVP). The second part is construction of the osmium pendent and third operation is complexation of the backbone and osmium pendent followed by precipitation, ultra purification and drying. Both the polymers have PVI backbone and polymer A was synthesized by polymerization of VI (20.75 g) by AIBN (0.06545 g), which initiates the free radical polymerization in 40 ml ethanol at 80 °C for 2 hrs (no stirring), followed by precipitation in acetone and filtration. ³⁸ Average molecular weight of the synthesized PVI was determined to be 46 kDa by the dilute solution viscometry and glass transition temperature of 177.1 °C was measured by the differential scanning calorimetry, which is very similar to literature value. ²¹ The osmium pendent was prepared by reacting K₂OsCl₆ (511 mg, 1.04 mmol) and bpy (342 mg, 2.19 mmol) in 40 ml DMF at 175 °C under the continuous sparging of argon for 1hr, followed by cooling, addition of ~15 ml ethanol and precipitation in ~500 ml of rapidly stirred diethyl ether. Dark red product was filtered and dried overnight in the fume hood. ²¹ The [Os(bpy)₂Cl₂]Cl was

reduced by dissolving it in a 16 ml of 2:1 solution of 1% sodium hydrosulphite solution. After 1 hr cooling in ice bath, crystallized [Os(bpy)Cl₂] was collected by filtration and dried (524 mg, yield 62 %). In final step, [Os(bpy)Cl₂] (155 mg, 0.271 mmol) was complexed with PVI (236 mg, 2.4 mmol) in a 90 ml of ethanol at 95 °C for three days. 21,39 At the end, product was purified over a Millipore YM-10 ultrafiltration membrane to remove unreacted species and stored as a 10 mg/ml solution in water. 36 Redox polymer **B** was also prepared in the similar manner. At each step of the polymer synthesis, redox potential of the synthesized compound can be confirmed with the predicted value 21,37 by cyclic voltammetry 40 as Gallaway *et al.* 12 observed during the reaction progress of poly(*N*-vinylimidazole[Os(terpyridine)(4,4'-dimethyl-2,2'-bipyridine)₂] $^{2+/3+}$), where they demonstrate that variation in the reaction conditions can have a profound effect on the synthesized polymer in terms of osmium loading and therefore on the mediator diffusivity and hence on the enzyme electrode performance.

Glucose Oxidase Electrode Preparation

Planar redox hydrogel film electrodes were produced on a 3 mm diameter, glassy carbon rotating disc electrodes (RDEs). RDEs were fabricated in-house from the type 1 glassy carbon rods (Alfa Aesar, MA). Prior to using, electrode surface were sanded with various ultrafine grit sandpapers (Buehler, IL) and polished to mirror finish with 0.3 µm alumina slurry followed by sonication in DI water to remove any residual alumina. No electrochemical features were observed on the bare RDEs after cleaning when tested at 50 mV/s scan rate, 1000 rpm rotation in the 250 mM, pH 7, 38 °C phosphate buffer.

GOx bioanodes were prepared by drop casting 4 μ l aliquot containing periodate oxidized GOx (39.5 wt%), redox polymer (59.5 wt%) and PEGDGE (3 mg/ml) (1 wt%) with a total mass loading of 0.726 mg/cm². We have chosen this composition because optimum performance of such electrodes have been reported⁴³ at ~ 40 % by mass GOx value. Resulting electrodes were cured in air at room temperature for ~14-16 hrs before testing.

Electrochemical Studies

Electrochemical measurements were conducted in the pH 7, 38 °C, 250 mM phosphate buffer electrolyte without any NaCl in it because negatively charged chloride ions screens the positively charged redox polymers that reduces the electrostatic repulsion between adjacent polymers and this causes long chains of the macromolecules to bundle up and prevent them to comply with the negatively charged enzyme surface, which results in a poor electron transfer between redox polymer mediator and the GOx enzyme. 43 The electrodes were rotated at 1000 rpm using a pine rotator (Pine Instrument Co., PA) in a one-compartment 100 ml water-jacketed cell. Platinum wire was used as counter electrode with an Ag|AgCl as a reference electrode (BAS, West Lafayette, IN) or cathode. Prior to testing, depending on the type of experiment, electrolyte was either sparged with N2, air or O2 for 40-45 mins. Concentration of O2 in the solution was considered as 0 mM, 0.18 mM and 0.86 mM for N_2 , air and O_2 saturated conditions respectively. 44 Data were collected with a VST Potentiostat and EC-Lab® software (Bio-logic USA, LLC, TN). All the potentials were ohmic resistance corrected by measuring the highfrequency (100 kHz) resistance or the real electrochemical impedence of the cell and it was

found to be 64±4 Ω , which is attributable to the migration resistance of the bulk electrolyte. This yields the buffer conductivity (\varkappa) of 55 mS cm⁻¹ from the relation $R_{\Omega} = (4\varkappa r_O)^{-1}$, where r_O is the electrode radius.

Results

Two water-soluble, osmium based redox polymers were synthesized for the GOx mediation purpose and their performance was analyzed quantitatively in the absence and presence of oxygen. Albeit similar study has been performed previously, ^{11,43} we have modeled such mediated enzyme electrodes (Chapter 3) in order to understand and have an accurate knowledge of the kinetics of such system, where apart from the glucose and mediator, oxygen also acts as a co-substrate of GOx, which affects the performance of such electrodes.

Redox mediator potential, loading and catalytic film performance

Figure 2.2 shows cyclic voltammograms (CVs) of two redox polymer mediated GOx electrodes in the absence of glucose substrate from which the mediator redox potential, E_m^0 , (Table 2.1) was calculated and it matches well with the value predicted by "Lever analysis" and the literature reports. It can be seen that in the presence of oxygen, redox mediator performance was unaffected. As shown in Table 2.1, osmium loading (m) in the synthesized redox polymers was determined via inductively coupled plasma mass spectrometry (ICP-MS) carried out by West Coast Analytical Service, Inc. (Santa Fe Springs, CA) and were comparable to the previously reported values $m_{\rm c}^{21}$ for the same polymers.

Representative polarization curves for glucose oxidation in the N_2 , air and O_2 saturated buffers are shown in Figure 2.3. Glucose oxidation current begins as the working electrode potential advances above the mediator redox potential, increases with increasing potential until the potential independent plateau current (i_{pl}) is reached. This plateau current depends on the mediator and substrate concentration, electron and substrate transport in the film, enzyme concentration and kinetics of the system. 21,45,46

Figure 2.4 depicts the effect of oxygen on the steady state current density at various glucose concentrations when electrodes were poised at 0.6 V/SHE and rotated at 1000 rpm in the presence of N_2 , air and O_2 saturated conditions. It can be observed that at low glucose concentrations (< 5 mM), reduction in current density in the presence of oxygen is approximately greater than 50% and this effect decreases as the glucose concentration increases.

Electron transport

The performance of the modern electrodes is mainly limited by the electron transport via redox polymer mediators. ^{5,21,47} Charge transport in such redox films are characterized by the apparent electron diffusion coefficient, D_m , which can be estimated from the Randles-Sevcik or the Cottrell analysis. ^{21,40} As shown in Figure 2.5(a), we obtain the mediator diffusivity (Table 2.1) by using Randle-Sevcik equation (Eq. 2.2), where peak current density (i_p) was found to vary linearly with square-root of the scan rate (v), indicative of the semi-infinite diffusion. ²¹

$$i_p = 0.4463 \left(\frac{F^3}{RT}\right)^{1/2} n^{3/2} C_m D_m^{1/2} v^{1/2}$$
 [2.2]

where F is Faraday's constant, R is gas constant, T is the solution temperature, n is number of electrons transferred in the redox reaction, C_m is the active mediator concentration and v is the scan rate. D_m in such redox polymers scales linearly with their osmium loading as demonstrated by Gallaway $et\ al.$, 21 and similar trend was observed for the synthesized redox polymers in the present work. It can be seen from the Figure 2.5(b) that oxygen does not impact the redox polymer mediator diffusivity, therefore it can be deduced that the reduction in GOx enzyme electrode performance in the presence of O_2 is entirely due to the loss of electrons at reduced active site of the GOx, which was not shown in the previously reported analyses. 11,43

Film thickness and active osmium concentration

Hydrogel film thickness is one of the important parameter that affects the performance of the redox polymer mediated enzyme electrodes in terms of mobility of the redox active centers or the charge propagation and the species transport.³⁴ Also, it has been shown that such films swell upon hydration.^{21,34} Dry and wet (Swollen) film thickness measurements has been approached in the literature using atomic force microscopy (AFM),⁴⁸ environmental scanning electron microscopy (ESEM),³⁴ profilometry²¹ and confocal microscopy.³⁵ Generally, the dry film thickness of such redox polymer films fall in the range of ~0.5-1.2 μm. When compared with the dry film thickness, upon hydration, a swelling factor of ~1.1 to 3 has been observed for

various redox polymer films. 21,34,35,48 As shown in Figure 2.6, in this work we measure the dry film thickness of 3 mm diameter GOx and polymer **A** containing films identical to those used in the RDE measurements on the thin mica sheets by AFM and we obtain a value of $\sim 0.75\pm 0.2~\mu m$ when measured at the three different location in the film, which is matched well with the previously reported values. 21

Apart from mediator diffusivity, the active osmium concentration is another pivotal parameter that governs the performance of such redox polymer mediated enzyme electrodes. ²¹ In the present work, we deposit ~ 4 M of redox polymer on one electrode, but it is important to have the quantitative knowledge of an active osmium concentration or an active osmium centers that facilitates the electron diffusion. Chakraborty *et al.* ²¹ used a Square-wave voltammetry (SWV) technique, ⁴⁹ to access the active osmium content for similar redox hydrogel based electrodes. SWV provides accurate information about the electro-active species by estimating the charge transferred due to faradic reactions only. In this work, we obtain the electro-active osmium concentration (C_m) (Table 2.1) from the integrated redox charge in the cyclic voltammetry, ^{31,40} which is comparable to the previously reported values. ^{21,35}

Electrode stability

Figure 2.7 depicts the stability of the polymer $\bf A$ and $\bf B$ mediated GOx electrodes (rotating at 1000 rpm) when electrolyte was continuously sparged with N_2 , Air and O_2 . Steep initial decrease in the current density was observed for polymer $\bf B$ mediated electrodes and this can be

attributed to the lower ΔE_T when compared with polymer **A**. Half-life (time at which the current density reduces to half of its maximum value) of such electrodes were reported to be ~60 hrs when operated in a flow cell assembly. ⁵⁰ In our studies, half life of ~24 hrs and ~15hrs was observed for polymer **A** and **B** mediated GOx electrodes in the case of N_2 saturated conditions but performance of the electrodes declined considerably in the presence of O_2 , which can be attributed to the competing reaction of O_2 with redox polymer at the GOx active site for electrons of the glucose substrate. Loss in performance in the presence of O_2 , can partly be attributed to the formation of H_2O_2 , which is known to inactivate the reduce form of GOx. ⁵¹ Other reasons for the decay in current for all the electrodes could be due to the denaturation or loss of enzyme or mediator from the cross-linked hydrogel, which is subjected to high shear over a long timescale of the experiments. ⁵²

Discussion

It can be seen from Figure 2.3 and 2.4 that in the presence of O_2 , enzyme electrode performance drops due to an electron scavenging action of O_2 at the reduced active site of the GOx (Equation 1.9). Sun salso conducted similar study using two different osmium based redox polymers in a flow-through cell assembly, where similar trend was observed in case of O_2 saturated conditions. We report the highest current density of ~ 2 mA/cm², for the glucose oxidizing redox hydrogel film on a planar bioanode prepared with GOx, mediated with polymer

A, operating at 38 $^{\circ}$ C and 1000 rpm, when 250 mM, pH 7 phosphate buffer (No NaCl) was saturated with N₂ gas, which to our knowledge is greater than a factor of ~1.5 higher than any previously reported values. ^{11,26,54} This can be attributed the superior mediator performance, higher loading of species on an electrode and increased electrolyte strength.

Despite of similar material loading (0.726 mg/cm²) in both redox polymer mediated GOx electrodes significant difference in the performance can be observed. It can be observed that the current densities produced by polymer **B** mediated electrodes are ~ 40% of polymer **A** based electrodes. This can be mainly attributed to two characteristics of the employed redox polymer. First, is the mediator redox potential, which determines the electron transfer driving force (ΔE_T) with respect to GOx. Polymer **A** has 100 mV greater ΔE_T than that of the redox polymer **B**, which can be one of the reason for better performance of the polymer **A** based electrodes. Secondly, superior performance of polymer **A** mediated GOx electrodes can also be attributed to the higher osmium loading (m) as compared to polymer **B**, which controls the diffusivity²¹ and active osmium concentration (C_m).

Presence of O_2 in the system greatly affects the performance of the GOx electrodes not by influencing of mediator transport but via impacting the kinetics of the GOx enzyme, which is elucidated in the Chapter 3 through mathematical modeling of such redox polymer mediated enzyme electrodes.

Conclusions

Using two different osmium based redox polymers, the impact of oxygen on the performance of mediated enzyme electrodes were studied. Lower current densities were observed for the electrodes comprising of low potential based mediator due to lower driving force with respect to GOx enzyme and osmium loading. In the presence of O_2 , reduction in performance of such redox polymer mediated enzyme electrodes was observed, attributed to the competition for electrons between O_2 and mediator at the reduced active site of GOx.

Acknowledgements

Authors are thankful to Deboleena Chakraborty for her guidance in the synthesis of the redox mediators and Hao Wen for sharing the GOx electrode preparation recipe.

 Table 2.1: Redox polymer properties

| RP | Structural Formula | E_m^0 (V SHE) | m (Os Wt %) | $D_m \times 10^{-9} \text{ cm}^2/\text{s})$ | <i>C_m</i> (mM) | ΔE_T (V) |
|----|---|-------------------|----------------|---|---------------------------|------------------|
| A | $poly(n-VI_{12}[Os(bpy)_2Cl]^{+/2+}$ | 0.43 | 9.34 | 2.18 ± 0.03 | 660 ± 35 | 0.55 |
| В | $poly(n\text{-VI}_{22}[Os(dm\text{-bpy})_2Cl]^{+/2+}$ | 0.33 | 7.3 | 1.50 ± 0.02 | 380 ± 28 | 0.45 |

FIGURES

Figure 2.1: Structure of synthesized redox mediators. A - poly(*N*-vinylimidazole[Os(2,2'-bipyridine)₂Cl] + $(2,2'-bipyridine)_2$ Cl] + (2,2'-bipyridin

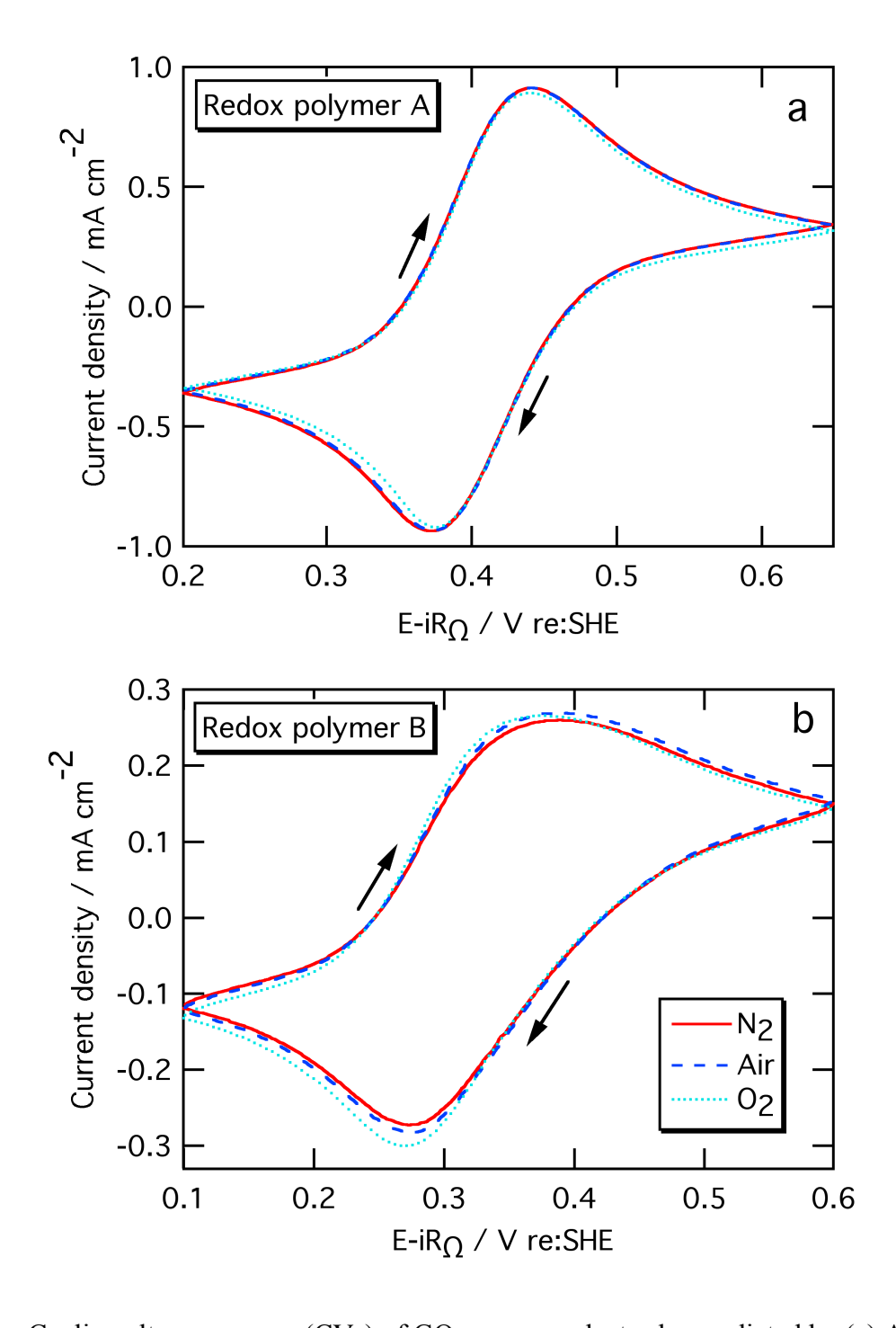


Figure 2.2: Cyclic voltammograms (CVs) of GOx enzyme electrodes mediated by (a) A and (b) B in the presence of N_2 , Air and O_2 saturated conditions. Experiments were conducted in the 245 mM phosphate buffer (No NaCl), pH 7, 38 °C, 50 mV/s scan rate. Redox hydrogel composition was 59.5 % redox polymer, 39.5 % GOx and 1 % cross linker by mass with a total material loading of 0.726 mg/cm².

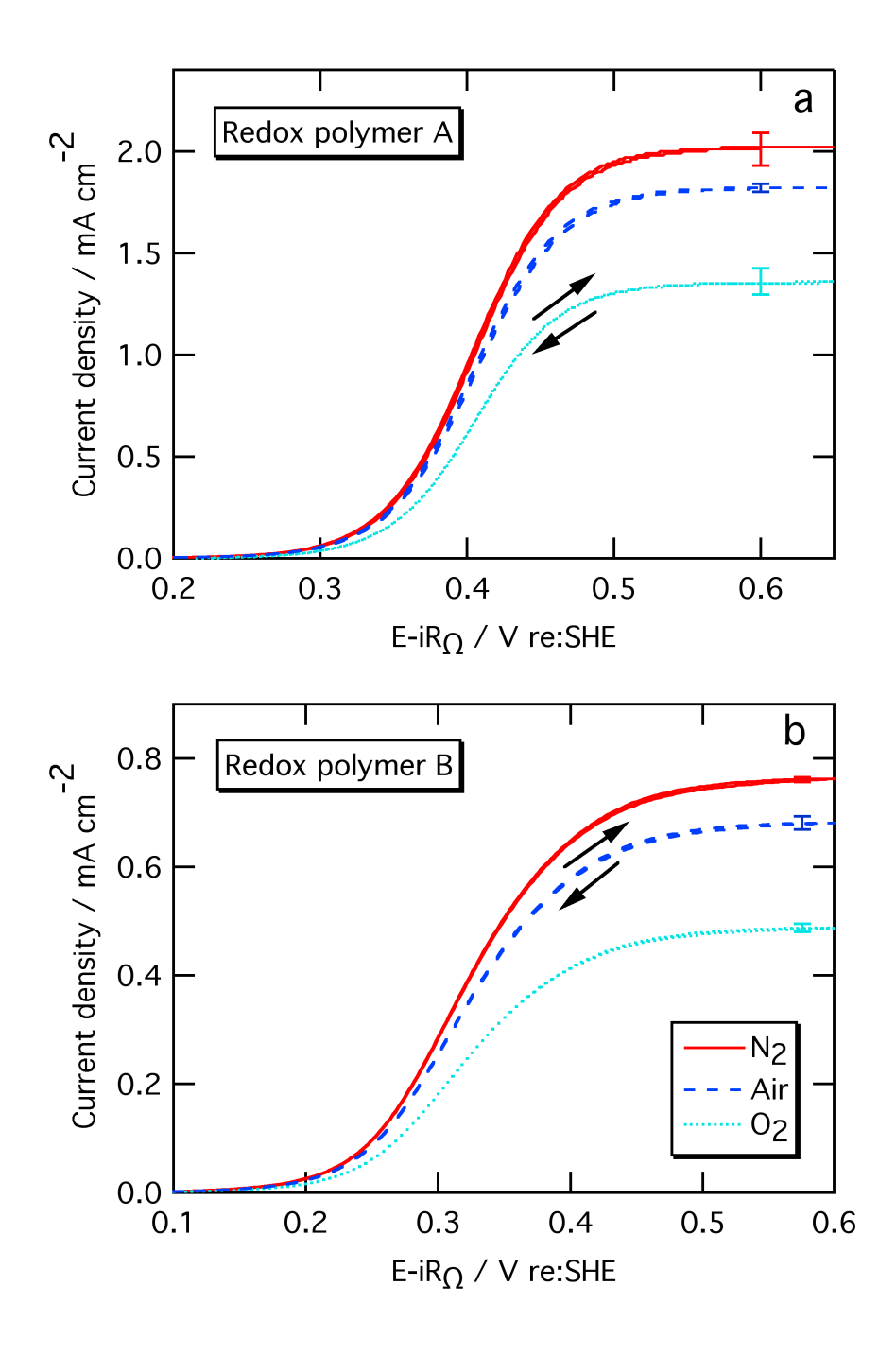


Figure 2.3: Anode performance of the GOx electrodes in the presence of N_2 , Air and O_2 . Polarization curves of (a) RP **A** and (b) RP **B** mediated GOx electrodes. Experiments conducted in the 38 °C, 245 mM phosphate buffer (No NaCl), pH 7 containing 50 mM glucose substrate at 1000 rpm rotation. Scan rate 1 mV/s. Total material loading of 0.726 mg/cm² with same composition as mentioned in Figure 2.2.

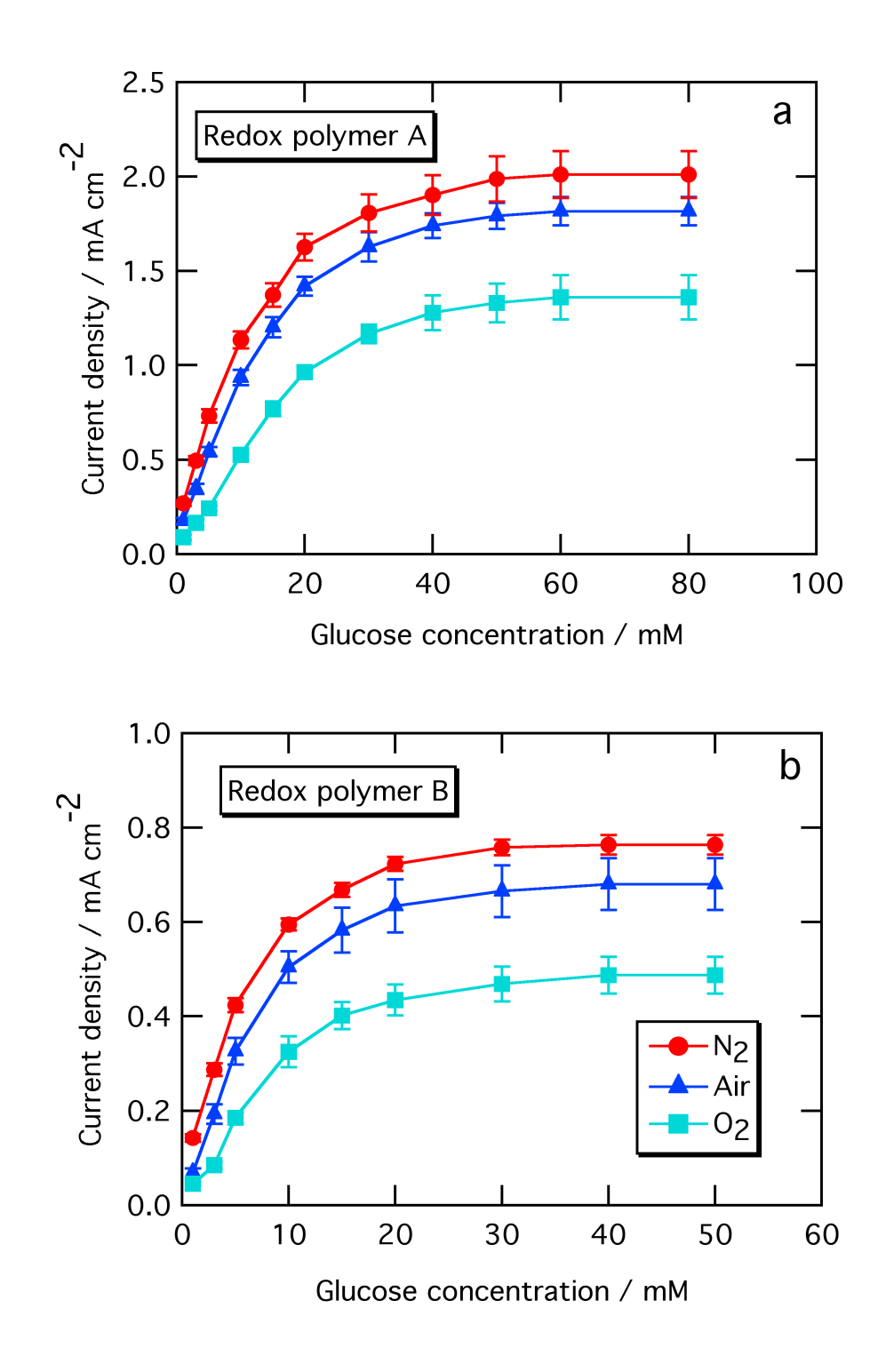


Figure 2.4: Substrate dependence curves of (a) RP **A** and (b) RP **B** mediated GOx electrodes. Electrodes were poised at 0.6~V | re:SHE and rotated at 1000~rpm. Other experimental conditions are same as mentioned in Figure 2.2

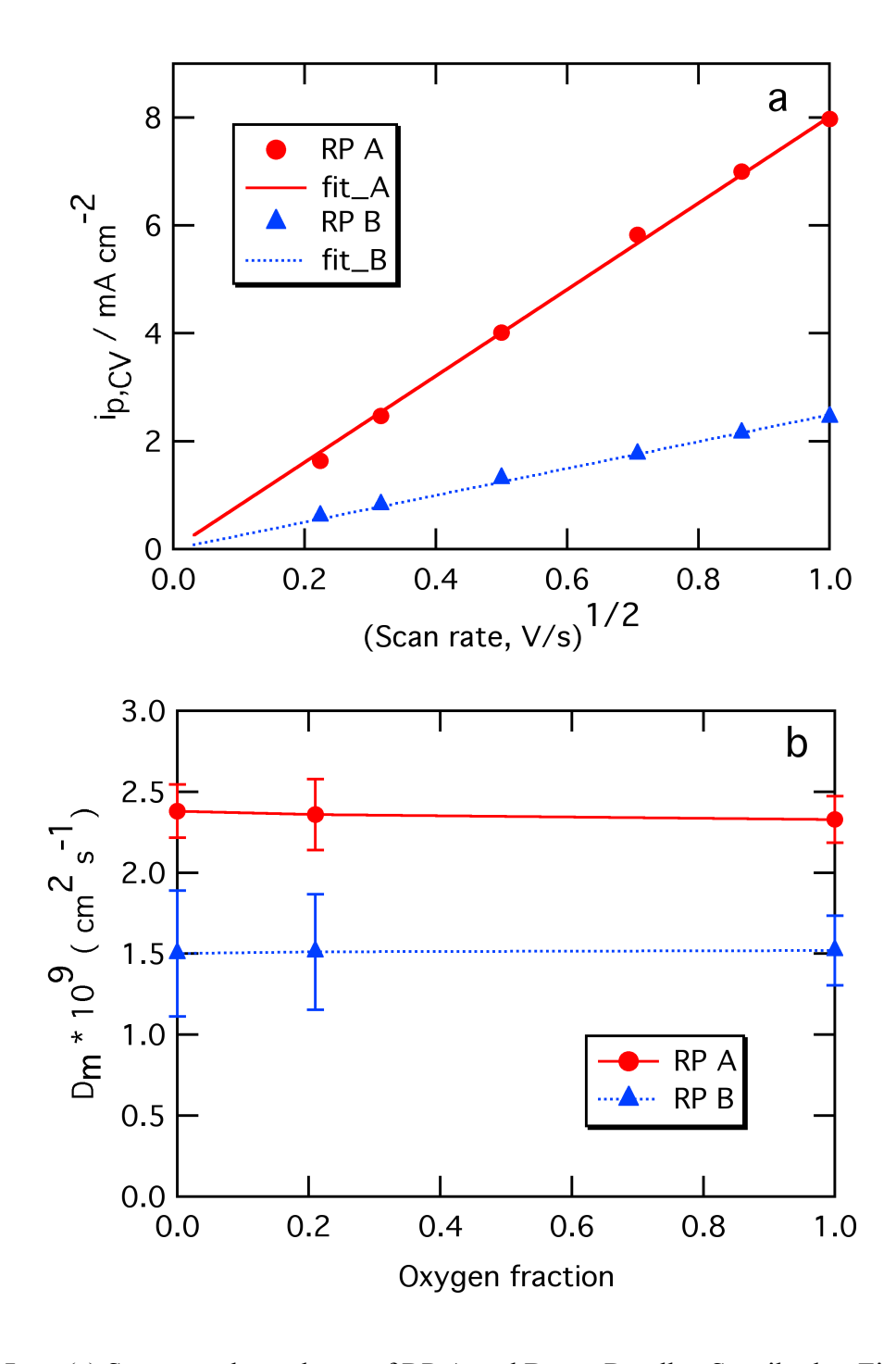


Figure 2.5: (a) Scan rate dependence of RP A and B as a Randles-Sevcik plot. Fitted line vanishes to the origin, indicating semi-infinite diffusion. (b) Apparent e^- diffusivity (D_m) of mediators as a function of oxygen fraction. Experimental conditions are same as mentioned in Figure 2.2

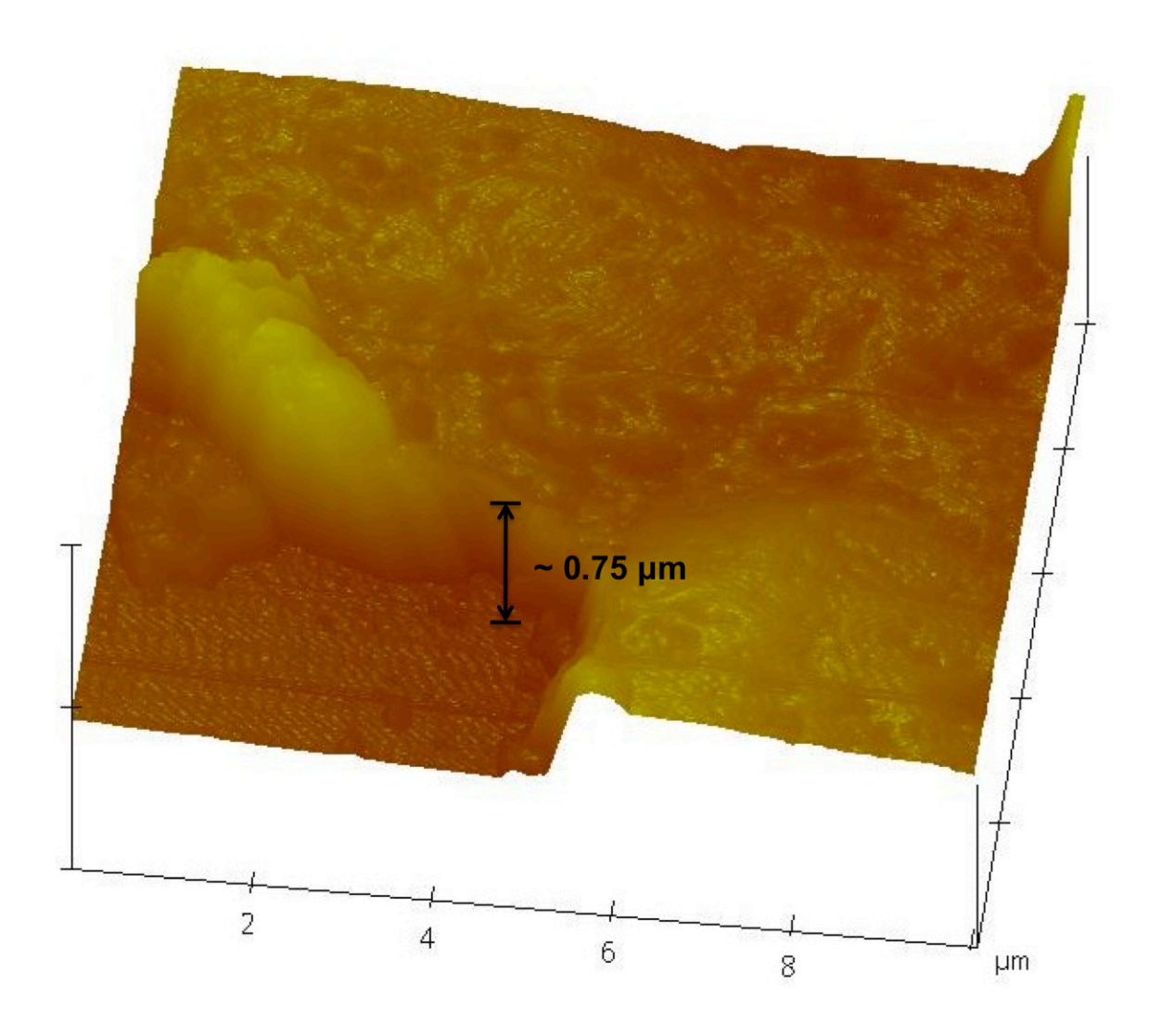


Figure 2.6: AFM image showing the cross section of RP A-GOx film. Material loading was 0.726 mg/cm^2 with 59.5 % redox polymer, 39.5 % GOx and 1 % cross linker by weight.

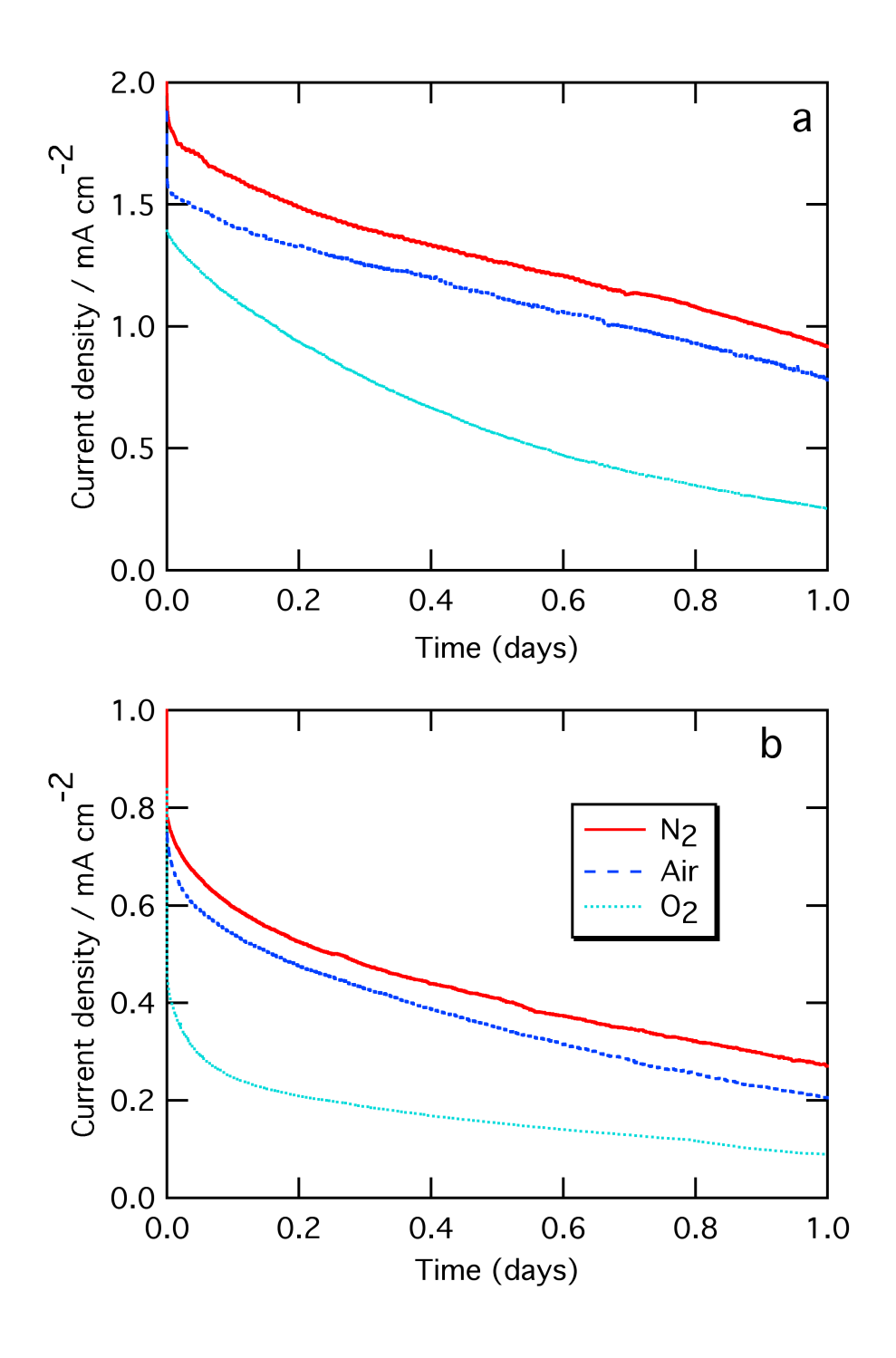


Figure 2.7: Glucose oxidation stability of the GOx electrodes in the chronoamperometry test mediated by (a) RP **A** and (b) RP **B** poised at $0.6 \text{ V} \mid \text{SHE}$. Experiments were conducted under N₂, Air and O₂ in 245 mM, pH 7 phosphate buffer (No NaCl) with 50 mM glucose at 38 °C, 1000 rpm.

REFERENCES

References

- 1. S. C. Barton, J. Gallaway and P. Atanassov, "Enzymatic biofuel cells for Implantable and microscale devices," *Chemical Reviews*, **104**(10), 4867-4886 (2004).
- 2. M. Rigla, M. E. Hernando, E. J. Gomez, E. Brugues, G. Garcia-Saez, I. Capel, B. Pons and A. de Leiva, "Real-time continuous glucose monitoring together with telemedical assistance improves glycemic control and glucose stability in pump-treated patients," *Diabetes Technology & Therapeutics*, **10**(3), 194-199 (2008).
- 3. A. Heller, "Implanted electrochemical glucose sensors for the management of diabetes," *Annual Review of Biomedical Engineering*, **1**, 153-175 (1999).
- 4. E. H. Yu and K. Scott, "Enzymatic Biofuel Cells-Fabrication of Enzyme Electrodes," *Energies*, **3**(1), 23-42 (2010).
- 5. S. C. Barton, "Enzyme catalysis in biological fuel cells" in Handbook of Fuel Cells Fundamentals, Technology and Applications (ed. Wolf Vielstich, H. Y., Hubert Andreas Gasteiger) (2009).
- 6. A. L. Ghindilis, P. Atanasov and E. Wilkins, "Enzyme-catalyzed direct electron transfer: Fundamentals and analytical applications," *Electroanalysis*, **9**(9), 661-674 (1997).
- 7. S. Shleev, A. Jarosz-Wilkolazka, A. Khalunina, O. Morozova, A. Yaropolov, T. Ruzgas and L. Gorton, "Direct electron transfer reactions of laccases from different origins on carbon electrodes," *Bioelectrochemistry*, **67**(1), 115-124 (2005).
- 8. D. Ivnitski, B. Branch, P. Atanassov and C. Apblett, "Glucose oxidase anode for biofuel cell based on direct electron transfer," *Electrochemistry Communications*, **8**(8), 1204-1210 (2006).
- 9. Y. D. Zhao, W. D. Zhang, H. Chen and Q. M. Luo, "Direct electron transfer of glucose oxidase molecules adsorbed onto carbon nanotube powder microelectrode," *Analytical Sciences*, **18**(8), 939-941 (2002).
- 10. O. Courjean, F. Gao and N. Mano, "Deglycosylation of Glucose Oxidase for Direct and Efficient Glucose Electrooxidation on a Glassy Carbon Electrode," *Angewandte Chemie-International Edition*, **48**(32), 5897-5899 (2009).
- 11. N. Mano, F. Mao and A. Heller, "On the parameters affecting the characteristics of the "wired" glucose oxidase anode," *Journal of Electroanalytical Chemistry*, **574**(2), 347-357 (2005).

- 12. J. W. Gallaway and S. A. C. Barton, "Effect of redox polymer synthesis on the performance of a mediated laccase oxygen cathode," *Journal of Electroanalytical Chemistry*, **626**(1-2), 149-155 (2009).
- 13. N. Mano, F. Mao and A. Heller, "Characteristics of a miniature compartment-less glucose-O-2 biofuel cell and its operation in a living plant," *Journal of the American Chemical Society*, **125**(21), 6588-6594 (2003).
- 14. N. S. Hudak and S. C. Barton, "Mediated biocatalytic cathode for direct methanol membrane-electrode assemblies," *Journal of the Electrochemical Society*, **152**(5), A876-A881 (2005).
- 15. H. Sakai, T. Nakagawa, Y. Tokita, T. Hatazawa, T. Ikeda, S. Tsujimura and K. Kano, "A high-power glucose/oxygen biofuel cell operating under quiescent conditions," *Energy & Environmental Science*, **2**(1), 133-138 (2009).
- 16. G. T. R. Palmore and H. H. Kim, "Electro-enzymatic reduction of dioxygen to water in the cathode compartment of a biofuel cell," *Journal of Electroanalytical Chemistry*, **464**(1), 110-117 (1999).
- 17. S. M. Zakeeruddin, D. M. Fraser, M. K. Nazeeruddin and M. Gratzel, "Towards Mediator Design Characterization of Tris-(4,4'-Substituted-2,2'-Bipyridine) Complexes of Iron(Ii), Ruthenium(Ii) and Osmium(Ii) as Mediators for Glucose-Oxidase of Aspergillus-Niger and Other Redox Proteins," *Journal of Electroanalytical Chemistry*, 337(1-2), 253-283 (1992).
- 18. S. Topcagic and S. D. Minteer, "Development of a membraneless ethanol/oxygen biofuel cell," *Electrochimica Acta*, **51**(11), 2168-2172 (2006).
- 19. M. J. Moehlenbrock and S. D. Minteer, "Extended lifetime biofuel cells," *Chemical Society Reviews*, **37**(6), 1188-1196 (2008).
- 20. W. E. Farneth and M. B. D'Amore, "Encapsulated laccase electrodes for fuel cell cathodes," *Journal of Electroanalytical Chemistry*, **581**(2), 197-205 (2005).
- 21. J. W. Gallaway and S. A. C. Barton, "Kinetics of redox polymer-mediated enzyme electrodes," *Journal of the American Chemical Society*, **130**(26), 8527-8536 (2008).
- 22. T. Delumleywoodyear, P. Rocca, J. Lindsay, Y. Dror, A. Freeman and A. A. Heller, "Polyacrylamide-Based Redox Polymer for Connecting Redox Centers of Enzymes to Electrodes," *Analytical Chemistry*, **67**(8), 1332-1338 (1995).
- 23. Z. Q. Gao, G. Binyamin, H. H. Kim, S. C. Barton, Y. C. Zhang and A. Heller, "Electrodeposition of redox polymers and co-electrodeposition of enzymes by coordinative crosslinking," *Angewandte Chemie-International Edition*, **41**(5), 810-+ (2002).

- 24. N. S. Hudak, J. W. Gallaway and S. C. Barton, "Formation of mediated biocatalytic cathodes by electrodeposition of a redox polymer and laccase," *Journal of Electroanalytical Chemistry*, **629**(1-2), 57-62 (2009).
- 25. E. S. Forzani, M. Otero, M. A. Perez, M. L. Teijelo and E. J. Calvo, "The structure of layer-by-layer self-assembled glucose oxidase and Os(Bpy)(2)CIPyCH2NH-Poly(allylamine) multilayers: Ellipsometric and quartz crystal microbalance studies," *Langmuir*, **18**(10), 4020-4029 (2002).
- 26. N. Mano, F. Mao and A. Heller, "Electro-oxidation of glucose at an increased current density at a reducing potential," *Chemical Communications*(18), 2116-2117 (2004).
- 27. A. Heller, "Electrical Wiring of Redox Enzymes," *Accounts of Chemical Research*, **23**(5), 128-134 (1990).
- 28. F. Mao, N. Mano and A. Heller, "Long tethers binding redox centers to polymer backbones enhance electron transport in enzyme "wiring" hydrogels," *Journal of the American Chemical Society*, **125**(16), 4951-4957 (2003).
- 29. D. A. Guschin, J. Castillo, N. Dimcheva and W. Schuhmann, "Redox electrodeposition polymers: adaptation of the redox potential of polymer-bound Os complexes for bioanalytical applications," *Analytical and Bioanalytical Chemistry*, **398**(4), 1661-1673 (2010).
- 30. A. Heller, Z. Q. Gao, G. Binyamin, H. H. Kim, S. C. Barton and Y. C. Zhang, "Electrodeposition of redox polymers and co-electrodeposition of enzymes by coordinative crosslinking," *Angewandte Chemie-International Edition*, **41**(5), 810-+ (2002).
- 31. E. J. Calvo, R. Etchenique, L. Pietrasanta, A. Wolosiuk and C. Danilowicz, "Layer-by-layer self-assembly of glucose oxidase and Os(Bpy)(2)CIPyCH2NH-poly(allylamine) bioelectrode," *Analytical Chemistry*, **73**(6), 1161-1168 (2001).
- 32. J. Hodak, R. Etchenique, E. J. Calvo, K. Singhal and P. N. Bartlett, "Layer-by-layer self-assembly of glucose oxidase with a poly(allylamine)ferrocene redox mediator," *Langmuir*, **13**(10), 2708-2716 (1997).
- 33. D. N. Blauch and J. M. Saveant, "Dynamics of Electron Hopping in Assemblies of Redox Centers Percolation and Diffusion," *Abstracts of Papers of the American Chemical Society*, **203**, 343-PHYS (1992).
- 34. A. Aoki, R. Rajagopalan and A. Heller, "Effect of Quaternization on Electron-Diffusion Coefficients for Redox Hydrogels Based on Poly(4-Vinylpyridine)," *Journal of Physical Chemistry*, **99**(14), 5102-5110 (1995).

- 35. D. Chakraborty and S. C. Barton, "Influence of Mediator Redox Potential on Fuel Sensitivity of Mediated Laccase Oxygen Reduction Electrodes," *Journal of the Electrochemical Society*, **158**(4), B440-B447 (2011).
- 36. J. W. Gallaway, *PhD Thesis*, *Redox Polymer Mediation for Enzymatic Biofuel Cells*, Columbia University (2007).
- 37. A. B. P. Lever, "Electrochemical Parametrization of Metal-Complex Redox Potentials, Using the Ruthenium(Iii) Ruthenium(Ii) Couple to Generate a Ligand Electrochemical Series," *Inorganic Chemistry*, **29**(6), 1271-1285 (1990).
- 38. B. B. Dambatta and J. R. Ebdon, "Kinetic-Studies of Free-Radical Polymerizations of 1-Vinylimidazole Initiated by Benzoyl Peroxide and Azoisobutyronitrile," *European Polymer Journal*, **22**(10), 783-786 (1986).
- 39. R. J. Forster and J. G. Vos, "Synthesis, Characterization, and Properties of a Series of Osmium-Containing and Ruthenium-Containing Metallopolymers," *Macromolecules*, **23**(20), 4372-4377 (1990).
- 40. a. F. A. J. Bard, *Electrochemical methods: fundamentals and applications* (2001).
- 41. D. Chakraborty, *PhD Thesis*, *Enzyme Electrocatalysis in Mediated Bioelectrodes*, Michigan State University (2010).
- 42. S. C. Barton, Y. H. Sun, B. Chandra, S. White and J. Hone, "Mediated enzyme electrodes with combined micro- and nanoscale supports," *Electrochemical and Solid State Letters*, **10**(5), B96-B100 (2007).
- 43. T. J. Ohara, R. Rajagopalan and A. Heller, "Glucose Electrodes Based on Cross-Linked [Os(Bpy)(2)](+/2+) Complexed Poly(L-Vinylimidazole) Films," *Analytical Chemistry*, **65**(23), 3512-3517 (1993).
- 44. S. A. M. Vanstroebiezen, A. P. M. Janssen and L. J. J. Janssen, "Solubility of Oxygen in Glucose Solutions," *Analytica Chimica Acta*, **280**(2), 217-222 (1993).
- 45. C. P. Andrieux and J. M. Saveant, "Kinetics of Electrochemical Reactions Mediated by Redox Polymer-Films Irreversible Cross-Exchange Reactions Formulation in Terms of Characteristic Currents for Stationary Techniques," *Journal of Electroanalytical Chemistry*, **134**(1), 163-166 (1982).
- 46. T. J. Ohara, R. Rajagopalan and A. Heller, "Glucose Electrodes Based on Cross-Linked [Os(Bpy)2cl]+/2+ Complexed Poly(1-Vinylimidazole) Films," *Abstracts of Papers of the American Chemical Society*, **207**, 94-PMSE (1994).
- 47. A. Heller, "Electron-conducting redox hydrogels: desgin, characteristics and synthesis," *Current opinion in Chemical Biology*, **10**, 664-672 (2006).

- 48. G. Ybarra, C. Moina, F. V. Molina, M. I. Florit and D. Posadas, "Morphology and swelling of Os(II) polyvinyl-bypyridile films The influence of pH and applied potential," *Electrochimica Acta*, **50**(7-8), 1505-1513 (2005).
- 49. M. V. Pishko, A. Mugweru and B. L. Clark, "Electrochemical redundant microsensor arrays for glucose monitoring with patterned polymer films," *Electroanalysis*, **19**(4), 453-458 (2007).
- 50. T. J. Ohara, R. Rajagopalan and A. Heller, "Wired Enzyme Electrodes for Amperometric Determination of Glucose or Lactate in the Presence of Interfering Substances," *Analytical Chemistry*, **66**(15), 2451-2457 (1994).
- 51. K. K., "The effect of hydrogen peroxide on glucose oxidase from *Aspergillus niger*," *Biochemistry*, **5**, 139-143 (1966).
- 52. G. Binyamin and A. Heller, "Stabilization of wired glucose oxidase anodes rotating at 1000 rpm at 37 degrees C," *Journal of the Electrochemical Society*, **146**(8), 2965-2967 (1999).
- 53. Y. Sun, *PhD Thesis*, *Mediated Enzyme Electrodes with Combined Micro- and Nanoscale Supports*, 2006).
- 54. A. Heller, "Electrical Connection of Enzyme Redox Centers to Electrodes," *Journal of Physical Chemistry*, **96**(9), 3579-3587 (1992).

Chapter 3: Kinetics of Osmium Redox Polymer Mediated Glucose Oxidase Electrodes

Abstract

The kinetic parameters of glucose-oxidizing osmium redox polymer mediated glucose oxidase (GOx) electrodes are estimated and elucidated in the presence and absence of oxygen via novel mathematical approach which incorporates the effect of competitive oxygen reduction. The glucose-oxidizing electrode described in the previous chapter was simulated on one dimension using a reaction-diffusion model in which the oxygen reduction reaction is treated as a first-order step. Results were found to be in excellent agreement with the experimental data. In the presence of oxygen, the redox mediator competes with oxygen for electrons at the reduced GOx active site. It is demonstrated that in the absence and presence of oxygen, turnover number (k_{cat}) of the enzyme remains constant indicative of a competitive inhibition mechanism. Fitting of the model to experimental data yields a rate constant, k_O , which characterizes the impact of oxygen on electrode performance.

Introduction

In biofuel cells or biosensors, enzymes convert chemical energy of substrates into electrical energy and this transformation can be enhanced greatly using electron transfer mediators such as osmium complexes, ferrocenes, quinones, which are either immobilized on the electrode surface or present in the solution as a homogeneous system. Despite the high diffusivities of dissolved mediators, an immobilized mediator is often preferred because redox

active species can be retained near the electrode surface to maintain the high mediation efficiency. Current generated at the electrode surface is a useful quantity for sensing of the substrate as an analyte, as in biosensors, or for producing power in a biofuel cell. In enzymatic biofuel cell (EFC) applications, it is desired to have high power output and therefore high current density and reaction rate. Mathematical models can be used to identify and optimize pivotal experimental parameters such as diffusivity of mediators, loading of biocatalysts, amount of substrates, mediators and inhibitors etc. that affect the performance of EFCs. Models must incorporate deliberation of various processes like electron and species transport, reaction kinetics and combination of these, which controls the overall performance. Mathematical treatments of such systems have been presented in the literature, which are based on either traditional species material balance with reaction and mass transport conditions ⁸⁻¹⁰ or based on metabolic control analysis ¹¹ (MCA) or statistical analysis methods. ¹²

Andrieux and Saveant investigated the redox polymer mediated system and related limiting processes to the concentration profiles internal and external to the film. $^{13-15}$ Bartlett *et al.* extended the analysis by considering Michaelis-Menten enzyme kinetics and presented one-dimensional catalytic film model with steady state material balances on the substrate and mediator considering transport only by diffusion and it has been extensively used for elucidating the kinetics of an immobilized and diffusive enzyme-mediator system. 8,16 Gallaway *et al.* used this approach to obtain the kinetic information of O_2 reducing laccase-based electrodes having different osmium redox polymer mediated redox hydrogels. 3 It was found that the rate constant

between laccase and O_2 was slightly lower than in the free solution. It was also shown that the rate constant between mediator and laccase scales linearly at low electron transfer driving force (ΔE_T) and becomes constant as ΔE_T increases. Tamaki $et~al.^{17}$ used this technique to model glucose oxidation on the high surface area carbon black redox polymer mediated enzyme electrode, where they claim that the mediator diffusivity is not a rate determining step for overall electrode kinetics. Using some of the limiting cases from the Bartlett et~al., Calvo and coworkers obtained the kinetic parameters for several layer-by-layer self-assembled ultrathin films (<100 nm) of osmium and ferrocene mediated glucose oxidase (GOx) electrodes having spatially ordered enzyme assemblies. $^{18-21}$

In glucose/ O_2 EFC, oxygen is required for the cathode but it also engages in a competing reaction at the GOx based anode, which decreases the overall efficiency of the cell (Equation 1.9). Using an efficient redox mediator or an oxygen insensitive enzyme like pyronase dehdrogenase²² such effect of oxygen can be minimized. Glykys *et al.*¹¹ used metabolic control analysis (MCA) analysis to probe an EFC based on the osmium redox polymer mediated GOx anode and laccase cathode. They applied the MCA analysis on the experimental data from the literature^{3,23} and albeit fitting to the experimental data was poor they conclude that variation in the O_2 concentration in solution would not affect the GOx kinetics as long as the mediator concentration is high. However, this prediction was not experimentally verified.

This work focuses on the extraction and elucidation of the kinetics of glucose-oxidizing osmium redox polymer mediated GOx films in the presence and absence of oxygen. Redox

hydrogel thickness (L) for such electrodes is usually ~1µm (as discussed in the chapter 2) therefore gradients in substrate concentration in the film are usually trivial³ due to high diffusion coefficient (~10⁻⁵ cm² s⁻¹) and saturated conditions but mediator concentration inside the film varies significantly, which can be attributed to slow electron transport, characterized via an apparent diffusion coefficient, D_m , of the order of 10^{-9} . Electrochemical regeneration of osmium based redox polymer mediators at the electrode is typically fast and reversible^{3,24} but the overall reaction rate may be limited by the enzyme kinetics if is ΔE_{et} is low,³ Michaelis constant with respect to the mediator is high,³ or an inhibitor is present.²⁵

We have adapted the model work of Bartlett *et al.*, ⁸ in order to consider the absence and presence of oxygen in the mediated glucose electrode. The governing equations described below are solved numerically using MATLAB[®]. The consequences of the several key parameters like mediator properties, glucose and oxygen concentration are explored via simulation and governing equations can be solved analytically for certain limiting cases.

The Model

In general enzyme-catalyzed electron transfer between two substrates can be described by the bi-bi-ping-pong mechanism where the first product is released before the second substrate attaches to the enzyme. ^{3,10,26} Figure 3.1a shows the general reaction scheme of reaction rate in the redox hydrogel film-modified enzyme electrodes, which may be limited by several factors namely electron transport via mediator, enzyme kinetics, substrate transport and may be affected

by the presence of inhibitors like methanol in the case of laccase based enzyme electrodes or oxygen for the GOx based electrodes. For example in case of mediated GOx electrodes, the glucose and mediator can be considered as an individual substrates of GOx. However when oxygen is present in such system, it can be considered as a third substrate, which is a natural oxidizing agent of GOx. Three reaction steps can therefore describe the overall glucose oxidation:

$$v_s S + E_{ox} \xrightarrow{k_E} v_s P + E_{red}$$
(aq.) (aq.) [3.1]

$$v_m M_{\text{ox}} + E_{\text{red}} \xrightarrow{k_m} v_m M_{\text{red}} + E_{\text{ox}}$$
(aq.) (3.2)

$$v_o O_2 + E_{\text{red}} \xrightarrow{k_o} v_o H_2 O_2 + E_{\text{ox}}$$
(aq.) (3.3)

The glucose-oxidizing enzyme anode in the presence of O_2 is illustrated in Figure 3.1a, adapted from Bartlett *et al.*, where S is glucose, P is glucono- δ -lactone, M_{ox} and M_{red} are the oxidized and reduced osmium moieties of the redox polymer, E_{ox} and E_{red} are the oxidized and reduced form of the enzymes. Stoichiometric coefficients v_s , v_p , v_m and v_o are 0.5, 0.5, 1 and 1 respectively. k_m , k_E and k_O are the second order rate constants describing the reaction between the enzyme and mediator, glucose and oxygen respectively. Assuming Michaelis-Menten kinetics for glucose we can write

$$k_E = \frac{k_{cat}}{K_S + [S]} \tag{3.4}$$

where k_{cat} and K_S are the turnover number of enzyme and apparent Michaelis constant with respect to glucose respectively. Apparent Michaelis constant for mediator can be defined as

$$K_M = \frac{k_{cat}}{k_m} .$$

Therefore we can write following non-linear second-order differential equations which describes the reaction and diffusion within the film:

$$\frac{\partial [M_{ox}]}{\partial t} = D_M \frac{\partial^2 [M]}{\partial x^2} - k_m [E_{red}][M_{ox}]$$
(aq.)

$$\frac{\partial[S]}{\partial t} = D_S \frac{\partial^2[S]}{\partial x^2} - \frac{k_{cat}[E_{ox}][S]}{K_S + [S]}$$
(aq.)

$$\frac{\partial [O_2]}{\partial t} = D_o \frac{\partial^2 [O_2]}{\partial x^2} - k_o [E_{red}][O_2]$$
(aq.)

$$\frac{\partial [E_{ox}]}{\partial t} = k_m [E_{red}][M_{ox}] - \frac{k_{cat}[E_{ox}][S]}{K_S + [S]} + k_o [E_{red}][O_2]$$
(aq.) (aq.) (aq.)

Now assuming that enzyme is bound within the film (not free to diffuse) and at steady state,

$$E_{red} = \frac{k_{cat} E_T[S]}{(K_S + [S])(k_m[M_{OY}] + k_O[O_2]) + k_{cat}[S]}$$
[3.9]

where $E_T = E_{ox} + E_{red}$ represents the total concentration of the immobilized enzyme, [S], [M_{OX}] and [O₂] indicates substrate, oxidized mediator and oxygen concentration respectively. D_m , D_S and D_O are the diffusivities of mediator, substrate and oxygen in the film respectively. Values of D_S and D_O are taken from the literature as 7×10^{-6} cm² s⁻¹ and 1.5×10^{-5} cm² s⁻¹ respectively. At steady state, eqs. (3.5), (3.6) and (3.7) reduce to the following by substitution of $[E_{ox}]$ or $[E_{red}]$ from equation (3.8):

$$D_A \frac{\partial^2 [M_{ox}]}{\partial x^2} = \frac{k_m k_{cat} E_T[S][M_{ox}]}{(K_S + [S])(k_m [M_{ox}] + k_O[O_2]) + k_{cat}[S]}$$
[3.10]

$$D_O \frac{\partial^2 [O_2]}{\partial x^2} = \frac{k_O k_{cat} E_T[S][O_2]}{(K_S + [S])(k_m[M_{ox}] + k_O[O_2]) + k_{cat}[S]}$$
[3.11]

$$D_S \frac{\partial^2[S]}{\partial x^2} = \frac{k_{cat} E_T[S](k_m[M_{ox}] + k_O[O_2])}{(K_S + [S])(k_m[M_{ox}] + k_O[O_2]) + k_{cat}[S]}$$
[3.12]

Following Bartlett *et al.*, ⁸ Eqs. (3.8), (3.9) and (3.10) can be made dimensionless by introducing following parameters:

$$s = \frac{[S]}{p_{S}[S]_{\infty}}; \quad a = \frac{[M_{oX}]}{p_{a}[M_{T}]_{\infty}}; \quad o = \frac{[O_{2}]}{p_{o}[O_{2}]_{\infty}}; \quad \chi = \frac{x}{L}; \quad \kappa = L\sqrt{\frac{k_{m}E_{T}}{D_{m}}}$$

$$\eta = \frac{D_{S}k_{m}K_{S}}{D_{m}k_{cat}}; \quad \gamma = \frac{K_{S}k_{m}[M_{T}]_{\infty}}{k_{cat}[S]_{\infty}}; \quad \beta = \frac{K_{S}k_{O}[O_{2}]_{\infty}}{k_{cat}[S]_{\infty}}; \quad \mu = \frac{[S]_{\infty}}{K_{S}}; \quad d = \frac{D_{S}}{D_{O}}$$
[3.13]

where $[M_T]_{\infty}$, $[S]_{\infty}$ and $[O_2]_{\infty}$ are the bulk concentration of mediator, glucose substrate and oxygen in the system respectively. Ratio of concentration of species into film to that of the bulk

solution is described by p_s , p_a and p_o , which denotes the substrate, mediator and oxygen partition coefficient respectively. s, a and o are the dimensionless concentrations of substrate, mediator and oxygen respectively. L is the thickness of the hydrogel. χ is the normalized distance from the electrode interface. κ , γ , η and μ have their usual meanings as described by Bartlett et al. 8 β and d are the additional parameters that stem from our model. β is similar to that of γ which describes the balance between two forms of the enzyme. Along with oxidized mediator, now oxygen also oxidizes the reduced form of GOx. When β >>1, GOx enzymes will be in the oxidized form and when β <<1, the reduced form of GOx predominates. But this situation is coupled with γ which also controls the oxidation state of GOx. The parameter d is the ratio of substrate diffusion to that of oxygen diffusion in the film. The system will be substrate limited when d<<1. Substitution of parameters from eq. (3.13) to equation (3.10), (3.11) and (3.12) gives

$$\frac{d^2a}{d\chi^2} = \frac{\kappa^2 as}{(\gamma a + \beta o)(1 + \mu s) + s}$$
 [3.14]

$$\frac{d^2o}{d\chi^2} = \frac{\kappa^2 os \eta^{-1} \beta d}{(\gamma a + \beta o)(1 + \mu s) + s}$$
 [3.15]

$$\frac{d^2s}{d\chi^2} = \frac{\kappa^2 a s \eta^{-1} \gamma}{(\gamma a + \beta o)(1 + \mu s) + s} + \frac{\kappa^2 o s \eta^{-1} \beta}{(\gamma a + \beta o)(1 + \mu s) + s}$$
[3.16]

Dimensionless boundary conditions for eqns. (3.14) - (3.16) are as follows:

at
$$\chi = 0$$
; $\frac{ds}{d\chi} = 0$; $\frac{do}{d\chi} = 0$; $a = a_e$ [3.17]

at
$$\chi = 1$$
; $s = 1 - \sigma_1 \left(\frac{ds}{d\chi} \right)$; $o = 1 - \sigma_2 \left(\frac{do}{d\chi} \right)$; $\frac{da}{d\chi} = 0$ [3.18]

Dimensionless parameters σ_1 and σ_2 characterizes the glucose and oxygen boundary conditions which accounts for the mass transfer correction of both the species at the film-solution interface.²⁷

$$\sigma_1 = \frac{\delta_1 D_S p_s}{L D_1}; \quad \delta_1 = 4.98 D_S^{1/3} v^{1/6} \omega^{-1/2}$$
 [3.19]

$$\sigma_2 = \frac{\delta_2 D_O p_O}{L D_2}; \quad \delta_2 = 4.98 D_O^{1/3} v^{1/6} \omega^{-1/2}$$
 [3.20]

where,

 D_I = Glucose diffusion coefficient in bulk solution.

 D_2 = Oxygen diffusion coefficient in the bulk solution.

 δ_I = Diffuse layer thickness of glucose at the film-solution interface

 δ_2 = Diffuse layer thickness of oxygen at the film-solution interface

 p_S = Partition coefficient of glucose at the film-solution interface

 p_O = Partition coefficient of oxygen at the film-solution interface

v =Kinematic viscosity of the electrolyte

 ω = Rotation rate of electrode in rpm.

Mostly because glucose and oxygen concentration gradients internal to the film are found to be negligibly small (Figure 3.1b), D_1 and D_2 are assumed to be equal to D_S and D_O respectively. The parameter a_e in eqn. (3.17) is dimensionless mediator concentration, which can be defined as:

$$a_e = \frac{1}{1 + \exp(-\varepsilon)}$$
 and $\varepsilon = \frac{(E - E^0)nF}{RT}$ [3.21]

where ε is the dimensionless potential obtained from the Nernst equation ²⁸ assuming that the electrode kinetics for the mediator at the electrode is fast and reversible. E is the potential at the electrode surface, E^0 is the formal potential of the mediator couple, n is the number of electrons transferred by mediator at the electrode surface, E^0 is the Faraday constant, E^0 is the universal gas constant and E^0 is the absolute temperature. Now the flux mediator at the electrode surface that is measured as a current can be given as ⁸

$$j_{obs} = -D_m \left(\frac{d[M_{ox}]}{dx}\right)_{x=0}$$
 [3.22]

and in dimensionless form

$$J_{obs} = \frac{Lj_{obs}}{D_m[M_T]} = -\left(\frac{da}{d\chi}\right)_{r=0}$$
 [3.23]

Therefore current measured at the electrode surface is

$$i = nFAj_{obs} ag{3.24}$$

where i is the current in ampere and A is the electrode area in cm².

Key assumptions of the model are i) Simple Michaelis-Menten kinetics for the reaction of enzyme and glucose substrate ii) Second order reaction between enzyme-mediator and enzymeoxygen iii) Both enzyme and mediator are confined within the film iv) Partition coefficients at the film-solution interface for mediator, substrate and oxygen is equal to 1. In the absence of O_2 , this model reduces to the two substrate ping-pong model proposed by Bartlett et al.⁸ where they have solved two non-linear differential equations numerically and approximate analytical solutions are presented for several limiting cases. Our model also incorporates the mass transfer correction ²⁷ for glucose and oxygen at the film-solution interface and *iR* correction was applied to all the electrode potentials to account for the Ohmic losses in the bulk electrolyte. 3,28 In Chapter 2, the charge transport of mediator (D_m) which is one of the critical parameter that governs the performance of such redox polymer mediated enzyme electrodes was quantified along with the active mediator concentration which is responsible for the current at the electrode surface. Nominal loading of the redox polymer mediator on one electrode is ~4 M but only 660 mM (~17%) of it is active for polymer A and 380 mM (~10%) for polymer B as determined by Coulometry²⁸ in chapter 2. Another variable that greatly influence the reaction rate and kinetics of such electrode is active or "wired" enzyme concentration that is responsible for the catalytic conversion of substrate into product. Several examples can be found in the literature in which the

kinetic parameters for GOx mediated reaction are taken from the analysis under aerobic conditions with O2 as a natural electron acceptor without any additional justification of the effect of redox mediator. ²⁹⁻³¹ One such example in which, Calvo et al. ¹⁸ obtained the active enzyme concentration of $\sim 2.2 \times 10^{-13}$ mol/cm² for self-assembled poly(allylamine) based osmium redox polymer mediated GOx electrodes by fitting the substrate variation data (like Figure 3.2a or 3.2c) to the ping-pong rate expression³² after assuming k_{cat} and K_{S} value of 700 s⁻¹ and 25 mM respectively which, are the kinetic parameters of GOx in free solution with O2 as the natural redox partner. In those spatially ordered enzyme assemblies only ~1% of the deposited enzymes was effectively wired by the redox mediator. In this work along with mediator and cross-linker, we drop cast nominal enzyme loading of $\sim 1.79 \times 10^{-9}$ mol/cm² on one electrode and with their approach for polymer A mediated GOx electrodes under N2 saturated conditions, we get active enzyme loading of 4.23×10^{-11} mol/cm⁻² which is ~ 2.35 % of the nominal loading. However, it is arguable to assume the kinetic parameters of the free solution for such redox polymer mediated enzyme studies. Also, the assumptions made in their analysis are limited for the thin films of $\sim 0.1 \, \mu m$ or less whereas in our case hydrogel film thickness is of the order of $\sim 1 \, \mu m$. This necessitates the extraction and elucidation of kinetic parameters for such system where species are confined and randomly distributed on the electrode surface. Gallaway et al.³ extracted and elucidated the kinetics of such several osmium redox polymer mediated laccase electrodes by slight modification in the two-substrate ping-pong model of Bartlett and Pratt.⁸

Here we have solved three equations (3.15), (3.16) and (3.17) using *bvp4c* solver of MATLAB[®] and code for all simulations are provided the Appendices section.

Results and discussion

Determination of kinetic parameters

Table 3.1(a) shows the formula and physical properties of the synthesized redox polymers. In chapter 2, they were used for the GOx mediation purpose and characterized in the presence and absence of O_2 . Table 3.2 shows the list of various parameters and nominal values that are used in the model. In absence of oxygen, the above model simplifies to traditional twosubstrate, Bartlett and Pratt presentation^{3,8} and pertinent kinetic parameters like k_{cat} , k_m and K_S of Table 3.1(b) were obtained using model as shown in Appendix A by fitting the appropriate substrate variation and polarization curve data for N_2 saturated conditions. Appendix ${\bf C}$ shows the input file for the various parameters used in the two-substrate model. From Figure 3.2, it can be seen that numerical predictions of the current density showed an excellent agreement to the experimental data for polymer A mediated electrodes whereas modest fitting was observed for polymer B mediated electrodes attributed to the Nernstian behavior assumption of fast and reversible kinetics for mediator couple at the electrode surface. It can be seen from the cyclic voltammograms of Figure 2.2 (Chapter 2) that kinetics of polymer **B** mediated electrodes are not as fast or reversible as predicted by the Nernst equation hence the moderate fitting.

Turn over number (k_{cat}) and apparent Michaelis constant (K_S) for GOx is in the free solution are normally ~1000 s⁻¹ and ~25 mM respectively which are generally obtained from the

spectrophotometric analysis under aerobic conditions. 33 Whereas in our analysis we obtain k_{cat} of \sim 17 and \sim 12 s⁻¹ for polymer A and polymer B mediated GOx electrodes, which is around two orders of magnitude lower than the values in the free solution where O2 was the final electron acceptor rather than the mediator. 34-36 Since the loading of active enzyme in the film is difficult to assess, the obtained turnover number can be compared with values from free solution by multiplying with nominal enzyme loading to yield the maximum enzyme velocity, $V_{max} = k_{cat} E_T$. Taking this approach we obtain V_{max} values of 0.31 and 0.21 $\text{M}^{-1} \text{s}^{-1}$ for polymer A and B respectively. Whereas V_{max} values for ultrathin GOx-osmium redox polymer mediated films falls in the range of ~ 0.015 - 0.023 M⁻¹ s⁻¹. Weller and co-workers 37,38 obtained the kinetic parameters of osmium redox polymer mediated GOx electrodes in the presence of N2, Air and O_2 using Eadie-Hofstee plots.³⁹ They report apparent K_S of 18.7, 37.5 and 64.5 mM for N_2 , Air and O2 saturated PVP-Os(bpy)2Cl mediated GOx electrodes respectively. However, this approach does not account for the mediator mass transport limitations.

When the two-substrate model was used to fit the experimental data of Air and O_2 saturated conditions for polymer A mediated electrodes, k_{cat} values remained the same as that of the N_2 saturated conditions indicative of the competitive inhibition kinetics of O_2 with K_S values of 12.3 mM, 17.1 mM and 35.1 mM for N_2 , Air and O_2 saturated conditions respectively. Increase in K_S value indicates that oxygen also binds with the enzyme, which can also be seen,

from the Figure 3.2a and 3.2c. In the presence of Air and O_2 , bimolecular rate constant of reaction between enzyme and oxygen, k_O was extracted using proposed three-substrate model (Appendix **B**) as described above by fitting the oxygen concentration and respective plateau current density data by keeping k_{cat} , K_S and k_m constant as obtained from the N_2 saturated conditions. In our model we show a linear rate expression for GOx-oxygen reaction because when we used the non-linear Michalies-Menten type of model similar to that of GOx-substrate reaction, errors in the extracted kinetic parameters were very large indicative of the fact that k_O , which is a bimolecular rate constant of the enzyme- O_2 reaction is an important quantity that characterize the whole system better than the individual turn over number and binding constant with respect to O_2 .

One thing to be noted over here is reported k_{cat} values in Table 3.1(b) are the glucose turnover number. To convert to mediator turnover rate, it must multiplied by two since two mediator moieties required to take two electrons from the reduced GOx active site which are then get transported to the electrode. 35,40 Obtained K_S values for both the mediated enzyme electrodes are almost equal and it is comparable to literature values for polymer A mediated GOx electrodes. 38 Extracted values of k_O for such immobilized redox hydrogel mediated system is approximately one magnitude lower than the value in free solution which is $\sim 1.6 \times 10^{-6} \, \text{M}^{-1} \, \text{s}^{-1}$ where measurements were made using stopped flow experiments and kinetic constants were either obtained from lineweaver-burk polts 41 or bi-bi ping-pong rate expression. 35,36 This could be due to hindrance offered in the GOx-oxygen binding, by the large concentration of osmium

molecules, which are present in the film as compared to oxygen.³ Also, it could be ascribed to the competing reaction between redox polymer and oxygen at the GOx active site, which might affect the electron scavenging capacity of oxygen like it does for the redox polymer.

Effect of glucose and oxygen concentration

Figure 3.3 shows the simulated dimensionless profiles of redox polymer mediator, M_{OX} , glucose substrate, S, oxygen, O_2 , reduced enzyme, E_{red} and catalytic reaction rate, R, within the film for redox polymer A mediated GOx electrodes in N_2 , Air and O_2 saturated conditions. It can be seen that when O_2 is present in the system, oxidized mediator concentration increases, which is discernible from the fact that O_2 being more efficient electron capturing agent due to its higher bimolecular rate constant with respect to GOx and higher diffusivity (D_O) as compared to that of the redox polymer (D_m). Albeit oxygen concentration in the film (~ 0.18 mM for Air and ~ 0.86 mM for O_2 saturated systems) 42 is much lower than that of the mediator concentration (~ 660 mM), it reduces the current density by >10% in air saturated conditions and >30% when electrodes are operated in the O_2 saturated solutions. We can also see that reduced GOx concentration in the film decreases in the presence of oxygen, because along with the mediator, oxygen also oxidizes the reduced GOx enzyme.

Figure 3.4 shows the simulation results for the effect of oxygen on the performance of the polymer A and B mediated GOx electrodes at 50 mM glucose concentration. We can see that increase in oxygen concentration in the system lowers the current density at the electrode surface

due to removal of electrons by O_2 from the reduced active site of GOx (Equation 1.9). This can be helpful in the design of glucose/ O_2 based EFC, where performance of the cell can be predicted at particular O_2 concentration in the system. Our study is limited to only two redox polymers therefore it would be difficult to comment on the effect of mediator redox potential on the bimolecular rate constants of the system unlike Gallaway *et al.*³ and Zakeeruddin *et al.*,⁴³ where they conclude their study based on the wide range of mediator redox potentials.

It can be recognized that parameter space of the simulation for such enzymatic mediated electrodes remains large and we have limited our discussion to the effect of oxygen concentration. Gallaway *et al.*²⁷ explored the consequences of other important parameters like mediator diffusivity, mediator concentration and electrode rotation speed, which are some of the major factors that needs significant attention while engineering the performance of such immobilized redox polymer mediated enzyme electrodes.

Conclusions

One-dimensional model of a redox polymer mediated, glucose-oxidizing GOx enzyme electrode was developed which accounts for the effect of oxygen and pertinent kinetic parameters were successfully extracted by fitting the model to the appropriate experimental data. Obtained kinetic parameter like k_{cat} and k_m is lower when compared with other homogeneous GOx-mediated systems but comparable when coupled with the appropriate enzyme concentrations. Bimolecular rate constant for GOx-oxygen reaction was found to be an order of magnitude lower than that of the free solution due to competition between mediator and oxygen

for the electrons at the reduced active site of GOx. Performance of the system was analyzed via simulation under various conditions. In the presence of oxygen, the reaction rate with respect to mediator and hence the current density at the electrode surface decreases due to unproductive reaction with oxygen.

Table 3.1: (a) Redox polymer properties. (b) Extracted kinetic parameters of the redox polymer-GOx films

(a)

| RP | Structural Formula | E_m^0 (V SHE) | $D_{m} \times 10^{9} \text{ cm}^{2}/\text{s})$ | ΔE_T (V) |
|----|---|-------------------|--|------------------|
| A | $poly(n\text{-VI}_{12}[Os(bpy)_2Cl]^{+/2+}$ | 0.43 | 2.18 ± 0.03 | 0.55 |
| В | $poly(n\text{-VI}_{22}[Os(dm\text{-bpy})_2Cl]^{+/2+}$ | 0.33 | 1.50 ± 0.02 | 0.45 |

(b)

| RP | k_{cat} (s ⁻¹) | $k_m (\text{M}^{-1} \text{s}^{-1})$ | K_S (mM) | $k_o \ (\times \ 10^{-5} \ \mathrm{M}^{-1} \ \mathrm{s}^{-1})$ | $V_{max} (\mathrm{M s}^{-1})$ |
|----|------------------------------|---------------------------------------|----------------|--|-------------------------------|
| A | 17.3 ± 0.6 | 211.9 ± 23.5 | 12.3 ± 0.9 | 1.66 ± 0.3 | 0.31 |
| В | 12.1 ± 1.9 | 35.9 ± 3.7 | 11.7 ± 2.3 | 0.37 ± 0.06 | 0.22 |

Table 3.2: Parameters and nominal values used in the model

| Parameters | Value | References |
|---|--|------------|
| Hydrogel film thickness, L | 1 μm | assumed |
| Diffusivity of polymer \mathbf{A} , D_m | $2.18 \pm 0.03 \text{ cm}^2 \text{ s}^{-1}$ | measured |
| Diffusivity of polymer B | $1.50 \pm 0.02 \text{ cm}^2 \text{ s}^{-1}$ | measured |
| Diffusivity of glucose substrate, D_S | $7 \times 10^{-6} \text{cm}^2 \text{s}^{-1}$ | 3 |
| Diffusivity of oxygen, D_O | $1.5 \times 10^{-5} \text{ cm}^2 \text{ s}^{-1}$ | 20 |
| Nominal enzyme loading, E_T | 18 mM | measured |
| Bulk substrate concentration, S_T | 50 mM | measured |
| Active mediator concentration for polymer \mathbf{A} , M_{ox} | $660 \pm 35 \text{ mM}$ | measured |
| Active mediator concentration for polymer \mathbf{B} , M_{ox} | $380 \pm 28 \text{ mM}$ | measured |
| Bulk oxygen concentration in Air saturated condition, O_T | 0.18 mM | 42 |
| Bulk oxygen concentration in oxygen saturated condition | 0.86 mM | 42 |
| Kinematic viscosity of electrolyte, v | $0.01 \text{ cm}^2 \text{ s}^{-1}$ | assumed |
| Electrode rotation speed, ω | 1000 rpm | measured |

FIGURES

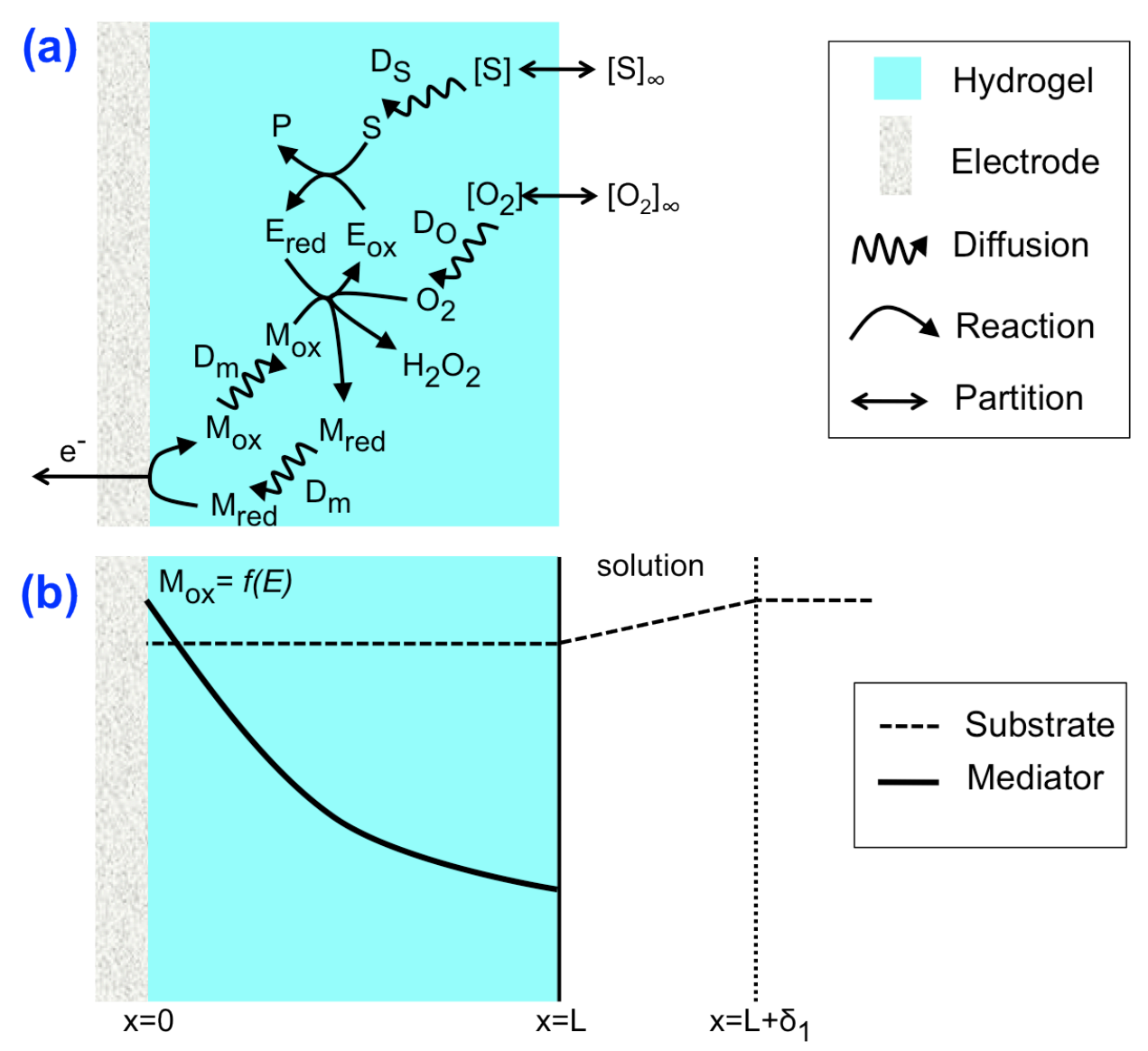


Figure 3.1: (a) Schematic representation of the immobilized redox polymer mediated enzyme electrode showing the processes considered in the model. (b) Sample concentration profiles for the one-dimensional film model. Diffuse layer thickness for glucose substrate is shown as $\delta_I.[S]_{\infty}$ and $[O_2]_{\infty}$ are the bulk concentration of glucose substrate and oxygen in the electrolyte. [S] and $[O_2]$ are the glucose and oxygen concentration in the film respectively. M_{ox} and M_{red} represents the oxidized and reduced form of the mediators respectively. D_s , D_m and D_o represents the diffusivities of substrate, mediator and oxygen respectively.

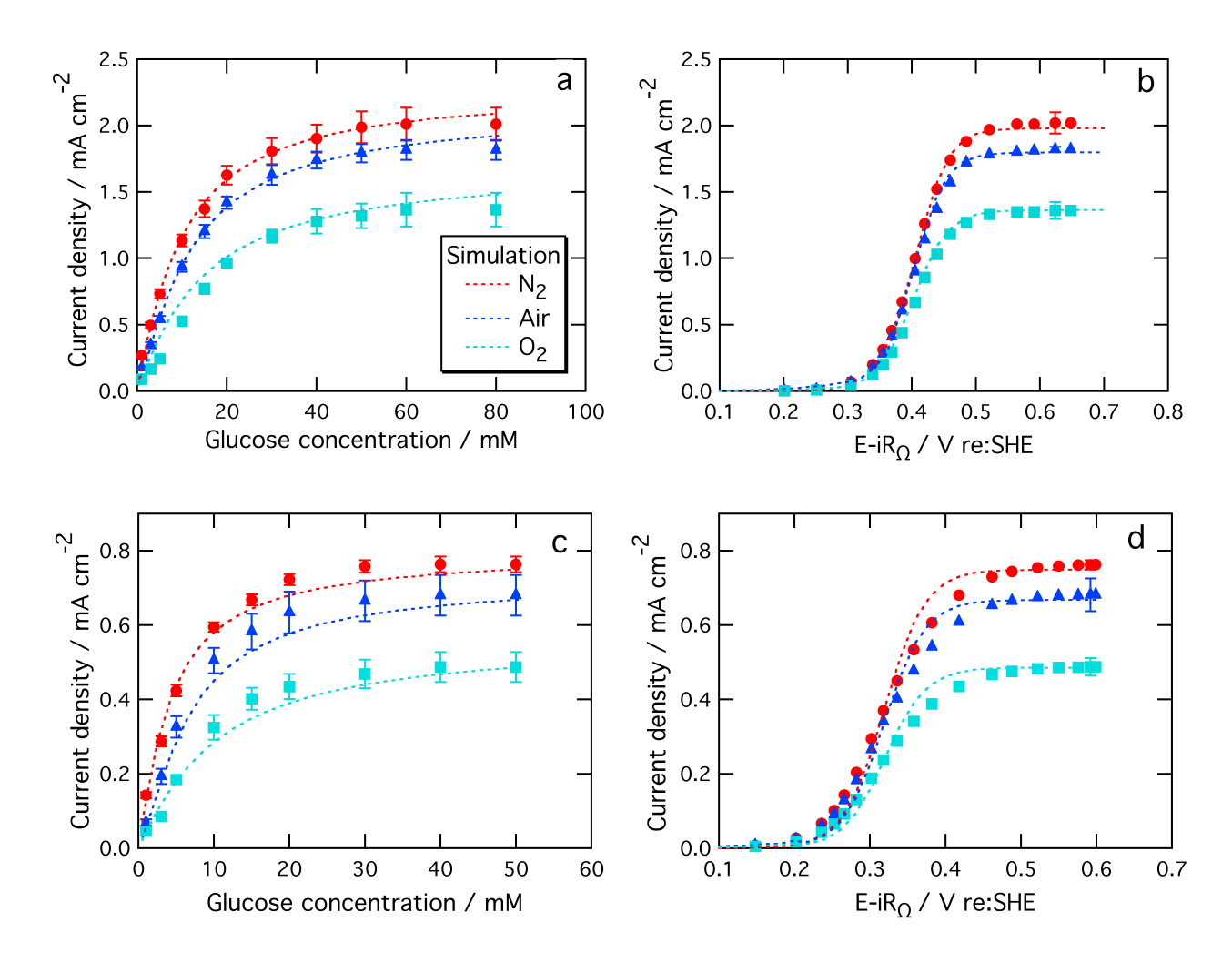


Figure 3.2: Comparison of experimental data to the numerical prediction. Kinetic parameters used in the fitted curve accounts for the mass transfer correction of glucose and oxygen at the film-solution interface. (a) and (c) are the plateau current density for polymer A and B mediated GOx electrodes for varying glucose concentration under N_2 , Air and O_2 . (c) and (d) are the ohmic resistance corrected polarization curves or polymer A and B in 50 mM glucose solution, 250 mM PBS buffer (pH 7, 38 $^{\circ}$ C). Dashed lines in all graphs indicate numerical model results simultaneously fitted to the glucose variation and polarization curves.

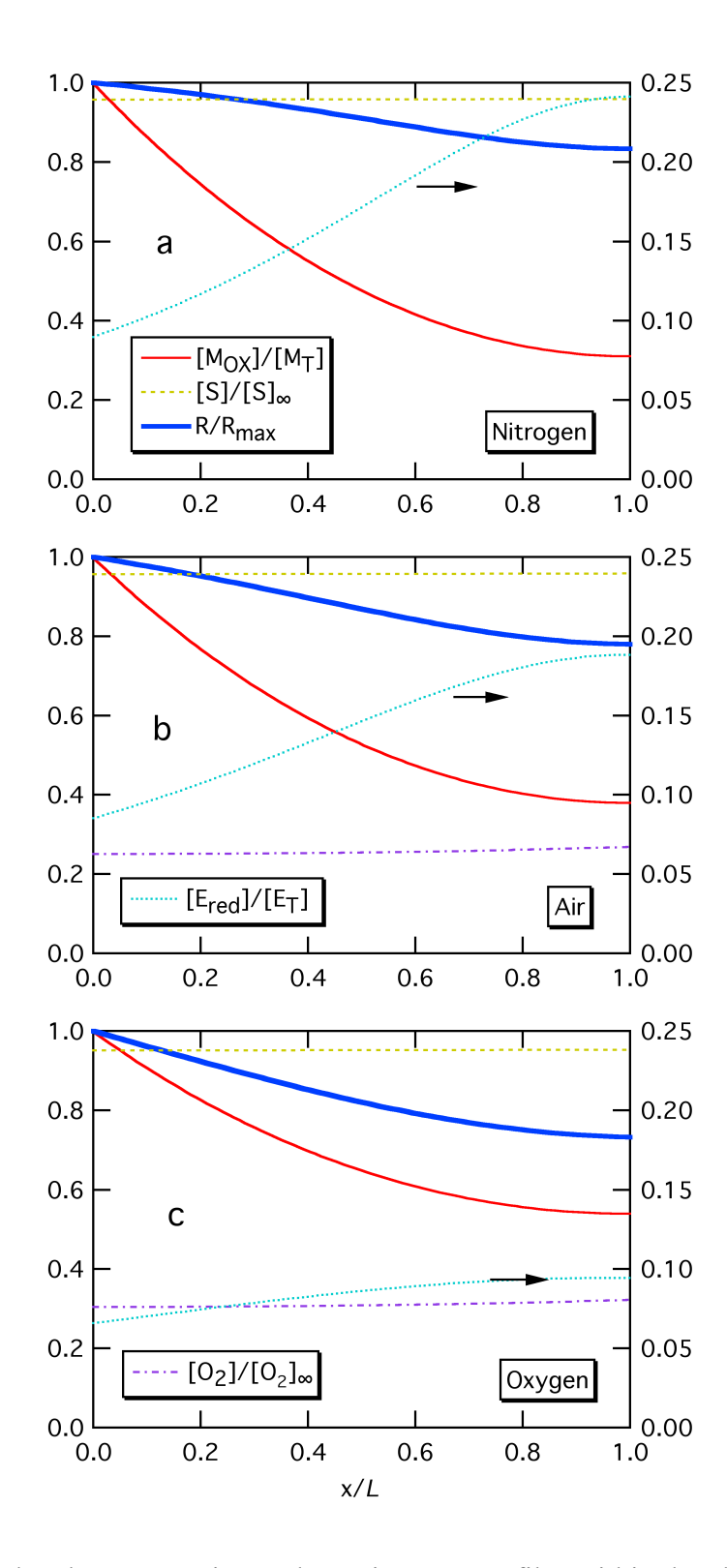


Figure 3.3: Simulated concentration and reaction rate profiles within the electrode film for **A** mediated GOx electrode in the presence of (a) N_2 (b) Air and (c) O_2 . Simulation parameters are taken from the Table 3.1 and 3.2. R/R_{max} represents the ratio of mediator reaction rate to its maximum value.

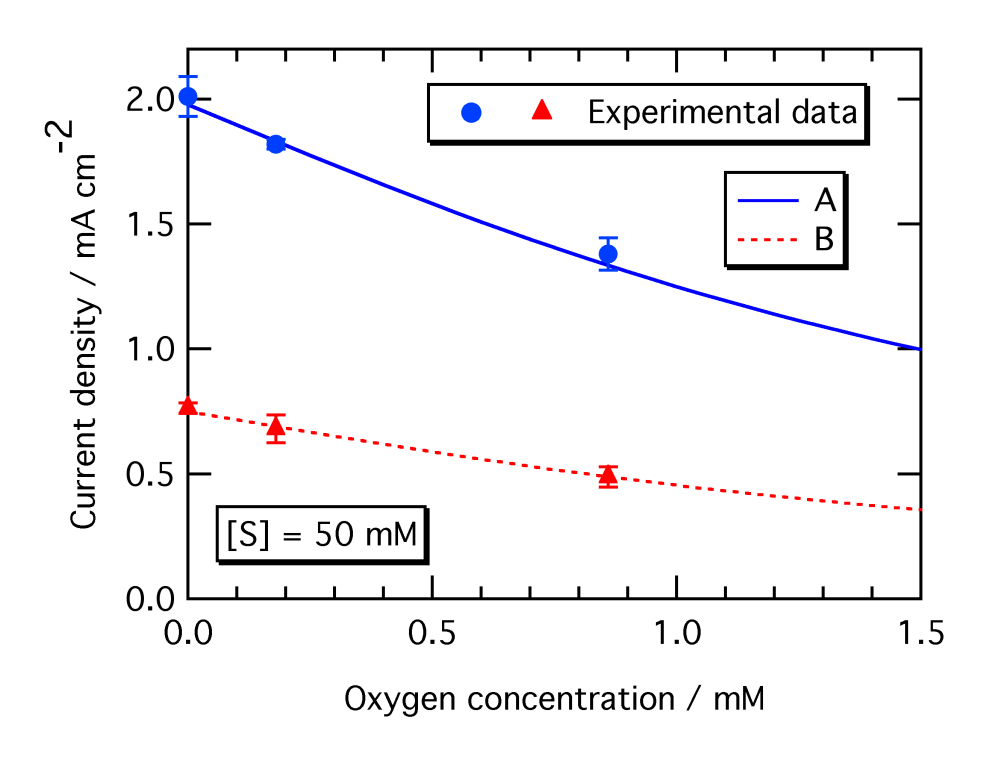


Figure 3.4: Simulation results for the effect of oxygen on GOx enzyme electrode performance at 50 mM glucose concentration, with all parameters as indicated in Table 3.1 and 3.2. Current at the electrode surface goes down with increase in O_2 concentration in the system. Measured experimental values are shown for polymer A and B mediated GOx electrodes.

REFERENCES

References

- 1. S. C. Barton, J. Gallaway and P. Atanassov, "Enzymatic biofuel cells for Implantable and microscale devices," *Chemical Reviews*, **104**(10), 4867-4886 (2004).
- 2. A. Chaubey and B. D. Malhotra, "Mediated biosensors," *Biosensors & Bioelectronics*, **17**(6-7), 441-456 (2002).
- 3. J. W. Gallaway and S. A. C. Barton, "Kinetics of redox polymer-mediated enzyme electrodes," *Journal of the American Chemical Society*, **130**(26), 8527-8536 (2008).
- 4. P. N. Bartlett, V. Flexer, M. V. Ielmini and E. J. Calvo, "Extracting kinetic parameters for homogeneous [Os(bpy)(2)ClPyCOOH](+) mediated enzyme reactions from cyclic voltammetry and simulations," *Bioelectrochemistry*, **74**(1), 201-209 (2008).
- 5. A. E. G. Cass, G. Davis, G. D. Francis, H. A. O. Hill, W. J. Aston, I. J. Higgins, E. V. Plotkin, L. D. L. Scott and A. P. F. Turner, "Ferrocene-Mediated Enzyme Electrode for Amperometric Determination of Glucose," *Analytical Chemistry*, **56**(4), 667-671 (1984).
- 6. I. Willner, G. Arad and E. Katz, "A biofuel cell based on pyrroloquinoline quinone and microperoxidase-1 monolayer-functionalized electrodes," *Bioelectrochemistry and Bioenergetics*, **44**(2), 209-214 (1998).
- 7. S. C. Barton, "Enzyme catalysis in biological fuel cells" in Handbook of Fuel Cells Fundamentals, Technology and Applications (ed. Wolf Vielstich, H. Y., Hubert Andreas Gasteiger) (2009).
- 8. P. N. Bartlett and K. F. E. Pratt, "Theoretical Treatment of Diffusion and Kinetics in Amperometric Immobilized Enzyme Electrodes .1. Redox Mediator Entrapped within the Film," *Journal of Electroanalytical Chemistry*, **397**(1-2), 61-78 (1995).
- 9. A. S. Bedekar, J. J. Feng, S. Krishnamoorthy, K. G. Lim, G. T. R. Palmore and S. Sundaram, "Oxygen limitation in microfluidic biofuel cells," *Chemical Engineering Communications*, **195**(3), 256-266 (2008).
- 10. S. C. Barton, "Oxygen transport in composite mediated biocathodes," *Electrochimica Acta*, **50**(10), 2145-2153 (2005).
- 11. D. J. Glykys and S. Banta, "Metabolic Control Analysis of an Enzymatic Biofuel Cell," *Biotechnology and Bioengineering,* **102**(6), 1624-1635 (2009).
- 12. S. W. Jeon, J. Y. Lee, J. H. Lee, S. W. Kang, C. H. Park and S. W. Kim, "Optimization of cell conditions for enzymatic fuel cell using statistical analysis," *Journal of Industrial and Engineering Chemistry*, **14**(3), 338-343 (2008).

- 13. C. P. Andrieux, J. M. Dumasbouchiat and J. M. Saveant, "Catalysis of Electrochemical Reactions at Redox Polymer Electrodes Kinetic-Model for Stationary Voltammetric Techniques," *Journal of Electroanalytical Chemistry*, **131**(Jan), 1-35 (1982).
- 14. C. P. Andrieux and J. M. Saveant, "Kinetics of Electrochemical Reactions Mediated by Redox Polymer-Films Irreversible Cross-Exchange Reactions Formulation in Terms of Characteristic Currents for Stationary Techniques," *Journal of Electroanalytical Chemistry*, **134**(1), 163-166 (1982).
- 15. C. S. J. M. Andrieux, *Catalysis at Redox Polymer Coated Electrodes*. (ed. Murray, R. W.) (John Wiley & Sons, Inc.: New York, 1992).
- 16. C. S. T. P. N. Bartlett, E. J. Calvo, V. Flexer, *Chapter 8. Modelling Biosensor Responses* (ed. Bartlett, P. N.) (2008).
- 17. T. Tamaki, T. Ito and T. Yamaguchi, "Modelling of Reaction and Diffusion Processes in a High-surface-area Biofuel Cell Electrode Made of Redox Polymer-grafted Carbon," *Fuel Cells*, **9**(1), 37-43 (2009).
- 18. E. J. Calvo, C. B. Danilowicz and A. Wolosiuk, "Supramolecular multilayer structures of wired redox enzyme electrodes," *Physical Chemistry Chemical Physics*, **7**(8), 1800-1806 (2005).
- 19. E. J. Calvo, F. Battaglini, C. Danilowicz, A. Wolosiuk and M. Otero, "Layer-by-layer electrostatic deposition of biomolecules on surfaces for molecular recognition, redox mediation and signal generation," *Faraday Discussions*(116), 47-65 (2000).
- 20. E. J. Calvo and A. Wolosiuk, "Wiring enzymes in nanostructures built with electrostatically self-assembled thin films," *Chemphyschem*, **6**(1), 43-47 (2005).
- 21. E. J. Calvo, R. Etchenique, C. Danilowicz and L. Diaz, "Electrical communication between electrodes and enzymes mediated by redox hydrogels," *Analytical Chemistry*, **68**(23), 4186-4193 (1996).
- 22. M. N. Zafar, F. Tasca, S. Boland, M. Kujawa, I. Patel, C. K. Peterbauer, D. Leech and L. Gorton, "Wiring of pyranose dehydrogenase with osmium polymers of different redox potentials," *Bioelectrochemistry*, **80**(1), 38-42 (2010).
- 23. T. J. Ohara, R. Rajagopalan and A. Heller, "Glucose Electrodes Based on Cross-Linked [Os(Bpy)(2)](+/2+) Complexed Poly(L-Vinylimidazole) Films," *Analytical Chemistry*, **65**(23), 3512-3517 (1993).
- 24. A. Heller, "Electrical Connection of Enzyme Redox Centers to Electrodes," *Journal of Physical Chemistry*, **96**(9), 3579-3587 (1992).

- 25. D. Chakraborty and S. C. Barton, "Influence of Mediator Redox Potential on Fuel Sensitivity of Mediated Laccase Oxygen Reduction Electrodes," *Journal of the Electrochemical Society*, **158**(4), B440-B447 (2011).
- 26. K. Kano and T. Ikeda, "Fundamentals and practices of mediated bioelectrocatalysis," *Analytical Sciences*, **16**(10), 1013-1021 (2000).
- 27. J. W. Gallaway, *PhD Thesis, Redox Polymer Mediation for Enzymatic Biofuel Cells*, Columbia University (2007).
- 28. A. J. Bard, and Faulkner, *Electrochemical methods: fundamentals and applications* (2001).
- 29. J. Hodak, R. Etchenique, E. J. Calvo, K. Singhal and P. N. Bartlett, "Layer-by-layer self-assembly of glucose oxidase with a poly(allylamine)ferrocene redox mediator," *Langmuir*, **13**(10), 2708-2716 (1997).
- 30. J. J. Gooding and E. A. H. Hall, "Parameters in the design of oxygen detecting oxidase enzyme electrodes," *Electroanalysis*, **8**(5), 407-413 (1996).
- 31. J. W. Parker and C. S. Schwartz, "Modeling the Kinetics of Immobilized Glucose-Oxidase," *Biotechnology and Bioengineering*, **30**(6), 724-735 (1987).
- 32. C. Bourdillon, C. Demaille, J. Moiroux and J. M. Saveant, "Step-by-Step Immunological Construction of a Fully Active Multilayer Enzyme Electrode," *Journal of the American Chemical Society*, **116**(22), 10328-10329 (1994).
- 33. V. Leskovac, S. Trivic, G. Wohlfahrt, J. Kandrac and D. Pericin, "Glucose oxidase from Aspergillus niger: the mechanism of action with molecular oxygen, quinones, and one-electron acceptors," *International Journal of Biochemistry & Cell Biology*, **37**(4), 731-750 (2005).
- 34. S. Nakamura and Y. Ogura, "Action Mechanism of Glucose Oxidase of Aspergillus Niger," *Journal of Biochemistry*, **63**(3), 308-& (1968).
- 35. G. Wohlfahrt, S. Trivic, J. Zeremski, D. Pericin and V. Leskovac, "The chemical mechanism of action of glucose oxidase from Aspergillus niger," *Molecular and Cellular Biochemistry*, **260**(1), 69-83 (2004).
- 36. Q. H. Gibson, V. Massey and B. E. P. Swoboda, "Kinetics + Mechanism of Action of Glucose Oxidase," *Journal of Biological Chemistry*, **239**(11), 3927-& (1964).
- 37. N. Mano, F. Mao and A. Heller, "On the parameters affecting the characteristics of the "wired" glucose oxidase anode," *Journal of Electroanalytical Chemistry*, **574**(2), 347-357 (2005).

- 38. B. A. Gregg and A. Heller, "Redox Polymer-Films Containing Enzymes .2. Glucose-Oxidase Containing Enzyme Electrodes," *Journal of Physical Chemistry*, **95**(15), 5976-5980 (1991).
- 39. J. F. Castner and L. B. Wingard, "Mass-Transport and Reaction Kinetic-Parameters Determined Electrochemically for Immobilized Glucose-Oxidase," *Biochemistry*, **23**(10), 2203-2210 (1984).
- 40. D. N. Blauch and J. M. Saveant, "Dynamics of Electron Hopping in Assemblies of Redox Centers Percolation and Diffusion," *Journal of the American Chemical Society*, **114**(9), 3323-3332 (1992).
- 41. I. H. Segel, *Enzyme kinetics : behavior and analysis of rapid equilibrium and steady-state enzyme systems* (Wiley, New York, 1975).
- 42. S. A. M. Vanstroebiezen, A. P. M. Janssen and L. J. J. Janssen, "Solubility of Oxygen in Glucose Solutions," *Analytica Chimica Acta*, **280**(2), 217-222 (1993).
- 43. S. M. Zakeeruddin, D. M. Fraser, M. K. Nazeeruddin and M. Gratzel, "Towards Mediator Design Characterization of Tris-(4,4'-Substituted-2,2'-Bipyridine) Complexes of Iron(Ii), Ruthenium(Ii) and Osmium(Ii) as Mediators for Glucose-Oxidase of Aspergillus-Niger and Other Redox Proteins," *Journal of Electroanalytical Chemistry*, 337(1-2), 253-283 (1992).

Chapter 4: Summary and Future Outlook

Mediated enzyme electrodes were prepared from the glucose-oxidizing enzyme glucose oxidase (GOx) from *Aspergillus niger* and two osmium based redox polymer mediators, which have redox potential difference of ~100 mV. These enzyme electrodes can be used as bioanodes for biofuel cell applications.

In Chapter 2, efforts have been made to characterize the GOx electrodes based on the mediator redox potential and osmium loading of the synthesized polymers in the presence of N_2 , Air and O_2 and such electrodes produced the highest current densities reported till date. For a complete biofuel cell based on mediated enzyme electrodes, it is desirable to have an anode mediator with lower redox potential, but suffers due to lower current density when ΔE_T , the electron transfer driving force or the overpotential between mediator and the enzyme decreases. Performance of such electrodes also deteriorates in the presence of inhibitors. For GOx based anodes, as we have seen in this work, reduction in the electrochemical performance and stability was observed due to competitive reaction of oxygen with mediator for electrons at the active site of GOx.

In Chapter 3, a one-dimensional model of a redox polymer mediated, glucose-oxidizing GOx enzyme electrode was demonstrated, which also accounts for the effect of oxygen and relevant kinetic behavior of the system was elucidated. To our knowledge, we are first to report the detailed kinetic parameters of such GOx based redox hydrogel films, where accurate estimation of the active enzyme loading is difficult. Therefore, obtained kinetic parameter like

 k_{cat} was multiplied with total enzyme loading (E_T) to yield a parameter called maximum enzyme velocity, V_{max} in order to have a fair comparison with the kinetics of the similar systems, where mediation of GOx was conducted using dissolved complexes or with redox polymers entrapped in an ultrathin films. V_{max} of the studied electrodes were found to be an order of magnitude higher than the literature findings, which can be ascribed to a superior mediation capacity of the synthesized polymers. Also, the bimolecular rate constant (k_O) for GOx-oxygen reaction was found to be an order of magnitude lower than in free solution, which can be attributed to the electron competition reaction with mediator or inhibition of oxygen-GOx binding by osmium moieties.

As a power-producing device, it is imperative to maximize the overall cell potential by identifying the optimal electrode design to achieve the optimum biofuel cell performance.

Optimum mediator potential of 0.66 V relative to standard hydrogen electrode (SHE) for laccase-catalyzed cathode has been proposed in the literature based on the experimental data and elucidation of kinetics via modeling of eight different osmium based redox polymers having potentials ranging from 0.85 to 0.11 V/SHE. In the present work, we have analyzed two redox polymer mediated GOx electrodes and similar study can also be undertaken for such bioanodes in order to have a realistic picture of the optimum biofuel cell performance.

The proposed model can be used to obtain the kinetic parameters of complex three-substrate enzymatic system. Optimum parameters, operating conditions and performance of the cell can be predicted and quantified via mathematical modeling. This would help to improve and optimize the system at molecular scale in the context of biofuel and biosensor applications.

Although osmium based redox mediators are widely used, issues regarding toxicity and cost limits their use for *in vivo* applications. With objective to develop low cost, lightweight, manufacturable and reproducible EFC system and to compete against Li-ion batteries having limited energy storage density for small power applications, novel mediator chemistry must be identified and synthesized.

With ability to extract power from the ambient fuels, biofuel cell technology has the potential to meet civilian and military needs for use as a compact, lightweight, small-scale power generating devices.

APPENDICES

Appendix A: MATLAB code for one dimensional film-model in N₂ saturated conditions*

```
function [jobs,out]=bp project N2(in)
 % Defining dimensionless variables
    kappa=in.L*sqrt(in.vm*in.kA*in.ET/in.DA);
    eta=(in.vm*in.DS*in.kA*in.Ks)/(in.vs*in.DA*in.kcat);
    gamma=(in.kA*in.Ao*in.Ks)/(in.kcat*in.ST);
    mu=(in.ST/in.Ks);
    sigma1 = (in.delta1 * in.DS * in.k) / (in.L * in.Ds);
Dimensionless parameter that characterizes the substrate
boundary condition
    eps = (in.n * in.F * (in.E-in.E0))/(in.R*in.T);
                                                             용
From the Nernst equation
    ae = 1/(1+exp(-eps));
Dimensionless potential boundary condition at the electrode
surface from the Nernst eqn
 % Dimensionless thickness of the hydrogel film
    x0 = linspace(0, 1, 100);
 % Forms the initial guess for bvp4c
    solinit = bvpinit(x0,[.5 0 1 0]);
 % Calls the bvp4c solver
    sol = bvp4c(@deriv, @bc, solinit);
        = sol.x;
                                    % Dimensionless mediator
         = sol.y(1,:);
concentration
    dadx = sol.y(2,:);
                                    % Dimensionless mediator
flux
                                    % Dimensionless substrate
         = sol.y(3,:);
concentration
```

^{*} This code was assembled with the kind help of my advisor Dr. Scott Calabrese Barton

```
dsdx = sol.y(4,:);
                            % Dimensionless substrate
flux
 % Extraction of current density at the elctrode surface in
mA/cm2
    jobs = (-1 * in.F * in.DA * in.Ao * sol.y(2,1) * 1000) /
in.L;
% Dimensionless non-linear differential equations
    Ra= kappa^2*a.*s./(qamma*a.*(1+mu*s)+s) .* (a >= 0) .* (s >= 0)
0);
    Rs= Ra.*(gamma/eta).*(Ra>=0);
 % Dimensionless reduced enzyme concentration in the film
    e2=s./((gamma*a.*(1+mu*s)+s)).* (a >= 0) .* (s >= 0);
 % Plot the results
    plot(x,a,'-r',x,s,'--g',x,Ra/max(Ra(:)),'-b',x,e2,'--
b');figure(gcf)
    axis([0,1,0,1]);
    xlabel('\chi');
    ylabel('Dimensionless concentration profile');
    legend('a - Oxidized mediator','s - Substrate','R /
Rmax','Reduced enzyme','Location','Southwest');
    function dzdx=deriv(x,z)
        a = z(1);
        va=z(2);
        s = z(3);
        vs=z(4);
        Ra= kappa^2*a*s/(gamma*a*(1+mu*s)+s) * (a >= 0) * (s >= 0)
0);
        Rs= Ra*(qamma/eta)*(Ra>=0);
        dvadx= Ra;
        dadx= va;
        dvsdx= Rs;
        dsdx= vs;
```

```
dzdx= [dadx; dvadx; dsdx; dvsdx];
    end %dzdx
    function res= bc(z0,z1)
        a0 = z0(1); a1 = z1(1);
        va0 = z0(2); va1 = z1(2);
        s0 = z0(3); s1 = z1(3);
        vs0= z0(4); vs1= z1(4);
     % Nernst BC on a at electrode-film interface
        res(1) = a0 - ae;
     % Zero flux BC on 's' at electrode-film interface
        res(2) = vs0;
     % Zero flux BC on 'a' at film-solution interface
        res(3) = va1;
     % Concentration BC on 's' at film-solution interface
        res(4) = s1 - 1 + (sigma1*vs1); % This BC incorporates
the MT resistance
        %res(4) = s1 - 1 ; %
     % force res to be a column vector
        res=res(:);
    end % bc
    out=sol;
    out.in=[kappa,eta,gamma,mu,ae,sigma1];
    out.a = a;
    out.dadx=dadx;
    out.s = s;
    out.dsdx=dsdx;
    out.Ra = Ra;
    out.Rs = Rs;
    out.jobs=jobs;
    out.e2=e2;
end % bp project N2
```

Appendix B: MATLAB code for one-dimensional film model in the presence of Air and O₂*

```
function [jobs,out]=bp project oxy(in)
 % Dimensionless variables
    kappa=in.L*sqrt(in.vm*in.kA*in.ET/in.DA);
    eta=(in.vm*in.DS*in.kA*in.Ks)/(in.vs*in.DA*in.kcat);
    gamma=(in.kA*in.Ao*in.Ks)/(in.kcat*in.ST);
    mu=(in.ST/in.Ks);
    beta=(in.ko*in.OT O*in.Ks)/(in.kcat*in.ST);
    d = (in.vo*in.DS*in.ST)/(in.vs*in.DO*in.OT O);
  응
beta=(in.kcat O*in.OT O*in.Ks)/((in.Ko+in.OT O)*in.kcat*in.ST);
% Beta for the two parameter model
    eps = (in.n * in.F * (in.E-in.E0))/(in.R*in.T);
                                                           % From
the Nernst equation
    ae = 1/(1+\exp(-\exp s));
Dimensionless potential boundary condition at the electrode
surface from the Nernst eqn
    sigma1 = (in.delta1 * in.DS * in.k) / (in.L*in.Ds);
Dimensionless parameter that characterizes the substrate
boundary condition
    sigma2 = (in.delta2 * in.DO * in.k) / (in.L*in.Do);
Dimensionless parameter that characterizes the oxygen boundary
condition
 % Dimensionless thickness of the hydrogel film
    x0=linspace(0,1,100);
 % Forms the initial guess for bvp4c
    solinit = bvpinit(x0, [1 \ 0 \ 1 \ 0 \ 1);
 % Calls the bvp4c solver
    sol = bvp4c(@deg, @bc, solinit);
```

^{*} This code was assembled with the kind help of my advisor Dr. Scott Calabrese Barton

```
x = sol.x;
                                       % Dimensionless mediator
         = sol.y(1,:);
concentration
                                       % Dimensionless mediator
    dadx = sol.y(2,:);
flux
                                       % Dimensionless oxygen
        = sol.y(3,:);
concentration
    dodx = sol.y(4,:);
                                       % Dimensionless oxygen
flux
        = sol.y(5,:);
                                       % Dimensionless substrate
    S
concentration
    dsdx = sol.y(6,:);
                                       % Dimensionless subsrate
flux
 % Extraction of current density in mA/cm2
jobs = (-1 * 96485.5 * 2.18e-9 * 659.7e-6 * sol.y(2,1) * 1000)
/ le-4; % Current density for 'lb'
 % Dimensionless non-linear differential equations
   Ra =
(kappa.^2.*a.*s)./((((gamma.*a)+(beta.*o)).*(1+(mu.*s)))+s).*(a>
=0).*(0>=0).*(s>=0);
    Ro =
(kappa.^2.*o.*s.*(beta*d/eta))./((((gamma.*a)+(beta.*o)).*(1+(mu
.*s)))+s).*(a>=0).*(o>=0).*(s>=0);
    Rs = (Ra.*gamma/eta)+(Ro./d).*(Ra>=0).*(Ro>=0);
 % Dimensionless reduced enzyme concentration in the film
e2=s./((((gamma.*a)+(beta.*o)).*(1+(mu.*s)))+s).*(a>=0).*(o>=0).
*(s>=0);
% Plot the results
    plot(x,a,'-r',x,s,'--g',x,o,'-k',x,Ra/max(Ra(:)),'-
b',x,e2,'--b');figure(gcf)
    axis([0,1,0,1]);
    xlabel('\chi');
    ylabel('Dimensionless concentration profile');
    legend('a - Oxidized mediator','s - Substrate','o -
```

```
Oxygen','R / R_{max}','Reduced enzyme','Location','Southwest');
      function dzdx = deq(x,z)
         a = z(1);
         va=z(2);
         o = z(3);
         vo=z(4);
         s = z(5);
         vs=z(6);
(\text{kappa}^2*a*s)/((((\text{gamma}*a)+(\text{beta}*o))*(1+(\text{mu}*s)))+s)*(a>=0)*(o>=0)
)*(s>=0);
         Ro =
(\text{kappa}^2*o*s*(\text{beta}*d/\text{eta}))/((((\text{gamma}*a)+(\text{beta}*o))*(1+(\text{mu}*s)))+s)
*(a>=0)*(o>=0)*(s>=0);
         Rs = ((Ra*qamma/eta)+(Ro/d))*(Ra>=0)*(Ro>=0);
         dvadx= Ra;
         dadx= va;
         dvodx= Ro;
         dodx= vo;
         dvsdx=Rs;
         dsdx= vs;
         dzdx= [dadx; dvadx; dodx; dvodx; dsdx; dvsdx];
      end % dzdx
      function res = bc(z0,z1)
         a0 = z0(1); a1 = z1(1);
         va0 = z0(2); va1 = z1(2);
         00 = z0(3); 01 = z1(3);
         vo0 = z0(4); vo1 = z1(4);
         s0 = z0(5); s1 = z1(5);
         vs0 = z0(6); vs1 = z1(6);
       % Nernst BC on a at electrode-film interface
         res(1) = a0 - ae;
```

```
% Zero flux BC on 'o' at electrode-film interface
        res(2) = vo0;
      % Zero flux BC on 's' at electrode-film interface
        res(3) = vs0;
      % Zero flux BC on 'a' at film-solution interface
        res(4) = val;
      % Concentration BC on 'o' at film-solution interface
        %res(5) = o1 - 1;
        res(5) = o1 - 1 + (sigma2*vo1); % This BC incorporates
the MT resistance
      % Concentration BC on 's' at film-solution interface
        %res(6) = s1 - 1;
        res(6) = s1 - 1 + (sigma1*vs1); % This BC incorporates
the MT resistance
      % force res to be a column vector
        res=res(:);
      end % bc
    out=sol;
    out.in=[kappa,eta,gamma,mu,beta,d,ae,sigma1,sigma2];
    out.a = a;
    out.dadx=dadx;
    out.o = o;
    out.dodx=dodx;
    out.s = s;
    out.dsdx=dsdx;
    out.Ra = Ra;
    out.Ro = Ro;
    out.Rs = Rs;
    out.jobs=jobs;
    out.e2=e2;
end % bp project oxy
```

Function for fitting the film model (for RP A mediated system in the presence of N_2)

% "xy=[]'" is a matrix of experimental data having 3 columns.
Three coulmns have substrate conc. (mol/cm3), potential (volts re:SHE) and current density (mA/cm2) data respectively.

```
p(1).data='ST';
p(2).data='E';

p(3).param='kcat'; p(3).init=17.5;
p(4).param='kA'; p(4).init=2.12e5;
p(5).param='Ks'; p(5).init=12e-6;
in=intest_1b;
out=funfit2(@bp_project_N2,xy,in,p,true);
```

Function for fitting the film model (for RP A mediated system in the presence of

O_2

```
% "xy" is a matrix of experimental data having 2 columns. Two
% coulmns have oxygen conc. (mol/cm3) and corresponding current
density (mA/cm2) respectively.

xy = [1e-20 0.18e-6 0.86e-6; 2.01 1.8157 1.3665]';
p(1).data='OT_O';
p(2).param='ko'; p(2).init=1.66e8;
in=intest_1b;
out=funfit2(@bp project oxy,xy,in,p,true);
```

Appendix C: Input file for the bp_project_N2(in) function (for RP A mediated system)

```
function in=intest 1b
% Diffusivitiy Values
  in hydrogel in cm2/s (Literature value from Calvo's 2005 paper)
  in.DO = 1.5e-5; % Diffusivity of the oxygen from Josh's
kinetics paper
% Concentration values
  in.ET = 17.96e-6; % Total enzyme concentration in
mol/cm3 ---> To convert in to mM multiply by 1e6
  in.ST = 50e-6; % Total bulk substrate concentration
in mol/cm3
  in.Ao = 659.7e-6; % Total mediator concentration in
mol/cm3 from CV integration
  in.OT O = 0.86e-6; % Total bulk oxygen concentration in
air saturated conditions in mol/cm3
  in.OT A = 0.18e-6; % Total bulk oxygen concentration in
oxygen saturated conditions in mol/cm3
% Kinetic parameters for N2 saturated conditions at 1000 rpm
  mediator in cm3/mol/s ---> To convert in to M-1 s-1 multiply by
1e-3
  in.Ks = 12.3e-6; % Michaelis constant for substrate in
mol/cm3 ---> To convert in to mM multiply by 1e6
  % At 0 rpm or No mass transfer correction
    in.kcat= 17.82;
    in.kA = 212e3;
    in.Ks= 14.735e-06;
% Kinetic parameters for O2 saturated conditions
                 % Second order rate constant for
in.ko = 1.66e8:
mediator in cm3/mol/s ---> To convert in to M-1 s-1 multiply by
1e-3
    in.kcat 0 = 1400; % Turn over number in s-1
```

```
in.Ko = 7e-6; % Michaelis constant for oxygen in
mol/cm3 ---> To convert in to mM multiply by 1e6
% Various constants
                       % Stoichiometric coeff. of mediator
  in.vm = 1;
                   % Stoichiometric coeff. of substrate
% Stoichiometric coeff. of product
  in.vs = 0.5;
in.vp = 0.5;
  in.vo = 0.5;
                       % Stoichiometric coeff. of oxygen
  in.E0 = 0.43;
                     % Reversible potential of the mediator
in volts re:SHE
  in.E = 0.0;
                     % Fixed potential of the system in
volts re:SHE
  in.n = 1;
                      % Number of electrons transfered at the
elecrode surface
  in.L = 1e-4;
                   % Hydrogel film thickness in cm
% Data in the following section will be used to incorporate the
effect of substrate mass transport
```

```
% kinematic viscosity in cm2/s
  in.v = 0.01;
 in.omega = 1000;
                          % RDE rotation speed in rpm
                          % Ds is the glucose diffusion in the
  in.Ds = 7e-6;
bulk solution in cm2/s
  in.Do = 1.5e-5;
                             % Do is the oxygen diffusion in
the bulk solution in cm2/s
                           % Partition coefficient of glucose
  in.k = 1;
and oxygen into the hydrogel film from the solution
  in.delta1 = 4.98 * (in.DS^(1/3)) * (in.v^(1/6)) * (in.omega^(-
1/2));% Thickness of the diffuse layer in cm at 1000 rpm
  in.delta2 = 4.98 * (in.DO^{(1/3)}) * (in.v^{(1/6)}) * (in.omega^{(-1/6)})
```

1/2));% Thickness of the diffuse layer in cm at 1000 rpm